

SYNTHESIS AND CHARACTERIZATION OF CONDUCTING  
COPOLYMERS OF THIOPHENE ENDED POLY(ETHYLENE OXIDE):  
THEIR ELECTROCHROMIC PROPERTIES AND USE IN ENZYME  
IMMOBILIZATION

A THESIS SUBMITTED TO  
THE GRADUATE SCHOOL OF NATURAL AND APPLIED SCIENCES  
OF  
MIDDLE EAST TECHNICAL UNIVERSITY

BY

HÜSEYİN BEKİR YILDIZ

IN PARTIAL FULFILLMENT OF THE REQUIREMENTS  
FOR  
THE DEGREE OF DOCTOR OF PHILOSOPHY  
IN  
CHEMISTRY

JANUARY 2007

Approval of the Graduate School of Natural and Applied Sciences.

---

Prof. Dr. Canan Özgen  
Director

I certify that this thesis satisfies all the requirements as a thesis for the degree of Doctor of Philosophy.

---

Prof. Dr. Ahmet M. Önal  
Head of the Department

This is to certify that we have read this thesis and that in our opinion it is fully adequate, in scope and quality, as a thesis for the degree of Doctor of Philosophy.

---

Prof. Dr. Levent Toppare  
Supervisor

Examining Committee Members

Prof. Dr. Duygu Kısakürek (METU, CHEM)

---

Prof. Dr. Levent Toppare (METU, CHEM)

---

Prof. Dr. Leyla Aras (METU, CHEM)

---

Prof. Dr. Ahmet M. Önal (METU, CHEM)

---

Prof. Dr. Mustafa Güllü (Ankara Üniv., CHEM)

---

**I hereby declare that all information in this document has been obtained and presented in accordance with academic rules and ethical conduct. I also declare that, as required by these rules and conduct, I have fully cited and referenced all material and results that are not original to this work.**

**Name, Last name : Hüseyin Bekir Yıldız**

**Signature :**

## ABSTRACT

### SYNTHESIS AND CHARACTERIZATION OF CONDUCTING COPOLYMERS OF THIOPHENE ENDED POLY(ETHYLENE OXIDE): THEIR ELECTROCHROMIC PROPERTIES AND USE IN ENZYME IMMOBILIZATION

Yıldız, Hüseyin Bekir

Ph.D., Department of Chemistry

Supervisor: Prof. Dr. Levent Toppare

January 2007, 132 pages

Thiophene ended poly(ethylene oxide) (ThPEO) and random copolymer (RPEO) of 3-methylthienyl methacrylate and *p*-vinylbenzyloxy poly(ethyleneoxide) units were synthesized chemically. Further graft copolymerization of RPEO and ThPEO with pyrrole (Py) and thiophene (Th) were achieved in H<sub>2</sub>O - sodium dodecylsulfate (SDS), H<sub>2</sub>O - *p*-toluenesulphonic acid (PTSA) and acetonitrile (AN) - tetrabutylammonium tetrafluoroborate (TBAFB) solvent electrolyte couples via constant potential electrolyses. Characterizations were performed by cyclic voltammetry (CV), nuclear magnetic resonance spectroscopy (NMR), and fourier transform infrared spectroscopy (FTIR). The morphologies of the films were examined by scanning

electron microscopy (SEM). Conductivities of the samples were measured by using four-probe technique. Moreover, spectroelectrochemical and electrochromic properties of the copolymers obtained from thiophene were investigated by UV-Vis spectrometry and colorimetry.

Immobilizations of alcohol oxidase and polyphenol oxidase enzymes were performed in the matrices obtained via copolymerization of ThPEO and RPEO with pyrrole. Immobilization was carried out via entrapment of enzyme in matrices during the polymerization of pyrrole. Temperature optimization, operational stability and shelf-life of the enzyme electrodes were investigated. Maximum reaction rate ( $V_{max}$ ) and Michaelis-Menten constant ( $K_m$ ) were determined.

It is known that wine includes phenolic groups that give astringency in high concentrations. Polyphenol oxidase (PPO) converts mono and diphenols to quinone. By analyzing the product, one can find out the amount of phenolic groups. By using the enzyme electrodes via immobilization of PPO, amount of phenolics in different wines were analyzed.

Keywords: Electrochemical polymerization, immobilization, alcohol oxidase, polyphenol oxidase, wine.

## ÖZ

### TİYOFEN SONLU POLİ(ETİLEN OKSİT) İLETKEN KOPOLİMERLERİNİN SENTEZ VE KARAKTERİZASYONU: ELEKTROKROMİK ÖZELLİKLERİ VE ENZİM TUTUKLAMASINDA KULLANIMI

Yıldız, Hüseyin Bekir  
Doktora, Kimya Bölümü  
Tez Yöneticisi: Levent Toppare

Ocak 2007, 132 sayfa

ThPEO olarak kodlanan tiyofen sonlu poli(etilen oksit) ve 3-metiltiyenil metakrilat ve p-vinilbenziloksi poli(etilen oksit) birimleri içeren ve RPEO olarak kodlanan kopolimer kimyasal olarak sentezlendi Sabit potansiyel altında yapılan elektroliz yardımıyla su-sodyum dodesil sülfat (SDS), su-paratoluen sülfonik asit (PTSA) ve asetonitril (AN)-tetrabütülamonyum tetrafloroborat (TBAFB) solvent-elektrolit çiftleri kullanılarak ThPEO ve RPEO'nin pirol (Py) ve tiyofenle (Th) kopolimerleri sentezlendi. Elde edilen kopolimerlerin karakterizasyonu, nükleer manyetik rezonans spektroskopisi (NMR), dönüşümlü voltametre, FTIR spektroskopisi, taramalı elektron mikroskobu kullanılarak yapıldı. Ayrıca tiyofen kullanılarak elde edilen kopolimerlerin

spektroelektrokimyasal ve elektrokromik özellikleri UV-Vis spektrometresi ve kolorimetre teknikleri kullanılarak araştırıldı.

RPEO ve ThPEO'nun pirol kullanılarak elde edilen kopolimerleri alkol oksidaz ve polifenol oksidaz tutuklamaları için kullanıldı. Enzim elektrotlarının optimum sıcaklıkları, kararlılıkları ve raf ömürleri tayin edildi. Kinetik parametreleri de ayrıca incelendi.

Polifenol oksidaz enzimi kullanılarak elde edilen enzim elektrotları şaraplarda bulunan ve fazla miktarı şarabın acılaşmasına sebep olan fenolik yapıların miktar tayininde kullanıldı. Türkiye'de üretilen iki farklı kırmızı şarabın fenolik miktar analizleri yapıldı.

Anahtar Kelimeler: Elektrokimyasal polimerleşme, enzim tutuklaması, alkol oksidaz, polifenol oksidaz, şarap.

**To the Memory of Mustafa Kemal ATATÜRK, the leader of Turkish  
Nation and founder of the Republic of Turkey**

## ACKNOWLEDGMENTS

First, I must thank Mustafa Kemal ATATÜRK, founder of the Republic of Turkey, for giving freedom and future to Turkish nation, and his revolutions for Turkey. Without him, I would have never been able to think and walk in the science road freely.

I wish to express my deepest appreciation to my advisor, Prof. Dr. Levent Toppare, for his support and tremendous encouragement. Through his endless enthusiasm for the subject matter, he was able to push me to achieve things which I initially believed impossible. He provided an academic environment of intellectual enrichment, advice and stimulation to excel and the lesson I learned under his guidance will serve me well in the future. He was not only my supervisor, but also was one of my friends and especially my second father in the university. I thank him very much for everything.

I would like to give my special thanks to Prof. Dr. Duygu Kısakürek for her inspiring discussions and wisdom for life.

I wish to express my sincere thanks to Prof. Dr. Yusuf Yağcı and Prof. Dr. Mustafa Güllü for their valuable discussions and help throughout this study.

I very much appreciate Prof. Dr. Wolfgang Schuhmann at the Department of Chemistry, Ruhr Universität-Bochum, giving me opportunity to work in his group. Members of the Schuhmann's group have made me feel very much at home. It was fun to work in that group.

Thanks also should go to my predecessor Dr. Senem Kıralp for her initial guidance in my early years in Toppare's group and her friendship

I also wish to express my endless thanks to my friends Dr. Jaime Castillo, Dr. Sonnur Işık Uppenkamp, Dr. Ertuğrul Şahmetlioğlu, Dr. Elif Şahin Işgın, Dr. Armağan Kınal, Sanem Ezgi Kınal, Yusuf Nur, Bekir Gökçen Mazı,

Ürün Doğan, Engin Okudan, Erhan Demircioğlu, Erkan Demircioğlu, Serkan Mulayim, Haluk Civan Çolak, Mustafa Boyacılar, Dr. Deniz Kılınc, Nurettin Eryaşayan, Olcay Mert, Murat Kaleli, Emre Çalık, Murat Ateş, Ali Sinan Dike and Özlem Türkarlan, for their friendship, moral supports and encouragement.

I also want to thank all the post and present members of Toppare's group for their helps, their friendships and for making lab life more fun.

My special thanks go to my parents, Tahsin and Naime Yıldız, and my sister, Elife Deniz, for their love and guidance throughout my life. Their support and active interest has enabled me to try when I otherwise would not have, allowing me to accomplish more than I thought possible. Their unwavering confidence has enabled me to continue when my efforts have fallen short, never doubting that next try will be successful one. Their unconditional love is something that I have relied on regardless of the time period or distance between us. I am proud to be their son and her brother and I am proud to say that this is the foundation on which all else has been possible.

Finally I must thank my fiancée, Sevgi Sıla Bilgin, for always being the best part of my day. I thank her for being my support system, and, at times, my only connection back to reality. I could not have done this without her constant encouragement and help. Words cannot describe how lucky I feel that she is in my life

Appreciation is extended to colleagues in the Department of Chemistry, Middle East Technical University.

## TABLE OF CONTENTS

ABSTRACT.....	iv
ÖZ.....	vi
ACKNOWLEDGMENTS .....	ix
TABLE OF CONTENTS .....	xi
LIST OF FIGURES.....	xvii
LIST OF TABLES .....	xxi
ABBREVIATIONS.....	xxii

### CHAPTERS

1. INTRODUCTION.....	1
1.1. Conducting Polymers.....	1
1.1.1. Brief History of Conducting Polymers .....	1
1.1.2. Applications of Conducting Polymers .....	4
1.1.3. Conductivity Mechanism in Conducting Polymers .....	5
1.1.3.1 Conductivity and Band Theory.....	5
1.1.3.2. Band Theory .....	6
1.1.3.3. Doping and Electrical Conductivity.....	9
1.1.3.4 Hopping Process .....	12
1.1.4. Synthesis of Conducting Polymers .....	12
1.1.4.1. Chemical Polymerization .....	13
1.1.4.2. Electrochemical Polymerization .....	13
1.1.4.3. Effects of Electrosynthesis Conditions.....	15

1.1.5. Mechanism of Electrochemical Polymerization.....	16
1.1.6. Electrochemical Methods.....	17
1.1.6.1 Cyclic Voltammetry.....	19
1.1.6.2. Constant Current (Galvanostatic) Methods.....	22
1.1.6.3. Constant-Potential Methods.....	22
1.1.7. Copolymers, Composites and Blends.....	22
1.1.8. Electrochromism and Electrochromic Materials.....	23
1.1.8.1 Transition Metal Oxides (TMOs).....	24
1.1.8.2 Conducting Polymers as Electrochromic Materials.....	25
1.2. Enzymes.....	26
1.2.1. Enzyme Classification.....	27
1.2.2. Enzyme Activity.....	28
1.2.3. Kinetics of Enzyme Reactions.....	29
1.2.4. Enzyme Immobilization.....	33
1.2.4.1. Adsorption.....	34
1.2.4.2. Covalent Binding.....	35
1.2.4.3. Entrapment.....	36
1.2.4.4. Microencapsulation.....	36
1.2.4.5. Crosslinking.....	37
1.2.5. Enzyme Immobilization by Electropolymerization.....	38
1.2.6. Applications of Immobilized Enzymes.....	40
1.2.7. Polyphenol Oxidase Immobilization.....	42
1.2.8. Alcohol Oxidase Immobilization.....	47
1.3. Aim of the Study.....	50
2. EXPERIMENTAL.....	51
2.1. Chemicals.....	51
2.2. Electrochemical Polymerization.....	52
2.2.1. Cyclic Voltammetry.....	52
2.2.2. Constant Current (Galvanostatic) Methods.....	53
2.2.3. Constant Potential (Potentiostatic) Methods.....	53
2.3. Instrumentation.....	53

2.3.1. Nuclear Magnetic Resonance Spectrometer ( <sup>1</sup> H-NMR).....	55
2.3.2. Fourier Transform Infrared Spectrophotometry (FTIR) .....	55
2.3.3. Gel Permeation Chromatography (GPC) .....	56
2.3.4. UV-Vis Spectrophotometry.....	56
2.3.5. Spectroelectrochemistry Experiments.....	56
2.3.6. Colorimetry Measurements .....	56
2.3.7. Scanning Electron Microscopy (SEM) .....	57
2.3.8. Four Probe Conductivity Measurements.....	57
2.4. Experimental Procedures.....	58
2.4.1. Synthesis of Conducting Copolymers of Thiophene Ended Poly (Ethylene Oxide) with Thiophene and Pyrrole .....	58
2.4.1.1. Synthesis of Thiophene Ended Poly(Ethylene Oxide) (ThPEO) .....	58
2.4.1.2. Cyclic Voltammetry Studies of ThPEO .....	59
2.4.1.3. Synthesis of Copolymers of ThPEO with Pyrrole by Electrochemical Polymerization.....	59
2.4.1.4. Synthesis of Copolymers of ThPEO with Thiophene by Electrochemical Polymerization.....	59
2.4.2. Synthesis of Copolymers of Random Copolymer (RPEO) 3- Methylthienyl Methacrylate and <i>p</i> -Vinylbenzyloxy Poly(Ethylene Oxide) with Thiophene and Pyrrole.....	60
2.4.2.1. Synthesis of 3-Methylthienyl Methacrylate Monomer .....	60
2.4.2.2. Synthesis of <i>p</i> -Vinylbenzyloxy Poly(Ethylene Oxide) Monomer (PEO-VB).....	60
2.4.2.3. Synthesis of Random Copolymer (RPEO) of 3-Methylthienyl Methacrylate and <i>p</i> -Vinylbenzyloxy Poly(Ethylene Oxide).....	61
2.4.2.4. Cyclic Voltammetry Studies of RPEO.....	62
2.4.2.5. Synthesis of Copolymers of RPEO with Thiophene by Electrochemical Polymerization.....	62
2.4.2.6. Synthesis of Copolymers of RPEO with Pyrrole by Electrochemical Polymerization.....	63
2.3.7. Spectroelectrochemical Studies of Copolymers .....	63

2.3.8. Switching Properties of Polymers.....	63
2.4.9. Enzyme Immobilization .....	64
2.4.9.1. Immobilization of Alcohol Oxidase.....	64
2.4.9.1.1. Preparation of Enzyme Electrodes PPy/AOX and RPEO-co-PPy/AOX.....	64
2.4.9.1.2. Determination of Alcohol Oxidase Activity .....	64
2.4.9.1.3. Determination of Kinetic Parameters of Free and Immobilized AOX .....	64
2.4.9.1.4. Determination of Optimum pH and Optimum Temperature of Immobilized AOX .....	65
2.4.9.1.5. Operational Stability and Shelf Life of Immobilized AOX...	65
2.4.9.2. Immobilization of Polyphenol Oxidase.....	65
2.4.9.2.1. Preparation of Enzyme Electrodes (PPy/PPO, RPEO-co-PPy/PPO and ThPEO-co-PPy/PPO) .....	65
2.4.9.2.2. Determination of PPO Activity .....	66
2.4.9.2.3. Enzyme Activity Measurements for Free and Immobilized PPO .....	67
2.4.9.2.4. Determination of Optimum pH and Temperature of Immobilized PPO.....	67
2.4.9.2.5. Operational Stability and Shelf Life of Immobilized PPO....	67
2.4.9.2.6. Determination of Phenolic Compounds in Red Wines.....	67
2.4.9.3. Protein Determination for Enzyme Electrodes .....	67
3. RESULTS AND DISCUSSION .....	69
3.1. Conducting Copolymers .....	69
3.1.1. Conducting Copolymers of Thiophene Ended Poly(Ethylene Oxide) (ThPEO) with Thiophene and Pyrrole.....	69
3.1.1.1. Characterization of Thiophene Ended Poly(Ethylene Oxide) (ThPEO).....	69
3.1.1.1.1. NMR Study of ThPEO .....	69
3.1.1.1.2. FTIR Study of ThPEO .....	70
3.1.1.1.3. GPC Study of ThPEO.....	70

3.1.1.1.4. Cyclic Voltammetry Study of ThPEO.....	70
3.1.1.2. Copolymers of ThPEO with Thiophene (ThPEO-co-PTh) .....	73
3.1.1.2.1. FTIR Study of ThPEO-co-PTh .....	74
3.1.1.2.2. Cyclic Voltammetry Study of ThPEO-co-PTh .....	74
3.1.1.2.3. Morphologies of ThPEO-co-PTh Films .....	76
3.1.1.2.4. Conductivity of ThPEO-co-PTh Film .....	76
3.1.1.2.5. Electrochromic Studies of ThPEO-co-PTh.....	77
3.1.1.3. Copolymers of ThPEO with Pyrrole (ThPEO-co-PPy) .....	79
3.1.1.3.1. FTIR Study of ThPEO-co-PPy.....	80
3.1.1.3.2. Cyclic Voltammetry Study of ThPEO-co-PPy .....	81
3.1.1.3.3. Morphologies of the ThPEO-co-PPy Films.....	82
3.1.1.3.4. Conductivity Measurements of ThPEO-co-PPy Film.....	82
3.1.2. Conducting Copolymers of Random Copolymer (RPEO) of 3- Methylthienyl Methacrylate and p-Vinylbenzyloxy Poly(Ethylene Oxide) with Thiophene and Pyrrole .....	83
3.1.2.1. Characterization of 3-Methylthienyl Methacrylate.....	83
3.1.2.2. Characterization of p-Vinylbenzyloxy Poly(Ethylene Oxide) (PEO-VB).....	83
3.1.2.3. Characterization of Random Copolymer (RPEO) of 3- Methylthienyl Methacrylate and p-Vinylbenzyloxy Poly(Ethylene Oxide).....	85
3.1.2.3.1. GPC Studies of RPEO .....	85
3.1.2.3.2. HNMR Studies of RPEO .....	85
3.1.2.3.3. FTIR Study of RPEO.....	87
3.1.2.4. Copolymers of RPEO with Pyrrole (RPEO-co-PPy).....	88
3.1.2.4.1. FTIR Study of RPEO-co-PPy .....	88
3.1.2.4.2. Cyclic Voltammetry Study of RPEO-co-PPy .....	90
3.1.2.4.3. Morphologies of RPEO-co-PPy Films .....	91
3.1.2.4.4. Conductivity Measurements of RPEO-co-PPy .....	93
3.1.2.5. Copolymers of RPEO with Thiophene.....	93
3.1.2.5.1. FTIR Study of RPEO-co-PTh .....	94
3.1.2.5.2. Cyclic Voltammetry Study of RPEO-co-PTh.....	95

3.1.2.5.3. Morphologies of the RPEO-co-PTh Films .....	95
3.1.2.5.4. Conductivity Measurements of RPEO-co-PTh.....	96
3.1.2.5.5. Electrochromic Studies of RPEO-co-PTh .....	96
3.2. Enzyme Immobilization Studies.....	99
3.2.1. Immobilization of Alcohol Oxidase.....	99
3.2.1.1. Protein Determination for AOX.....	100
3.2.1.2. Kinetic Studies of Free and Immobilized AOX.....	101
3.2.1.3. Influence of Temperature on the AOX Activity .....	102
3.2.1.4. Influence of pH on the AOX Activity .....	104
3.2.1.5. Operational Stability and Shelf Life of the AOX Electrodes .....	106
3.2.2. Immobilization of Polyphenol Oxidase .....	109
3.2.2.1. Protein Determination for Polyphenol Oxidase.....	109
3.2.2.2. Kinetic Studies for Polyphenol Oxidase .....	109
3.2.2.3. Influence of Temperature on the PPO Activity .....	110
3.2.2.4. Influence of pH on the AOX Activity.....	111
3.2.2.5. Operational Stability and Shelf Life of the PPO Electrodes.....	114
3.2.2.6. Determination of Total Phenolic Amount in Red Wines .....	117
4. CONCLUSION .....	118
REFERENCES .....	120
VITA .....	132

## LIST OF FIGURES

Figure 1.1. Common conducting polymers. ....	4
Figure 1.2. The conductivity range .....	5
Figure 1.3. The $\pi$ -system model.....	6
Figure 1.4. Molecular orbital (MO) diagram.....	7
Figure 1.5. Energy level diagrams for three types of solids .....	8
Figure 1.6. Neutral and Doped Forms of Polyacetylene .....	10
Figure 1.7. Band Structures of a) Neutral Polymer b) Lightly Doped Polymer c) Heavily Doped Polymer.....	11
Figure 1.8. Bipolarons of Polythiophene.....	11
Figure 1.9. Polaron and Bipolaron of Polypyrrole.....	12
Figure 1.10. Electrochemical Polymerization of Conducting Polymers .....	14
Figure 1.11. Electrochemical polymerization mechanism of pyrrole .....	18
Figure 1.12. Cyclic voltammograms of a) triangular potential waveform and b) current/potential response. ....	19
Figure 1.13. Cyclic voltammogram of ferrocene (5 mM in LiClO <sub>4</sub> (0.2 M)/ACN). The inset shows the definition of scan rate.....	20
Figure 1.14. Plot of initial velocity against substrate concentration for enzyme catalyzed reaction.....	31
Figure 1.15. Lineweaver- Burk plot.....	32
Figure 1.16. Principal methods of immobilization .....	34
Figure 1.17. Enzyme immobilization by electropolymerization.....	40
Figure 1.18. Schematic representation of polyphenol oxidase activity .....	43
Figure 1.19. Catalytic cycle for the hydroxylation of monophenol to o-diphenol (I) and dehydrogenation of o-diphenol to o-quinones (II) by tyrosinase.....	44
Figure 2.1. H-shaped electrolysis cell .....	54

Figure 2.2. Cyclic voltammetry cell.....	55
Figure 2.3. Four- probe conductivity measurement. ....	58
Figure 2.4. Synthesis route of p-vinylbenzyloxy poly(ethylene oxide) (ThPEO- VB) .....	61
Figure 2.5. Synthesis route of random copolymer (RPEO) of 3-methylthienyl methacrylate and p-vinylbenzyloxy poly(ethyleneoxide).....	62
Figure 2.6. Assay reactions of PPO .....	66
Figure 3.1. Chemical synthesis route of thiophene ended poly (ethylene oxide) (ThPEO).....	70
Figure 3.2. <sup>1</sup> HNMR spectrum of ThPEO. ....	71
Figure 3.3. FTIR spectrum of ThPEO.....	72
Figure 3.4. Cyclic voltammogram of ThPEO.....	73
Figure 3.5. Electrochemical synthesis route for copolymerization of ThPEO-co- PTh.....	74
Figure 3.6. FTIR spectrum of ThPEO-co-PTh in AN-TBABF medium.....	75
Figure 3.7. Cyclic voltammograms of a) PTh, b) ThPEO-co-PTh .....	75
Figure 3.8. Scanning electron micrographs of a) ThPEO-co-PTh (electrode side), b)ThPEO-co-PTh (solution side) .....	76
Figure 3.9. Spectroelectrochemical studies on ThPEO-co-PTh (a: 1.0 V; b: 0.9 V; c: 0.8 V; d: 0.6 V; e: 0.4 V; f: 0.2 V).....	77
Figure 3.10. CIE color space .....	78
Figure 3.11. Photographs of a) reduced state of ThPEO-co-PTh and b) oxidized state of ThPEO-co-PTh .....	79
Figure 3.12. Electrochemical synthesis route for copolymerization.....	79
Figure 3.13. FTIR spectrum of ThPEO-co-PTh in water-SDS medium.....	80
Figure 3.14. Cyclic voltammograms of a) PPy, b) ThPEO-co-PPy.....	81
Figure 3.15. Scanning electron micrographs of a) ThPEO-co-PPy (electrode side), b) ThPEO-co-PPy (solution side). ....	82
Figure 3.16. <sup>1</sup> HNMR spectrum of PEO-OVB. ....	84
Figure 3.17. <sup>1</sup> HNMR spectrum of RPEO .....	86
Figure 3.18. FTIR spectrum of RPEO.....	87
Figure 3.19. Electrochemical synthesis route for RPEO-co-PPy .....	88

Figure 3.20. FTIR spectrum of RPEO-co-PPy in water-SDS medium.....	89
Figure 3.21. FTIR spectrum of RPEO-co-PPy in water-PTSA medium .....	90
Figure 3.22. Cyclic voltammograms of a) RPEO-co-PPy and b) PPy.....	91
Figure 3.23. SEM micrographs of (a) electrode side of RPEO-co-PPy; (b) solution side of RPEO-co-PPy in water-PTSA medium. ....	92
Figure 3.24. SEM micrographs of (a) electrode side of RPEO-co-PPy; (b) solution side of RPEO-co-PPy in water-SDS medium.....	92
Figure 3.25. Electrochemical synthesis route for RPEO-co-PTh .....	93
Figure 3.26. FTIR spectrum of RPEO-co-PTh in AN-TBAFB medium .....	94
Figure 3.27. Cyclic voltammograms of a) PTh and b) RPEO-co-PTh .....	95
Figure 3.28. SEM micrographs of (a) electrode side of RPEO-co-PTh; (b) solution side of RPEO-co-PTh in AN-TBAFB medium. ....	96
Figure 3.29. Spectroelectrochemical spectrum of RPEO/PTh (a: 0.2 V, b: 0.4 V, c: 0.5 V, d: 0.6 V, e: 0.7 V, f: 0.8 V, g: 1.0 V, h: 1.2 V, i: 1.4 V).....	98
Figure 3.30. The photographs of a) reduced state of RPEO-co-PTh and.....	98
Figure 3.31. Reaction scheme for the enzymatic measurement of primary alcohols .....	99
Figure 3.32. Calibration curve for Jansenn’s Method .....	100
Figure 3.33. Calibration curve for protein determination.....	100
Figure 3.34. Effect of incubation temperature on alcohol oxidase activity for free enzyme (◆); PPy/AOX (■) and RPEO-co-PPy/AOX (▲) in a) methanol; b) ethanol; c) n-propanol.....	103
Figure 3.35. Effect of pH on alcohol oxidase activity for free enzyme (◆); PPy/AOX (■) and RPEO-co-PPy/AOX (▲) in a) methanol; b) ethanol; c) n-propanol .....	105
Figure 3.36. Operational stabilities of PPy/AOX (◆) and RPEO-co-PPy/AOX (■) electrodes in a) methanol; b) ethanol; c) n-propanol.....	107
Figure 3.37. Shelf life of PPy/AOX (◆) and RPEO-co-PPy/AOX (■) electrodes in a) methanol; b) ethanol; c) n-propanol. ....	108
Figure 3.38. Calibration curve for Besthorn’s Hydrazone method.....	109
Figure 3.39. Temperature dependence of a) ThPEO enzyme electrode,.....	111

Figure 3.40. pH dependence of a) ThPEO enzyme electrode, b) RPEO enzyme electrode.....	113
Figure 3.41. Operational stability of a) ThPEO enzyme electrode, b) RPEO enzyme electrode.....	115
Figure 3.42. Shelf life of a) ThPEO enzyme electrode, b) RPEO enzyme electrode.....	116

## LIST OF TABLES

Table 1.1. Comparison between inorganic materials and conducting polymers ...	25
Table 1.2. Applications of immobilized enzymes.....	41
Table 3.1. Synthesis of 3-thiophene-ended polyethyleneoxide .....	73
Table 3.2. Electrochemical, electronic and electrochromic properties of PTh and ThPEO-co-PTh.....	78
Table 3.3. The <sup>1</sup> HNMR spectrum of 3-methylthienyl methacrylate.....	83
Table 3.4. <sup>1</sup> HNMR peaks of (PEO-OVB). .....	84
Table 3.5. Preparation of random copolymer (RPEO) of 3-methylthienyl methacrylate and PEO –VB .....	85
Table 3.6. <sup>1</sup> HNMR peaks of RPEO.....	86
Table 3.7. Electrochemical, electronic and electrochromic properties of PTh and RPEO/PTh.....	97
Table 3.8. Kinetic parameters for free and immobilized alcohol oxidase for methanol, ethanol and n-propanol substrates .....	102
Table 3.9. Kinetic parameters for free and immobilized PPO.....	111
Table 3.10. Total phenolics in two different red wines, determined by the two enzyme electrodes .....	117

## ABBREVIATIONS

- ThPEO : Thiophene ended poly(ethylene oxide)  
RPEO : Random copolymer of 3-methylthienyl methacrylate and *p*-vinylbenzyloxy poly(ethylene oxide)  
PANI : Polyaniline  
PA : Polyacetylene  
EDOT : 3,4-ethylenedioxythiophene  
PEDOT : Poly(3,4-ethylenedioxythiophene)  
BFEE : Borontriflouride diethyletherate  
TBAFB : Tetrabutylammonium tetraflouroborate  
AN : Acetonitrile  
EO : Ethyleneoxide  
SDS : Sodiumdodecyl sulfat  
PTSA : *p*-Toluenesulfonic acid  
NMR : Nuclear magnetic resonance spectroscopy  
FTIR : Fourier transform infrared spectroscopy  
CV : Cyclic voltammetry  
SEM : Scanning electron microscopy  
AIBN :  $\alpha,\alpha$ -Azobisisobutylnitrile  
VBCl : *p*-Vinylbenzyl chloride  
DCM : Dichloromethane  
TEA : Triethylamine  
Py : Pyrrole  
PPy : Polypyrrole  
Th : Thiophene

PTh : Polythiophene  
CB : Conduction band  
VB : Valence band  
PPO : Polyphenol oxidase  
AOX : Alcohol oxidase  
POD : Peroxidase  
MBTH : 3-Methyl-2-benzothiozolinone  
MO : Molecular orbital  
RNA : Ribonucleic acid  
HOMO : Highest occupied molecular orbital  
LUMO : Lowest occupied molecular orbital  
 $E_g$  : Band gap energy  
CIE : La Commission Internationale de L'Eclairage  
L a b : Luminance, hue, saturation  
EC : Commission on Enzymes of the International Union of Biochemistry

## **CHAPTER 1**

### **INTRODUCTION**

#### **1.1. Conducting Polymers**

Polymers are normally thought of as insulators. Examples include cable insulation, valve bases, capacitor dielectrics and housing equipment. In the last decade however, a rapidly advancing field has been developed on the basis of the ability of certain polymers to conduct charge. The principal reason of wide application of polymers in electronics is due to being good dielectric materials with readily controllable properties. More recently, polymers with additional intrinsic properties have been developed such as intrinsically conducting polymers exhibiting not only conductivities similar to metals but also the processability of traditional polymers [1].

##### **1.1.1. Brief History of Conducting Polymers**

The field of conducting polymers has expanded exponentially since the first discovery of high conductivity in a plastic, doped polyacetylene, in 1977 [2]. This notorious work has spawned an entire arena of scientific research. Fortunately, this massive area has been extensively reviewed [3-7]. In the year 2000, twenty-three years after the first experiment demonstrating that certain plastics conduct electricity, the Nobel Prize was awarded to Alan J. Heeger, Alan G. MacDiarmid, and Hideki Shirakawa for “the discovery and development of conducting polymers” [8, 9]. In his Nobel Lecture, Alan Heeger

offers two brief explanations for the importance of the discovery of conducting polymers: 1. “they didn’t exist before,” and 2. “they offer a unique combination of properties not available from any other known materials.” The first simplistic statement embodies the academic curiosity that has attracted so many researchers in a list of varying disciplines, including chemists, physicists, and materials scientists, to study these fascinating polymers. The second explanation encompasses the potential use of conducting polymers in a vast number of applications by replacing old materials and by developing new technologies based on their unique and unprecedented abilities. The commercialization of conducting polymer technologies has now arrived. Today, they can be found as electrode materials for solid-state electrolyte capacitors [10] and antistatic coatings in photographic film. A plethora of industrial companies are racing to develop a number of new products that take advantage of the unique properties of conducting polymers. The last three decades have been an exciting time of discovery. Within the next three decades, conducting polymers will likely be ubiquitous in our daily lives.

Polyacetylene is one of the most studied conducting polymers of today. It can be viewed as the simplest conjugated polymer and has been studied extensively since the initial reports of high conductivity doped complexes in 1977 [11, 12]. Polyacetylene serves as a model for developing both the electronic and physical properties of electronically conducting polymers with unique properties in both its reduced semi-conducting and highly doped conducting forms. Polyacetylene is highly crystalline, which has allowed direct analysis of both the doped and undoped forms [13-18].

Polythiophenes (PThs) have received a great deal of attention due to their electrical properties, environmental stability in doped and undoped states, non-linear optical properties, and highly reversible redox switching [19]. Thiophene possesses a rich synthetic flexibility, allowing for the use of several polymerization methods and the incorporation of various side chain functionalities. Thus, it is of no great surprise that polythiophenes have become the most widely studied of all conjugated polyheterocycles [20]. The polymerization of thiophene, to yield interactable polythiophene, was first

carried out in a controlled manner in the early 1980s [21-24]. Even in such an unyielding form, this polymer displayed many promising optical and electronic properties.

Comparable to thiophene, pyrrole is a five-membered heterocycle, yet the ring nitrogen results in a molecule with distinctly different behavior and a far greater tendency to polymerize oxidatively. The first report of the synthesis of polypyrrole (PPy) that alluded to its electrically conductive nature was published in 1968 [25]. This early material was obtained via electrochemical polymerization and carried out in 0.1 N sulfuric acid to produce a black film. Since this date, a number of improvements, which have resulted from in-depth solvent and electrolyte studies, have made the electrochemical synthesis of polypyrrole the most widely employed method [26-28]. The properties of electrosynthesized polypyrrole are quite sensitive to electrochemical environment in which it is obtained. The use of various electrolytes yields materials with pronounced differences in conductivity, film morphology, and overall performance [29-32]. Furthermore, the water solubility of pyrrole allows aqueous electrochemistry [33], which is prime importance for biological applications [34].

Polyaniline (PANI) is perhaps the oldest of the conducting polymers. Reference dating back to 1862 can be found describing a material known as aniline black [35]. A few reports surfaced on polyaniline in the 1960s [36-38], most notably a study investigating the effects of acids on conductivity of polyaniline [39], but it was not until the 1980s that its electrically conducting properties became fully appreciated [40]. Polyaniline has become an extremely well-studied conducting polymer, due to its low cost and remarkable stability under variety of conditions [41, 42]. This has resulted in polyaniline being the conjugated polymer choice for many technological applications and led to its development as a commercial product.

In the late 1970s Heeger and MacDiarmid found that polyacetylene  $[(CH)_n]$  produced by Shirikawa's method exhibited a 12 order of magnitude increase in electrical conductivity when exposed to oxidizing agents. Since that discovery, a vast array of other conducting polymers has been synthesized.

Structures of repeating units of several conjugated polymers; polyacetylene (PA), polyaniline (PANI), polypyrrole (Ppy), polythiophene (PTh), poly(3,4-ethylenedioxythiophene) (PEDOT) are shown in Figure 1.1.

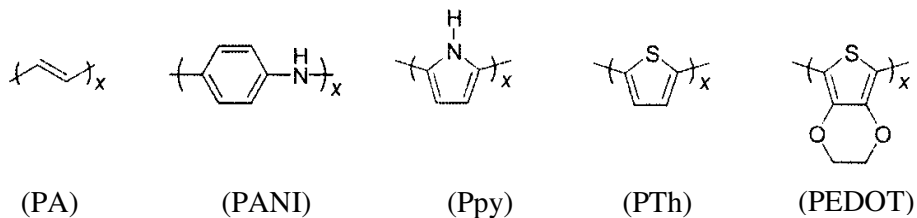


**Figure 1.1.** Common conducting polymers.

### 1.1.2. Applications of Conducting Polymers

The applications of conducting polymers can be divided into three main classes. The first use is in their neutral form, which provides the advantage of their semi-conducting and luminescent properties. Examples of applications are semiconducting materials for field effect transistors [43] and active material in an electroluminescent device [44, 45]. The second category of applications involves using the polymer in its doped or conducting form, and some representative applications in this category are electrostatic charge dissipation and EMI shielding [46, 47], electrode materials for capacitors [48, 49] and enzyme immobilization [48-50]. The third category uses the ability of polymer to reversibly switch between its conducting and reduced forms. Upon switching between two states, the polymer undergoes color, conductivity, and volume changes. Applications that use these properties include battery electrodes [51], actuators [52], sensors [53], drug delivery [54], electrochromics [55-58]. Of these applications, the use conducting polymers as enzyme immobilization matrices are the most pertinent to the work in this thesis.

### 1.1.3. Conductivity Mechanism in Conducting Polymers

#### 1.1.3.1 Conductivity and Band Theory

Conducting polymers offer a unique property in that their conductivity can be turned over eight or more orders of magnitude in the same material. Figure 1.2 shows the typical conductivity ranges. The three most common conducting polymers (polyacetylene, polypyrrole and polythiophene) shown span the range of conductivities from metal to insulator depending level for materials commonly considered metals, semiconductors and insulators although the factor that determines this classification is really the temperature dependence of conductivity rather than the conductivity magnitude.

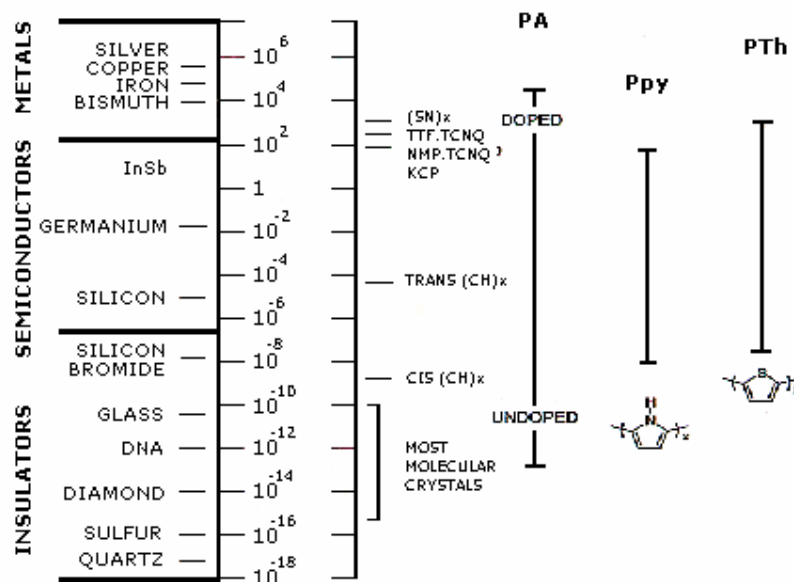
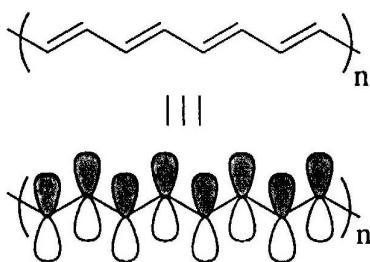


Figure 1.2. The conductivity range.

### 1.1.3.2. Band Theory

Apart from polyaniline, all of these systems share one common structural feature, namely a rigid nature brought about by the  $sp^2$  carbon-based backbone. The utilization of the conjugated construction affords polymer chains possessing extended  $\pi$ -systems, and it is this feature alone that separates conducting polymers from their other polymeric counterparts. Using this generic, lowest energy (fully bonding) molecular orbital (MO) representation as shown by  $\pi$ -system model, the picture of primary concern that is generated by these networks consists of a number of  $\pi$  and  $\pi^*$  levels (Figure 1.3). However, unlike the discrete orbitals that are associated with conjugated organic molecules, the energies of the polymers' MOs are so close so in energy that they are indistinguishable. In fact, for long chains orbital separation is so small that band formation occurs as illustrated by the MO diagram (Figure 1.4).



**Figure 1.3.** The  $\pi$ -system model

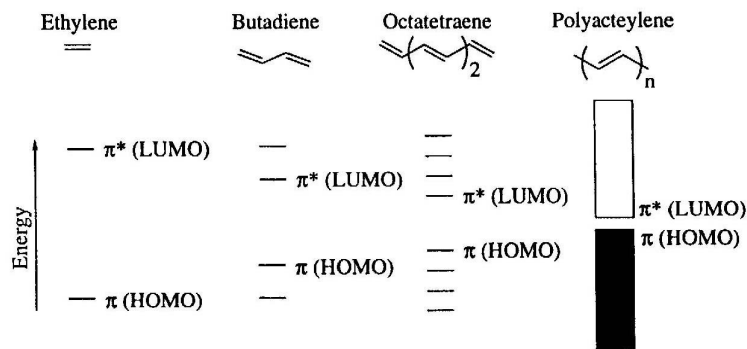


**Figure 1.4.** Molecular orbital (MO) diagram.

The electrical properties of any material are a result of the material's electronic structure. The presumption that conducting polymers form bands through extensive molecular orbital overlap leads to the assumption that their electronic properties can be explained by band theory. With such an approach, the bands and their electronic population are the chief determinants of whether or not a material is conductive. Here, materials are classified as one of three types shown in Figure 1.5., being metals, semiconductors, or insulators. Metals are materials that possess partially-filled bands, and this characteristic is the key factor leading to the conductive nature of this class of materials. Semiconductors, on the other hand, have filled (valence bands) and unfilled (conduction bands) bands that are separated by a range of forbidden energies (known as the "band gap"). The conduction band can be populated, at the expense of the valence band, by exciting electrons (thermally and or photochemically) across this band gap. Insulators possess a band structure similar to semiconductors except here the band gap is much larger than and inaccessible under the environmental conditions employed.

Conducting polymers in their neutral state are insulators or, at best, weak semiconductors. Hence, there is enough of an energy separation

between the conduction band and valence bands that thermal energy alone is insufficient to excite electrons across the band gap. To explain the conductive properties of these polymers, several concepts from band theory and solid state physics have been adopted. For electrical conductivity to occur, an electron must have vacant place (a hole) to move and occupy. When bands are completely filled or empty, conduction can not occur. Metals are highly conductive because they possess unfilled bands. Semiconductors possess an energy gap small enough that thermal excitation of electrons from the valence to conduction bands is sufficient for conductivity; however, the band gap in insulators is too large for thermal excitation of an electron across the band gap.

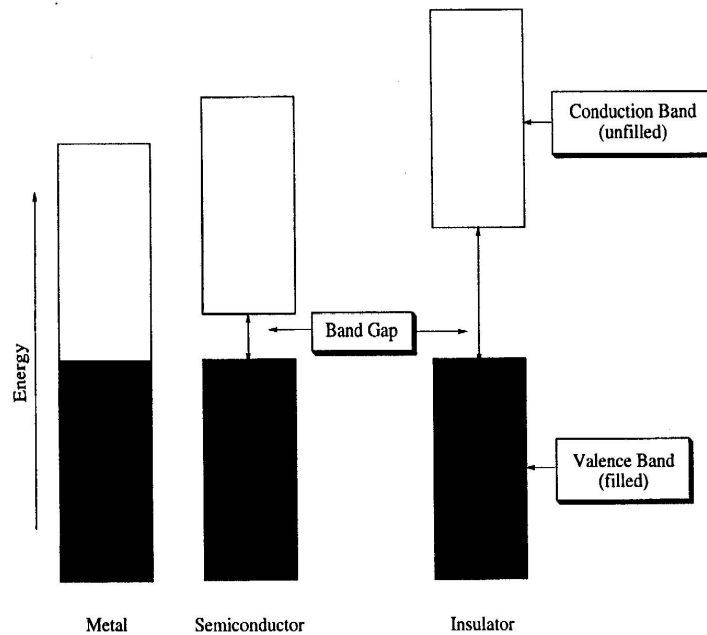


**Figure 1.5.** Energy level diagrams for three types of solids.

### 1.1.3.3. Doping and Electrical Conductivity

So, we can ask that how this more than 8 order of magnitude increase in electrical conductivity for polyacetylene occurs. The diffuse of the extended  $\pi$ -system readily allows electron removal from, or injection, into the polymer. The term 'doping' has been borrowed from semiconductor physics with 'p-doping' and 'n-doping' being used to describe polymer oxidation and reduction, respectively. Doping in regards to semiconductors is quite different, as it is a very distinct process carried out at low levels 1% as compared to conducting polymers doping (usually 20-40%). However, the manner by which doping transforms a neutral conducting polymer into a conductor remained a mystery for many years.

Electron Paramagnetic Resonance (EPR) studies have shown that both neutral and heavily doped conducting polymers possess no net spin, interpreted as no unpaired electrons, while moderately doped materials were discovered to be paramagnetic in nature. Conducting experiments showed that it was the 'spin-less' heavily doped form that is the most conductive for a given conducting polymer. Such behavior marks an abrupt departure from simple band theory, which centers around spin-containing charge carries.

Polyacetylene turns out to be a special case when considering its neutral and dopes forms. Comparison of the two neutral forms, shown in Figure 1.6, reveals them to be structurally identical, and thus, their ground states are degenerate in energy. Two successive oxidations on one chain yield radical cations that, upon radical coupling, become non-associated charges termed positive 'solitons'.

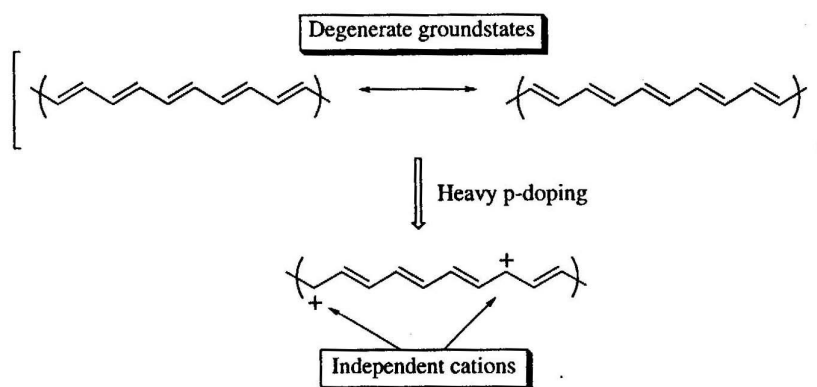


**Figure 1.6.** Neutral and Doped Forms of Polyacetylene.

In contrast to polyacetylene, the other conducting polymers shown in Figure 1.2 has no degenerate ground states (i.e. they do not have two equivalent resonance forms), and thus, do not show evidence of soliton formation. In this example, the oxidation of the conducting polymer is believed in destabilization (raising of the energy) of the orbital from which the electron is removed. Energy of this orbital is increased and can be found in energy region of the band gap as shown in Figure 1.7. Initially, if only one electron level is removed, radical cation is formed and is known as a 'polaron' (Figure 1.7b). Further oxidation removes this unpaired electron yielding a dicationic species termed a 'bipolaron' (Figure 1.7c). High dopant concentrations create a bipolaron-'rich' material and eventually lead to band formation of bipolaron levels. Such a theoretical treatment, thereby, explains the appearance, and subsequent disappearance, of the EPR signal of a conducting polymer with increased as the neutral polymer transitions to the polaronic form and subsequently to the spinless bipolaronic state [59].

Contrary to independent charges of polyacetylene, the bipolaron unit remains intact and entire propagates along the polymer chain. Figure 1.8 shows this behavior using polythiophene as the example. In the case of unsubstituted polythiophene, the bipolaronic unit is believed to spread over six to eight rings. This ‘bipolaron length’ is by no means an absolute number as different polymer backbone and substituent types yield various lengths [60]. Figure 1.9 shows the polaron and bipolaron unit of polypyrrole.

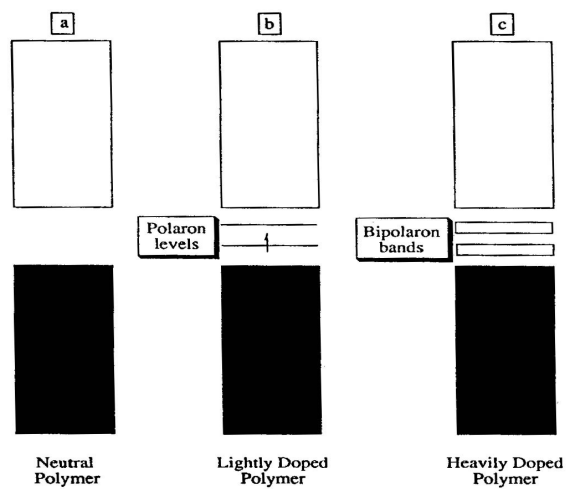


**Figure 1.7.** Band Structures of a) Neutral Polymer b) Lightly Doped Polymer c) Heavily Doped Polymer.

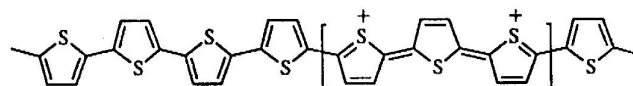


**Figure 1.8.** Bipolarons of Polythiophene.

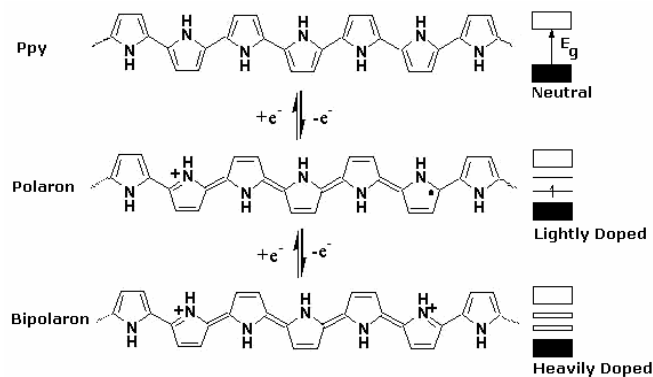


**Figure 1.9.** Polaron and Bipolaron of Polypyrrol.

#### 1.1.3.4 Hopping Process

The conduction process is well described by a variable range hopping process in which electrons are localized on individual monomer rings. The hopping process produces a generous supply of potential carriers. There are mainly three types of transport for the carrier mobility; single chain or intramolecular transport, interchain transport, interparticle transport. These three show a resistive network determining the effective mobility of the carriers. Thus, the mobility and therefore, conductivity are determined on both a macroscopic (interparticle) and microscopic (intra and interchain) level.

#### 1.1.4. Synthesis of Conducting Polymers

Synthesizing new and novel structures, increasing the order of the polymer backbone (and also conductivity), good processability, easier synthesis, more defined three dimensional structure, stability in both conducting and non-conducting states, solubility in certain solvents such as water and many other application unique properties are some of important targets in conducting polymer synthesis. The synthesis of conducting polymers is divided in two categories: chemical polymerization and electrochemical polymerization. Many

conducting polymers can be synthesized by both chemical and electrochemical methods [61, 62].

#### **1.1.4.1. Chemical Polymerization**

In chemical synthesis, monomers are polymerized using appropriate catalysis or reagents. The morphological, physical and electrochemical properties are influenced by reaction conditions such as the species and concentrations of catalyst, reagents and solvent, the monomer concentration, the reaction temperature and so on. Chemical synthesis is considered to be suitable for producing large amounts of homogeneous polymer [63].

Oxidative chemical polymerization is the least expensive, simple and most widely used chemical synthesis of conducting polymers [64]. In this method, a stoichiometric amount of oxidizing reagent is used to form polymer that is in its doped or conducting form.

Heterocyclic monomers are usually polymerized with  $\text{FeCl}_3$  as the chemical oxidant [65, 66] although other oxidants can also be used. Reduction to neutral state is accomplished by addition of strong base such as ammonium hydroxide or hydrazine. Benzene can also undergo oxidative polymerization with  $\text{AlCl}_3/\text{CuCl}_2$  to yield poly(p-phenylene).

#### **1.1.4.2. Electrochemical Polymerization**

Electrochemical polymerization is an efficient method for synthesizing smooth polymer films on conductive substrates, and it allows for easy probing of electrical and optical properties. It represents one of the simplest and most straightforward methods for elaboration of modified electrodes in which inherent electrochemical and optical properties of the conjugated polymer backbone of polymers are associated with specific properties afforded by covalently bound functional groups. In this procedure, the oxidation potential at which the system polymerizes is well defined and finely controlled and the

properties of the deposited polymer allows for the preparation of a variety of different conducting polymers prepared from the same monomer system by simply varying specific electrochemical parameters such as applied potential electrolyte, temperature, electrode [67].

The electrochemical synthesis of polyheterocyclics can be made with anodic oxidation or cathodic coupling. Anodic process provides the oxidation of monomer to a polymer with proton elimination whereas the cathodic one is based on the reduction of the dihalogen-substituted (usually dibromo substituted) monomer to a polymer with halogenide release. Anodic coupling is preferred because it uses the unmodified monomer and the polymer, being more easily oxidized (doped), is produced in the conductive state and therefore, allows the continuous deposition of the material up to considerable thickness. This method is used for polymers such as polypyrrole and polythiophene. When anodic one is precluded by the non-oxidizability of the monomer, the occurrence of demolitive oxidation in the course of coupling or when the requirement of definite positions of coupling are not guaranteed by highly selective spin densities in the radical cation, cathodic coupling is used. Moreover, this technique has the advantage of being applicable to electrode materials subject to anodic corrosion such as small band gap semiconductors.

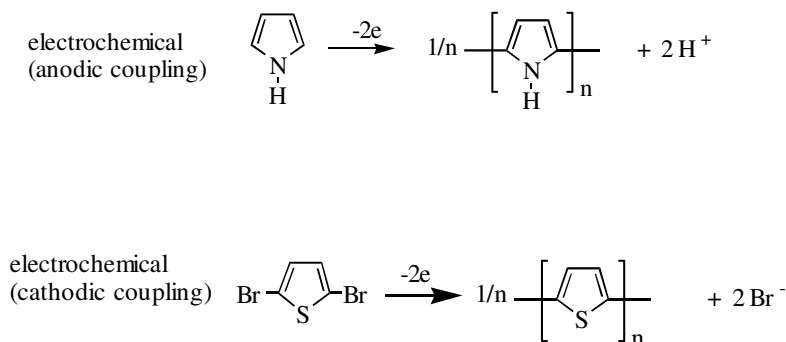


**Figure 1.10.** Electrochemical Polymerization of Conducting Polymers.

### 1.1.4.3. Effects of Electrosynthesis Conditions

Electropolymerization involves many experimental variables such as solvent, monomer concentration, electrolyte type, temperature, electrode material and applied electrical conditions.

The solvent must be of sufficiently high dielectric constant to ensure the ionic conductivity of the electrolytic medium, i.e., to dissolve and dissociate the supporting electrolyte, and possess a potential window open at the potential required to oxidize or reduce the monomer. The degree of nucleophilicities of solvent and electrolyte is very important because polymerization reaction is sensitive to the nucleophilicity of the environment in the region of the electrode surface due to the presence of radical cation intermediates.

The monomer concentration is generally high (0.1 M or more) to avoid competitive reactions of the radical cations or of the oxidized polymer with nucleophiles in the medium, but this parameter mostly depends on the oxidation potential of the monomer. As the monomer is more easily oxidized the competition of parasitic reactions decreases so that even millimolar concentration may be used for efficient electropolymerization.

The type of supporting electrolyte, and the particularly the anion in the case of anodic coupling, is most important. The anion part of the electrolyte must be 'innocent' type such as perchlorate, tetrafluoroborate or hexafluorophosphate.

The working electrode material should be so selected that it does not get oxidized concurrently with the monomer. To enable this condition, anodes are made from inert conducting materials such as platinum, Indium-Tin Oxide (ITO), gold and titanium. The cathode may be any suitable metal such as copper, stainless steel, aluminum, platinum and gold.

The decrease in conductivity observed in the material with use of potentials or current densities beyond the optimum is related to the fact that poly(heterocycle)s are overoxidized at the potentials used for their formation

[68, 69]. The degradation of the polymer may compete with its electrodeposition at highly anodic potentials or when the monomer concentration in the medium becomes too low to sustain the rate of polymer deposition imposed by the applied electrical conditions [70].

### **1.1.5. Mechanism of Electrochemical Polymerization**

Most of the conjugated polymers are synthesized by electrochemical means. Electropolymerization is accomplished by placing the monomer in a suitable solvent-electrolyte medium and oxidizing at a mild potential. A polymer film grows at the anode in a reaction that is thought to occur as illustrated in Figure 1.11.

The proposed electrochemical polymerization of pyrrole starts with the formation of radical near the electrode resulted from the oxidation of the monomer at the appropriate electrode potential. Monomer has a higher oxidation potential than that of dimers and oligomers. Thus, the generation of monomer radical cation is slow, but the radical-radical coupling, deprotonation and subsequent oxidation are fast [71]. The polymerization proceeds via radical-radical coupling mechanism, chain growth then continues until the charge on the chain is such that a counterion is incorporated [72]. Eventually, the solubility limit is exceeded and the polymer precipitates on the electrode surface. The initial layer of polymer deposited on the electrode surface plays an intricate role in determining the remainder of the structure. The initial layer becomes a reactant and determines the course of the remainder of polymerization process. On the other hand, electrochemical conditions such as the electrode material, the solvent, the counter ion, and the monomer itself also influence the nature of the process occurring.

Figure 1.11 represents the proposed mechanism of polymerization. It is known that polymerization starts from 2,5 positions of pyrrole monomers (1.11b). Then the reaction proceeds with the elimination of two protons (1.11c). This process is followed by the oxidation of one of the pyrrole units of dimer (1.11d), which then combines with another radicalic monomer cation (1.11e)

and the trimer is formed (1.11f). As mentioned before, the dimer formation starts via  $\alpha$ - $\alpha$  coupling, but further polymerization allows also  $\alpha$ - $\beta$  and  $\beta$ - $\beta$  linkages [73]. As a result, a crosslinked polymer is obtained. Figure 1.11g represents idealized structure of polypyrrole. However, it has been mentioned that after dimer formation polymerizations through 3 and 4 positions have comparable formation enthalpies, thus, the polymer grows from both  $\alpha$ - and  $\beta$ -positions. These couplings do not extend conjugation; actually, branching of this type reduces the conjugation length of the main chain of the polymer [74].

The anion is incorporated into polymer to ensure the electrical neutrality of the film (Figure 1.11g). Generally it originates from the anion of the supporting electrolyte and act as the dopant. Furthermore, some scientists estimate that counter ion also plays an important role during the polymerization process [75]. It not only balances the charge on the polypyrrole main chain, but also stabilizes the cation radicals formed during polymerization process.

#### **1.1.6. Electrochemical Methods**

Electrochemical methods are very useful established for the synthesis of conducting polymers as well as allowing unique characterization information. Cyclic voltammetry, constant current and constant potential methods are utilized extensively to study monomers and polymers electrochemically.

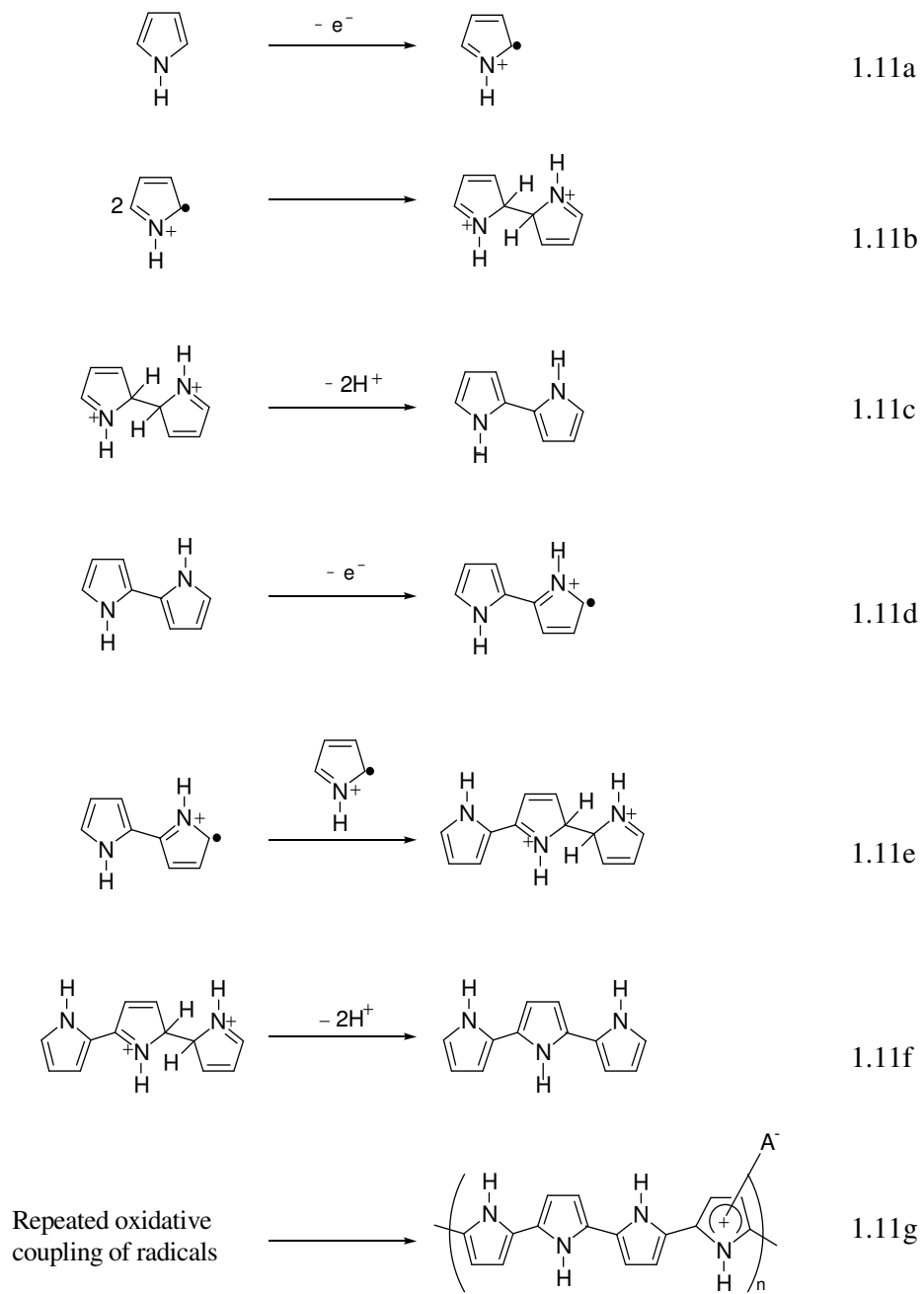


**Figure 1.11.** Electrochemical polymerization mechanism of pyrrole.

### 1.1.6.1 Cyclic Voltammetry

Cyclic voltammetry provides information about the properties and characteristics of electrochemical systems and also gives insight into any complicating side processes, electron transfer reactions, and kinetic properties. This method has been widely used to examine the redox behavior of surface-deposited electroactive films qualitatively as a function of specific experimental conditions (sweep rate, solution composition, pH, temperature, etc.).

In this method, a triangular potential waveform is the input and the current/potential response to this perturbation is monitored (Figure 1.12.).

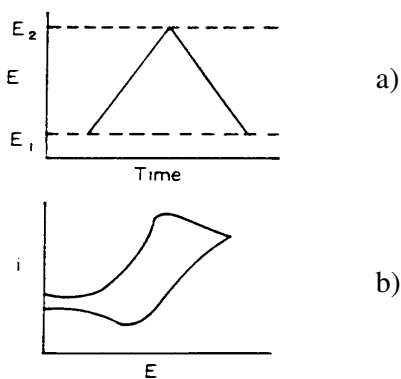


**Figure 1.12.** Cyclic voltammograms of a) triangular potential waveform and b) current/potential response.

In a typical experiment, the potential starts at a reducing value, and is scanned anodically until monomer oxidation and polymerization occurs.

Subsequently, the potential is scanned cathodically back to the original value, where the reduction of polymer which has deposited on the electrode occurs [76].

A typical voltammogram of a reversible process, standard ferrocene solution is shown in Figure 1.13. Reversibility involves the oxidized and reduced forms are in equilibrium and their concentrations can be predicted by the Nernst equation. A test for reversibility of the redox reaction is the difference in potential between the anodic ( $E_{p,a}$ ) and cathodic ( $E_{p,c}$ ) peaks are given with the following equation :

$$E_{p,a} - E_{p,c} = 2.203 RT/nF = 0.056/n \quad (1)$$

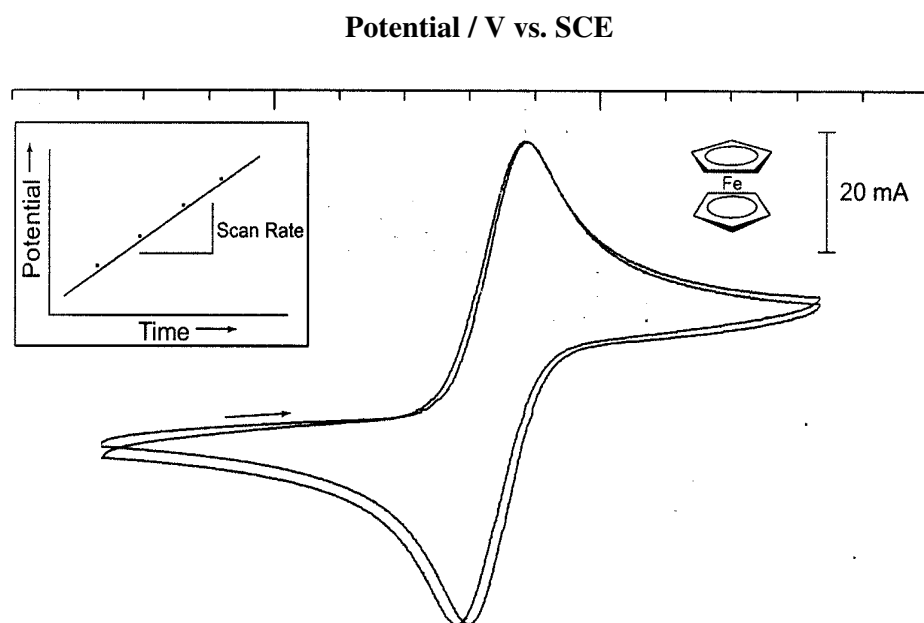


**Figure 1.13.** Cyclic voltammogram of ferrocene (5 mM in LiClO<sub>4</sub> (0.2 M)/ACN). The inset shows the definition of scan rate.

In ferrocene electrochemistry, a typical example for freely diffusing species, as the potential is increased, easily oxidized species near the electrode surface react, and a current response is measured. When the direction of the scan is reversed, the oxidized species near the electrode surface are reduced, and

again a current response is measured. The Randles-Sevcik equation [77] states that the peak current is given by

$$i_p = (2.69 \times 10^5) n^{3/2} A D^{1/2} C^b v^{1/2} \quad (2)$$

where  $n$  is the number of electrons in the reaction,  $A$  is the surface area of the electrode ( $\text{cm}^2$ ),  $D$  is the diffusion coefficient ( $\text{cm}^2\text{s}^{-1}$ ),  $C^b$  is the bulk concentration of the electroactive species ( $\text{mol cm}^{-3}$ ),  $v$  is the scan rate ( $\text{V s}^{-1}$ ). From this equation it can be concluded that for a diffusion-controlled system, the peak current is proportional to the square root of the scan rate in a reversible system. For these processes, it was assumed that the reactants and products are soluble in solution and the surface processes (adsorption of reactants and products) can be neglected. However, the rules change in electroactive polymer electrochemistry, because the polymer is adhered to electrode surface. Therefore, the process is not diffusion-controlled, and cannot be described by the Randles-Sevcik equation discussed above. Instead, the peak current for a surface bound species is given by the following equation [78]

$$i_p = n^2 F^2 \Gamma v / 4RT \quad (3)$$

where  $F$  is the Faradays constant and  $\Gamma$  is the concentration of surface bound electroactive centers ( $\text{mol cm}^{-2}$ ). Therefore, if a species is surface bound, both the anodic and cathodic peak current will scale linearly with scan rate.

The redox processes for films of conducting polymers in solution or on electrodes are rarely reversible because the extensive changes in polymer structure that occur on oxidative or reductive doping preclude compliance with the kinetic limitations of the Nernst equation.

CV method can also be used to electrochemically grow conducting polymer films. Typically the voltammograms obtained during film growth are irreversible but the CVs can possess the reversible redox responses of polymer upon subsequent scans. The deposition of electroactive polymer upon monomer oxidation increases the conductive surface area of the electrode, hence

increasing the current response. One of the disadvantages of this growth method is that overoxidation of the monomer or polymer can easily occur if scan limits are not set properly.

#### **1.1.6.2. Constant Current (Galvanostatic) Methods**

Constant-current, or controlled-current, electrolysis (CCE) is experimentally extremely simple. One simply passes a direct current of fixed magnitude between the anode and cathode for the necessary time. This may be done by using current sources either with a variable voltage in series with the cell (as resistor) or a fixed voltage source and a variable resistor. The major disadvantage of constant-current electrolysis is the lack of selectivity. All possible redox processes may take place since the electrode potential continually changes. Another disadvantage is that the involvement of species present in the system in addition to the monomer is inevitable. For that reason, complications may arise in initiation and propagation steps.

#### **1.1.6.3. Constant-Potential Methods**

Constant potential electrolysis is achieved with a three-electrode system. The potential of the working electrode (WE) with respect to a reference electrode (RE) is adjusted to a desired value and kept constant by a potentiostat while current is allowed to vary. The voltage between the working and the reference electrodes may be called the polymerization potential. By keeping the potential constant, creation of undesired species is prevented; therefore the initiation becomes selective, that is, through the monomer itself.

#### **1.1.7. Copolymers, Composites and Blends**

Conducting polymers are promising for commercial applications because of their facile synthesis, good environmental stability, and long term stability of electrical conductivity. However, several drawbacks restrict their processing and applications for practical uses. These films are insoluble, hard and brittle and have a variety of conductivity values depending on the electrolysis conditions.

In order to obtain a material suitable for applications in various technological fields certain limitations need to be overcome [79].

The formation of copolymers and composites is one of the most useful tools in polymer science in that the physical and mechanical properties of a polymer can be controlled and enhanced. To improve the mechanical and physical properties of conducting polymers is to synthesize block and/or graft copolymers involving conventional and conducting sequences [80-85]. In recent years, this tool has been employed for the study of conducting polymers such as polyacetylene [86], polypyrrole [87] and polythiophene [88]. These polymers and composites are important due to their resultant mechanical properties [89,90]. Electropolymerization of the conducting component on the electrode previously coated with the insulating polymer is a common approach for the preparation of conducting composites and copolymers. Several groups have reported that the electrochemical polymerization of pyrrole and thiophene may occur on an ordinary insulating polymer film [91, 92]. In these cases, monomer and solvent molecules and electrolyte anions swell the polymer film as they diffuse into the polymer coating and polymerization starts in the interface between the electrode surface and the insulating polymer film and finally a conducting polymer film is obtained.

Polycarbonate and polystyrene [93], poly(methylmethacrylate) [94], polyimide [95], polyamide [96], polysiloxanes [97], polytetrahydrofuran [98, 99] were previously used as the host matrices.

#### **1.1.8. Electrochromism and Electrochromic Materials**

Electrochromism is the property whereby a reversible change in the electronic state of a material induces color changes. As an electrochromic material undergoes electron transfer, new optical bands appear and the material exhibits coloration. Electron transfer in the opposite direction reverses the electrochemical process and the materials revert to the colorless state. The color change is commonly between a transparent (bleached) state and a colored state.

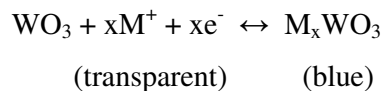
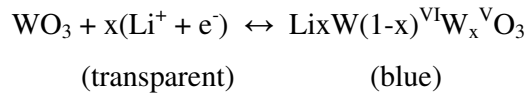
Electrochromic materials can be useful in various applications such as optical displays, automotive applications (e.g. dimming rear view mirrors) and

smart windows for buildings. Self dimming rear-view mirrors are designed to avoid dazzle from the headlights of a following car. This technology uses an electrochromic film to produce a mirror with variable specular reflectance. Most new luxury cars have adapted self dimming mirrors. Smart windows are designed to automatically control the amount of visible or infrared light entering a room when they are used in conjunction with thermal and optical sensing devices [100]. When electrochromic materials can control infrared emissivity, these also can be used for the thermal emittance control (e.g. infrared camouflage and aerospace) and optoelectronic devices [101].

### 1.1.8.1 Transition Metal Oxides (TMOs)

Oxide thin films of many transition metals such as iridium [102, 103], rhodium [104], ruthenium [105], tungsten [106, 107], manganese [108], etc have been reported to have electrochromic properties. These types of materials are classified as inorganic electrochromic materials.

Tungsten trioxide ( $\text{WO}_3$ ) has been the most commonly used electrochromic material. It changes its color from yellow to green in bulk form and has been studied since 1815 [109]. Tungsten oxide has a nearly cubic structure by  $\text{WO}_6$  octahedral that share corners. The empty space in the cube enables the insertion of guest ions interstitial sites. When all tungsten sites are in the oxidation state  $\text{W}^{\text{VI}}$ , the thin film is transparent. By electrochemical reduction,  $\text{W}^{\text{V}}$  sites are generated and induce blue coloration. The generally accepted mechanism for this process is the intercalation of metal cations such as  $\text{Li}^+$ ,  $\text{H}^+$ , etc. The electrochemical reaction with a  $\text{Li}^+$  cation is expressed by the following generalized equation.



Even though tungsten oxide has been utilized for smart windows, these windows have had little success because of the lifetime requirement (> 10 years) and their high price. The sputtering process on the glass substrate under vacuum is mainly responsible for the high cost of manufacturing [110]. Furthermore, TMOs show slow response times for obtaining full contrast.

### 1.1.8.2 Conducting Polymers as Electrochromic Materials

In recent years, conducting polymers have emerged as promising candidates for electrochromics. Conducting polymers are lightweight, mechanically flexible, exhibit dynamic color change at a low potential and offer low fabrication costs [111]. They also offer a high degree of color tailorability by modification of various polymer systems. This can be achieved by monomer functionalization or copolymerization as well as with the use of blends, laminates and composites. Table 1.1. gives a comparison between inorganic and polymeric electrochromic materials.

**Table 1.1.** Comparison between inorganic materials and conducting polymers

Property	Inorganic materials	Conducting polymers
Method of preparation	Needs sophisticated techniques such as vacuum evaporation, spray pyrolysis, sputtering, etc.	Easily prepared by simple chemical, electrochemical polymerization and the films can be obtained by simple techniques such as dip-coating, spin coating, etc.
Processibility	Poor	Can be processed easily
Cost for making device	High	Low compared to inorganic materials
Colors obtainable	Limited number of colors	Depends on the doping percentage, choice of the monomer, operating potential, etc. Hence, large number of colors are available with the polymeric materials
Contrast	moderate	Very high
Life time	$10^3 \sim 10^5$ cycles	$10^4 \sim 10^6$ cycles

The color changes elicited by doping are due to the modification of the polymer's band electronic structure. The undimensional character of the polymer system energetically favors the localization on the chain of the charge created by doping and the relaxation of the lattice around this charge. This confinement of the charge then creates the defects that produce in the gap new electronic states which cause the color changes. In polymers with a nondegenerate ground state and an aromatic-like structure the lattice relaxation is towards the quinoid structure and defects, polarons (single charged of spin  $\frac{1}{2}$ ) and bipolarons (double charges, spinless), are related to the amount of charge in the polymer, usually indicated as the doping level. As the doping level increases the bipolaron states overlap in bipolaron bands, and the bipolaron bands may merge with valence and conduction bands leading to metallic-like state.

Polyanilines, polypyrroles, and polythiophenes have been the most actively investigated systems for electrochromic properties [112-117]. Spectroelectrochemical techniques provide a practical method for reversibly doping and undoping conjugated polymers while simultaneously observing optical responses. In particular, small band-gap conjugated polymers have attractive intrinsic properties such as transparency in the doped state, stability for electrochemical doping process and significant absorption changes in the infrared/visible range by doping. Additionally, by modification of substituents of low band gap conducting polymers, the band gap can be changed further and provide a wide range of color changes within the visible spectrum. Unlike low band-gap conducting polymers, high band-gap polymers show the transparent state in the neutral state and color in the doped state. By adapting both polymers in the device, electrochromic devices with a dual polymer system have been fabricated for improved contrast.

## **1.2. Enzymes**

Life depends on a well-orchestrated series of chemical reactions. Many of these reactions, however, proceed too slowly on their own to sustain life. Hence nature has designed catalysts, which we now refer to as enzymes, to greatly accelerate the rates of these chemical reactions. The catalytic power of

enzymes facilitates life processes in essentially all life-forms from viruses to man. Many enzymes retain their catalytic potential after extraction from the living organism, and it did not take long for mankind to recognize and exploit the catalytic power of enzyme for commercial purposes. In fact, the earliest known references to enzymes are from ancient texts dealing with the manufacture of cheeses, breads, and alcoholic beverages, and for the tenderizing of meats. Today enzymes continue to play key roles in many food and beverage manufacturing processes and are ingredients in numerous consumer products, such as laundry detergents (which dissolve protein-based stains with the help of proteolytic enzymes). Enzymes are also of fundamental interest in the health sciences, since many disease processes can be linked to the aberrant activities of one or a few enzymes. Hence, much of modern pharmaceutical research is based on the search for potent and specific inhibitors of these enzymes. The study of enzymes and the action of enzymes has thus fascinated scientists since the dawn of history, not only to satisfy erudite interest but also because of the utility of such knowledge for many practical needs of society [118].

The macromolecular components of almost all enzymes are composed of protein, except for a class of RNA modifying catalysts known as ribozymes. Ribozymes are molecules of ribonucleic acid that catalyze reactions on the phosphodiester bond of other RNAs. Enzymes are found in all tissues and fluids of the body. Intracellular enzymes catalyze the reactions of metabolic pathways. Plasma membrane enzymes regulate catalysis within cells in response to extracellular signals, and enzymes of the circulatory system are responsible for regulating the clotting of blood. Almost every significant life process is dependent on enzyme activity.

### **1.2.1. Enzyme Classification**

Presently more than 2000 different enzymes have been isolated and characterized. The sequence information of a growing number of organisms opens the possibility to characterise all the enzymes of an organism on a genomic level. The smallest known organism, *Mycoplasma genitalium*, contains 470 genes of which 145 are related to gene replication and transcription. Baker's

yeast has 7000 genes coding for about 3000 enzymes. Thousands of different variants of the natural enzymes are known. The number of reported 3-dimensional enzyme structures is rapidly increasing. In the year 2000 the structure of about 1300 different proteins were known. A systematic list based on a numerical notation, the EC number, has been laid down by the *Commission on Enzymes of the International Union of Biochemistry*. The systematic name of the enzyme consists of two parts: The first part describes the substrates and the second part defines the type of reaction catalyzed. According to this approach, all enzymes catalyze one of six types of reactions. The enzymes are classified into six major categories based on the nature of the chemical reaction they catalyze [119]:

1. Oxidoreductases catalyze oxidation or reduction of their substrates
2. Transferases catalyze group transfer
3. Hydrolases catalyze bond breakage with the addition of water
4. Lyases remove groups from their substrates
5. Isomerases catalyze intramolecular rearrangements
6. Ligases catalyze the joining of two molecules at the expense of chemical energy

### **1.2.2. Enzyme Activity**

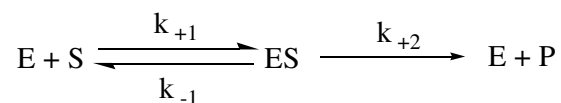
It is usually best to determine the activity of an enzyme at its optimum with respect to pH, concentration of substrate, presence of activators, etc. The method employed should yield results which are independent of the concentration of the enzyme solutions. With most enzymes the amount of change produced by the enzyme is only proportional to the enzyme concentration in the early part of the reaction [120].

The potency of an enzyme is expressed in units. The unit activity is the amount of change or destruction of a given quantity of a substrate under certain definite conditions. Quite often the number of units is defined as  $\mu\text{moles}$  of substrate transformed to product/min per mg of total enzyme-polymer

conjugate. Another way of expressing the activity of an enzyme is by specific activity, the number of  $\mu\text{moles}$  of substrate transformed to product/min/mg of protein, under certain specified conditions of temperature, pH, etc.

### 1.2.3. Kinetics of Enzyme Reactions

Enzymes possess unique catalytic function, so their efficiency is usually determined by measuring their effect on the rate of chemical reaction. The rates of enzyme catalyzed reactions were first studied in the latter part of nineteenth century, when no enzyme was available in pure form and the methods of assay were primitive. Furthermore, instead of measuring initial rates of reaction at various initial substrate concentrations, the commonly used method was to follow the course of reaction over a period of time [121]. In 1913, Michaelis and Menten [122] measured initial rates of the breakdown of sucrose into glucose and fructose catalyzed by invertase at different substrate concentrations and controlled pH by allowing the autorotation of the product. It was postulated that the enzyme and its substrate form an enzyme-substrate complex to account for rectangular hyperbolic relationship between the substrate concentration and the reaction velocity. They proposed a mechanistic scheme for the enzyme-catalyzed reaction involving single substrate and single intermediate and equilibrium between the free enzyme and the enzyme-substrate and enzyme-product complexes, where E is the free enzyme, S is the substrate, ES is the enzyme-substrate complex and P is the reaction product.



Michaelis and Menten derived the rate equation based on the assumption that the rate of breakdown of the ES to product was much slower than the dissociation of ES into enzyme and substrate therefore,

$$k_{+2} \ll k_{-1}$$

However, the formulation of Michaelis and Menten, which treats the first step of enzyme catalysis as an equilibrium, makes unnecessary and unwarranted assumptions about the rate constants. Thus, a more valid derivation was proposed by Briggs and Haldane [123] based on the initial rate of reaction. It was assumed that almost immediately after the reaction starts a steady state is achieved in which the concentration of the intermediate (enzyme-substrate complex) is constant.

$$d[ES]/dt = k_{+1} [E][S] - k_{-1} [ES] - k_{+2} [ES] = 0 \quad (1)$$

Since the total enzyme concentration,  $[E]_0$  can be written as the sum of  $[E]$  and  $[ES]$ ,

$$d[ES]/dt = k_{+1}[E]_0[S] - (k_{-1}[S] + k_{+2}) [ES] = 0 \quad (2)$$

dividing (2) by  $k_{+1}$  and solving for  $[ES]$

$$[ES] = \frac{[E]_0 [S]}{(k_{-1} + k_{+2}) / k_{+1} + [S]}$$

the rate equation is

$$v = k_{+2} [ES] = \frac{k_{+2}[E]_0 [S]}{(k_{-1} + k_{+2}) / k_{+1} + [S]}$$

$$v = \frac{v_{\max} [S]}{K_m + [S]}$$

$K_m$  is known as *Michaelis constant*, is the equilibrium constant for dissociation of enzyme-substrate complex and inversely related to the affinity of the enzyme for its substrate. The  $v_{\max}$  is the *maximum velocity of reaction* which is attained when the entire enzyme is in the form of enzyme substrate complex.

It was shown that this theory and equation could account accurately for their results with invertase, and because of the definitive nature of their experiments, which have served as a standard for almost all subsequent enzyme kinetic measurements. Today, Michaelis and Menten are regarded as the founders of modern enzymology and equation 1 is generally known as the *Michaelis-Menten equation*. The initial rate of reaction obeying Michaelis-Menten equation as a function of the substrate concentration at constant enzyme concentration is given in Figure 1.14.

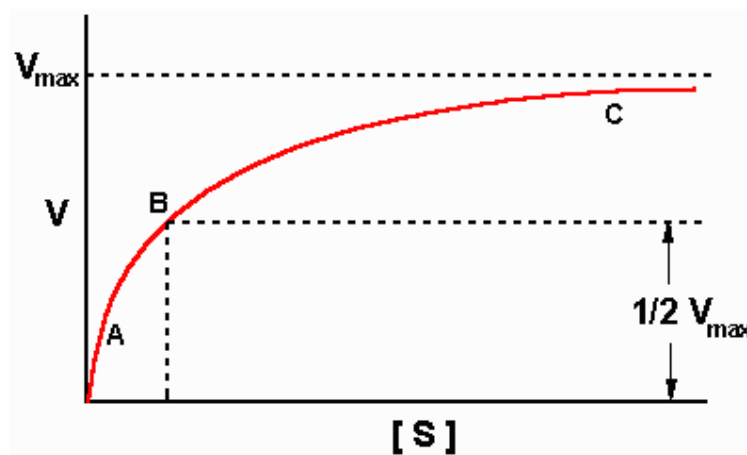


**Figure 1.14.** Plot of initial velocity against substrate concentration for enzyme catalyzed reaction.

At very low substrate concentrations, velocity is directly proportional to  $[S]$  so that reaction is apparently first order in  $S$ . At very high substrate concentrations, velocity will approach to  $v_{max}$  and the reaction is apparently zero order in  $S$ . Under these conditions, the enzyme is said to be saturated with substrate. Graphical representation of Michaelis and Menten equation is desirable if a series of initial velocities at different substrate concentrations is

measured, so that the kinetic parameters,  $K_m$  and  $v_{max}$  can be determined. However, the plot of  $v$  against  $S$ , generating a rectangular hyperbola which is unsatisfactory in practice due to difficulty in drawing hyperbolas accurately and then estimating asymptotes. Therefore, in order to determine these kinetic parameters, for an enzyme catalyzed reaction, a linear relation would be more useful. Lineweaver and Burk [124] have preferred to rewrite the Michaelis and Menten equation in a form that permits the results to be plotted as a straight line,

$$\frac{1}{v} = \frac{K_m}{v_{max}} \frac{1}{[S]} + \frac{1}{v_{max}}$$

The plot of  $1/v$  versus  $1/[S]$  will give a straight line of slope  $K_m/v_{max}$  and y intercept of  $1/v_{max}$  (Figure 1.15)

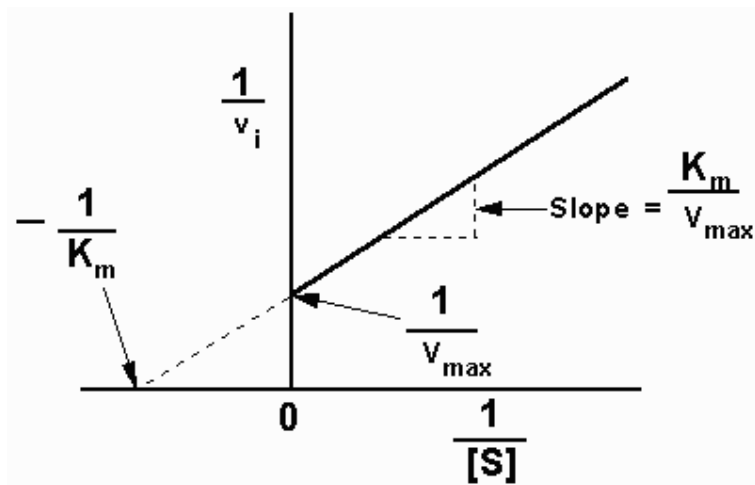


**Figure 1.15.** Lineweaver- Burk plot

#### **1.2.4. Enzyme Immobilization**

Immobilization can be defined as the physical confinement or localization of enzyme molecules within or on a support material, while retaining their biochemical activity. In this process, enzyme molecules are in distinct phase which allows exchange with, but is separated from, the bulk phase in which substrate molecules are dispersed and monitored.

The technology for immobilization of cells and enzymes evolved steadily for the first 25 years of its existence [125], but in recent years it has reached a plateau, if not a slight decline. However, the expansion of biotechnology, and the expected developments that will accrue from advances in genetic technology, has revitalized enthusiasm for immobilization of enzymes and cells [126]. Research and development work has provided a bewildering array of support materials and methods for immobilization. Much of the expansion may be attributed to developments to provide specific improvements for a given application [127]. Surprisingly, there have been few detailed and comprehensive comparative studies on immobilization methods and supports. Therefore, no ideal support material or method of immobilization has emerged to provide a standard for each type of immobilization. Selection of support material and method of immobilization is made by weighing the various characteristics and required features of the enzyme/cell application against the properties, limitations, characteristics of the combined immobilization/support.

In solution, soluble enzyme molecules behave as any other solute in that they are readily dispersed in the solution and have complete freedom of movement. Enzyme immobilization is a technique specifically designed to greatly restrict the freedom of movement of an enzyme. Most cells are naturally immobilized one way or another, so immobilization provides a physical support for cells. There are five principal methods for immobilization of enzymes/cells: adsorption, covalent binding, entrapment, microencapsulation, and crosslinking (Figure 1.16). The relative merits of each are discussed briefly below.

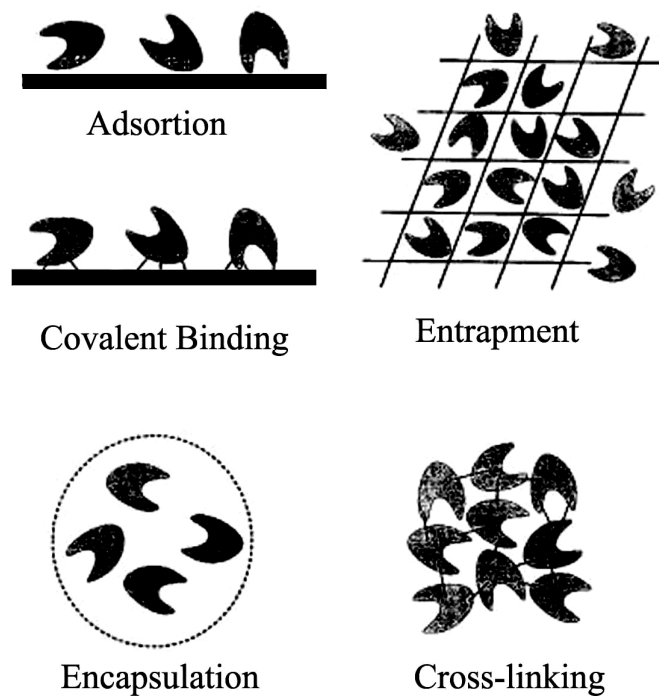


**Figure 1.16.** Principal methods of immobilization.

#### 1.2.4.1. Adsorption

The adsorption of an enzyme onto an insoluble support is the oldest method of enzyme immobilization. It is exceedingly easy to perform. In this method, enzyme and support material are mixed under appropriate conditions and following a period of incubation, finally the insoluble material is separated from the soluble material by centrifugation or filtration [128].

Numerous surface-active materials including anion-cation exchange resins, activated charcoal, silica gel, alumina, controlled-porosity glasses, ceramics, etc, have been used in the preparation of enzyme-adsorption complexes. Depending on the nature of the surface, the enzyme binding may be the result of ionic interactions, physical adsorption, hydrophobic bonding, or Van der Waals interactions [128].

Adsorption methods offer advantages of simplicity, a wide variety of adsorbents (a large number of adsorbents a variety of physical shapes (sheets, fibers, etc) can be used. However, yields (enzyme bound per unit adsorbent) are low, and the enzyme is partially or totally inactivated.

The major disadvantage of this method is that the enzyme is not firmly bound to the support. Changes in experimental conditions such as pH, ionic strength, temperature and type of solvent can cause desorption of the enzyme from the support as they affect such linkages. In some cases the substrate itself can also cause leakage of its enzyme from the support [128].

#### **1.2.4.2. Covalent Binding**

Covalent attachment of enzyme molecules to functionalized support, based on the formation of a covalent bond between the enzyme molecules and support material, is the most prevalent and experimentally easy to conduct. This method involves adding the enzyme to a suspension of the polymer, allowing the coupling to proceed, and removing any noncovalently bound enzyme by subsequent washings [129].

Since the immobilization is dependent on the formation of covalent bonds between the enzyme and the support and a derivatized enzyme produced, consequently, the derivatized enzyme may exhibit superior chemical and physical properties relative to its soluble counterpart. Another advantage of the method is its high degree of development. [129]

However, the successful attachment of an enzyme to a support requires elaborate preparations of both the enzyme and the support, which can exhibit low efficiency in coupling procedure, can give derivatives of low catalytic efficiency. It is important that the amino acids essential to the catalytic activity of the enzyme are not involved in the covalent linkage to the support. This may be difficult to achieve, and enzymes immobilized in this fashion generally lose activity upon immobilization. This problem may be prevented if the enzyme is immobilized in the presence of its substrate- a step in procedure which would tend to have a protective effect on the catalytic site of the enzyme during immobilization [129].

### **1.2.4.3. Entrapment**

The entrapment method is based on the localization of an enzyme within the lattice of a polymer. Unlike other methods of immobilization, entrapment does not result in a direct link between the matrix and the active component. Entrapment methods are performed by dissolving the enzyme solution of chemicals required for synthesis of the enzyme phase and treating this solution so that a distinct phase is formed [128].

Entrapment is an attractive method of immobilization where the size differential between substrate and catalysis is large, where the biocatalyst is susceptible to chemicals or deactivation and where strong interaction with the surfaces of a support matrix is undesirable or can not be achieved directly.

Method offers the advantages of the overall experimental simplicity. The need for only small amounts of enzyme to produce a water-insoluble enzyme conjugate, no alteration in the enzyme's intrinsic properties (no chemical modification of enzyme).

The main problems with entrapped enzymes usually stem from diffusional restrictions. To be an effective barrier, a matrix must have pores within a limited size range, being sufficiently small to retain the catalyst while not impeding the free diffusion of substrate and product. Enzyme molecules are physically entrapped within the polymer lattice and permeate out of the matrix; however, appropriately sized substrate and product molecules can transfer across and within network of polymer to insure a continuous transformation [128].

### **1.2.4.4. Microencapsulation**

Microencapsulation differs from other immobilization methods in that it is mainly based on maintaining the solution environment around the enzyme rather than involving physical or chemical forces. In this process, the original solution containing the enzyme is wholly immobilized instead of selectively immobilizing enzyme molecule.

In this method, enzyme molecules being larger than the mean pore diameter of the sphere retained within the encapsulated sphere and cannot

diffuse out while small substrate and product molecules can be readily diffuse into the capsule [128].

Procedure involves the following steps: An aqueous solution of the enzyme is first added to organic phase containing small amount of water or emulsifying agent, and two phase mixture is obtained, next a second organic phase containing the polymer and the organic solvent for polymer, small colloids are formed, and by evaporation out the organic solvent further precipitation will result in a thicker membrane. Finally, by sedimentation or centrifugation small microcapsules are separated from organic phase.

Compared to classical entrapment method, the major advantage including the possibility of formation of high surface area per unit enzyme immobilized (high concentrations of enzymes in the original solution) that provides an extremely large surface area for contact of substrate and enzyme. In this method, no changes in the inherent properties of the enzyme are expected, since no chemical modification is required, and the enzyme molecules are free in solution. However, a great deal of technology is needed to make uniform spheres and provide high activity retention [129].

#### **1.2.4.5. Crosslinking**

This type of immobilization (Figure 1.17) is support-free and involves joining the cells (or the enzymes) to each other to form a large, three-dimensional complex structure, and can be achieved by chemical or physical methods [130]. Chemical methods of crosslinking normally involve covalent bond formation between the cells by means of a bi- or multifunctional reagent, such as glutaraldehyde and toluene diisocyanate. However, the toxicity of such reagents is a limiting factor in applying this method to living cells and many enzymes. Both albumin and gelatin have been used to provide additional protein molecules as spacers to minimize the close proximity problems that can be caused by crosslinking a single enzyme. Physical crosslinking of cells by flocculation is well known in the biotechnology industry and does lead to high cell densities. Flocculating agents, such as polyamines, polyethyleneimine, polystyrene sulfonates, and various phosphates, have been used extensively and

are well characterized. Crosslinking is rarely used as the only means of immobilization because the absence of mechanical properties and poor stability are severe limitations. Crosslinking is most often used to enhance other methods of immobilization, normally by reducing cell leakage in other systems.

### **1.2.5. Enzyme Immobilization by Electropolymerization**

Electropolymerization is an efficient enzyme immobilization method used in biosensor development. Conducting polymers such as, polythiophene, polyaniline, polyindole polypyrrole [131] can be grown electrochemically on an electrode surface, and it could be demonstrated that electrochemical polymerization is an easy and attractive approach for the immobilization of enzymes at electrode surface. However, conducting polymers have additionally been used in amperometric enzyme electrodes with the intention of coupling the electron-transfer reaction between enzyme and electrode via the ramified conducting network of the polymer. Some of these electropolymers can also serve as mediator, decreasing the work potential and thereby avoiding interference from other species.

In recent years, there has been a growing interest in electrochemical microdevices owing to their potential application in monitoring and diagnostic tests in clinical laboratories. In particular, the development of microfabricated biosensors constitutes an attractive avenue for the *ex vivo* and *in vivo* measurements of metabolites, for example glucose, hormones, neurotransmitters, antibodies and antigens. However, the stable immobilization of macromolecular enzymes on conductive microspheres with complete retention of their biological recognition properties is a crucial problem for the commercial development of miniaturized biosensors. Effectively, most of the conventional procedures of enzyme immobilization such as cross-linking, covalent binding and entrapment in gels or membranes suffer from a low reproducibility and a poor spatially controlled deposition. Apart from these conventional methods, the immobilization of enzymes in electropolymerized films is gaining importance [131-133]. Effectively, the electrochemical formation of polymer layers of controlled thickness constitutes a reproducible

and nonmanual procedure of biosensor fabrication. This approach has received considerable attention due to increase demand for miniaturized biosensors [134].

The electrochemical method involves the entrapment of enzymes in organic polymers during their electrogeneration on an electrode surface. The polymer formation is carried out by controlled potential electrolysis of an aqueous solution containing monomers and enzymes. Recently, a more sophisticated approach involving the adsorption of amphiphilic monomers and enzymes before the electropolymerization step has been described [133]. Another electrochemical method involves, initially, the electropolymerization of functionalized conducting polymers. Then the attachment of enzymes to the polymer surfaces can be obtained by chemical grafting or by affinity of the enzyme at the functional group [135, 136]. In comparison to the physical entrapment of enzymes within polymer films such as polypyrrole, polythiophene, polyacetylene or polyaniline, this approach preserves a better access of substrate to the immobilized enzymes and facilitates macromolecular interactions. However, the amount of immobilized enzymes is restricted to a monolayer at the interface polymer-solution. Ten years ago, an elegant strategy of biosensor construction based on the entrapment of enzymes in polymer films during their electrogeneration on electrode surface appeared [137, 138]. This method involves the application of an appropriate potential to the working electrode soaked in aqueous solution containing both enzyme and monomer molecules. Enzymes present in the immediate vicinity of the electrode surface are thus incorporated in the growing polymer. In addition, the entrapment of enzymes occurs without chemical reaction that could affect their activity. The advantage of electrochemical polymerization is that films can be prepared easily in a rapid one-step procedure. Furthermore, this method enables exact control of the thickness of the polymer layer based on the measurement of the electrical charge passed during the electrochemical polymerization. One major advantage of electrochemical deposition procedures over more conventional methods is the possibility to precisely electrogenerate a polymer coating over small electrode surfaces of complex geometry. Moreover, the recent design of electrochemical micro cell allows the electrogeneration of polymer films from small volumes of

electrolyte. The amount of enzyme required for its entrapment within the polymeric film is thus markedly reduced. Most of the electrochemically deposited polymer films used for the enzyme immobilization are conducting polymers for example, polyacetylene, polythiophene, polyaniline, polyindole and polypyrrole.

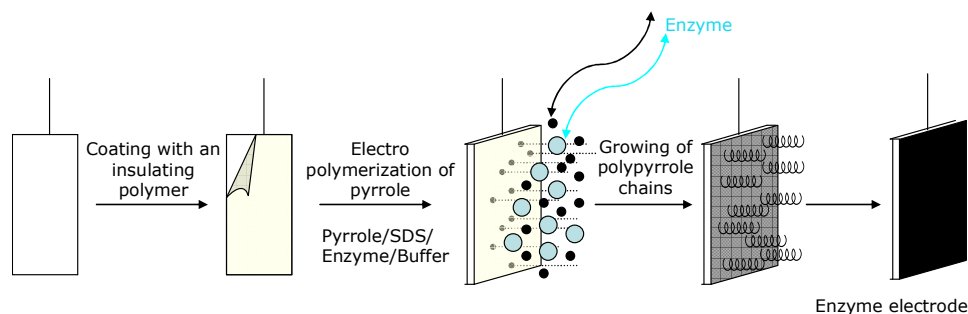


**Figure 1.17.** Enzyme immobilization by electropolymerization.

Often, the thickness of the growing polymer film is controlled by measuring the charge transferred during the electrochemical polymerization process. However, most authors have their individual way of electrode surface pretreatment, choose specific concentrations for the enzyme and the monomer, and use different electrolyte salts and hence counter anions incorporated in the growing polymer film.

### 1.2.6. Applications of Immobilized Enzymes

Immobilized enzymes have been widely used for the processing of a variety of products spanning industries from food to environmental control. In addition to their use in processing, they have also been found useful in many bioanalytical and biomedical applications. Presently, immobilized enzymes are routinely in the medical field, such as in the diagnosis and treatment of various

diseases. For example, immobilized antibodies, receptors or enzymes are used in biosensors and ELISA for the detection of various bioactive substances in the diagnosis of disease states; encapsulated enzymes are also used in bioreactors for the removal of waste metabolites and correction of inborn metabolic deficiency [139].

**Table 1.2.** Applications of immobilized enzymes.

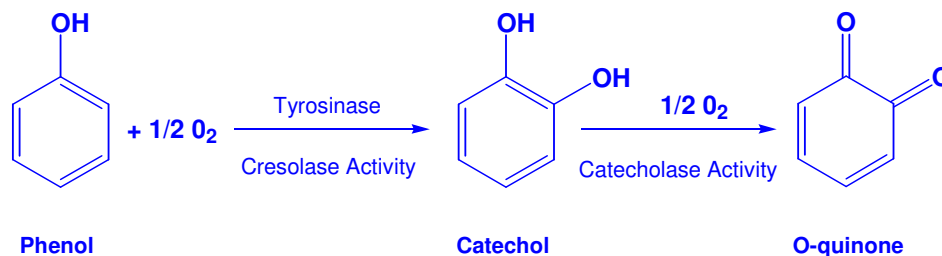
Pharmaceuticals	Selective hydrolysis of penicillin Production of monoclonal antibodies Steroid conversions Antibiotic modification
Food industry	Isomerization of glucose to fructose Hydrolysis of starch oligomers to glucose Inversion of sucrose Treatment of milk Amino acid synthesis Ethanol production
Analytical	Enzyme electrodes based on changes in pH, redox potential, current response, etc.
Medical	In vivo devices for treatment of failure of kidney, pancreas Detoxification following drug overdose Treatment of certain leukaemias by asparaginase

### 1.2.7. Polyphenol Oxidase Immobilization

Polyphenol oxidases (PPO; oxygen oxido-reductase or tyrosinase; EC 1.14.18.1) are copper containing enzymes, which are widely distributed in micro organisms, animals and plants [140, 141]. Enzymatic browning of fruits and vegetables resulted mainly due to PPO's oxidation of natural phenolic compounds into *o*-quinones, which are polymerized into brown, red or black pigments [142, 143]. The most important factors determining the rate of enzymatic browning are the concentration of enzyme and phenolic substrate, pH, temperature and oxygen availability [144].

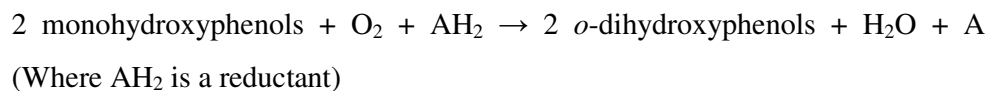
In general, the observed coloration on bruised, cut or sliced fruits and vegetables is related to enzymatic browning [145]. However, browning can also originate from non-enzymatic reactions such as the Maillard reaction [146], which occurs mainly in heat-processed food products [147]. PPO has an enormous impact on the quality of fruits and vegetables due to the loss of texture, color and nutritional value of products [144]. As a result, PPO has received attention from researchers in the area of food processing and food technology. Commercially important plant products particularly susceptible to adverse browning reactions include fruits such as apples, bananas, grapes, pineapples, peaches and apricots as well as vegetables such as potatoes, cabbages and lettuces [148]. In certain instances, such as the manufacture of tea [149], coffee and cocoa [150], enzymatic browning is considered actually a desirable reaction [151].

The names of tyrosinase, catecholase, catechol oxidase and polyphenolase are used interchangeably with polyphenol oxidase [145]. Polyphenol oxidases catalyze the hydroxylation of monophenols to *o*-diphenols and subsequent oxidation of *o*-diphenols to corresponding *o*-quinones (Figure 1.18) [142, 152]. Unstable and highly reactive *o*-quinones can react with one another as well as with *o*-diphenols in the presence of O<sub>2</sub>. In addition, *o*-quinones are strongly electrophilic in nature making them susceptible to nucleophilic attack [152]; as a result, *o*-quinones can react with amino acids, peptides and proteins [153, 154].



**Figure 1.18.** Schematic representation of polyphenol oxidase activity.

Tyrosinase catalyzes two distinct oxidation reactions as shown in Figure 1.19. In cycle I, tyrosinase completes the oxidation of monophenols in the presence of oxygen as it proceeds through four enzymatic forms ( $E_{\text{deoxy}}$ ,  $E_{\text{oxy}}$ ,  $E_{\text{oxy-M}}$ , and  $E_{\text{met-D}}$ ); in cycle II, *o*-diphenols are oxidized as the enzyme goes through five enzymatic rearrangements ( $E_{\text{deoxy}}$ ,  $E_{\text{oxy}}$ ,  $E_{\text{oxy-D}}$ ,  $E_{\text{met}}$  and  $E_{\text{met-D}}$ ). The two cycles lead to the formation of *o*-quinones, which spontaneously react with each other to form oligomers [155]. A typical lag period observed during tyrosinase-catalytic reaction is related to its monophenolase activity. The hydroxylation of monohydroxyphenols by tyrosinase is as follows:



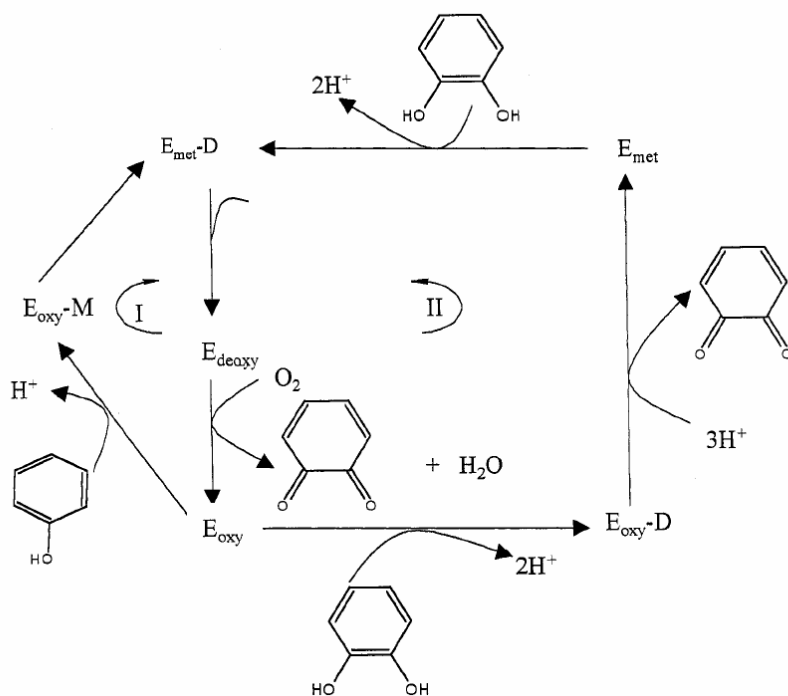


**Figure 1.19.** Catalytic cycle for the hydroxylation of monophenol to o-diphenol (I) and dehydrogenation of o-diphenol to o-quinones (II) by tyrosinase [156].

Tyrosinase has two separate binding sites in its active center, one for the substrate (monohydroxyphenol) and another for the reductant (o-dihydroxyphenol or exogenously added  $AH_2$ ) (157, 158). When exogenous  $AH_2$  is not added, the hydroxylation reaction is characterized by a lag period, which is a dynamic equilibrium between the enzymatic and chemical steps to obtain the steady state with respect to the diphenol concentration [141]; to reach such a concentration, a small amount of enzyme must be present in the oxy form [159]. The lag period is an autocatalytic mechanism, which depends on the concentrations of DOPA (dihydroxy phenylalanine), a monophenol substrate [160]. Exogenous addition of the reductants (ascorbate, hydroxylamine and hydroquinone) can also shorten the lag period. Furthermore, the lag is dependent

on various factors, including substrate and enzyme concentration, pH and transition metal ion concentration. The absence of a lag period for diphenolase activity can be explained by the binding and transformation of o-diphenols into o-quinones by the Emet and Eoxy forms [158].

The catecholase or diphenolase activity of tyrosinase also has important applications, since this activity can be used in the analysis of phenols and its derivatives. Phenolic pollutants are frequently found in surface waters and in the effluent of industrial discharge sources. Some of the industrial sources of phenol discharge include oil refineries, coke and coal conversion plants, plastics and petrochemical companies, dyes, textiles, timber, mining, and the pulp and paper industries. Virtually all phenols are toxic. Moreover, they have a high oxygen demand and can deplete the oxygen in the body of water [161]. As a consequence, this may affect the ecosystem of water sources where phenols are discharged.

A successful application of soluble tyrosinase in the “cleansing” of polluted waters have reported by Atlow et al. [162]. Tyrosinase causes the precipitation of phenols, which can then be filtered out from surface waters and industrial discharge sources. The enzyme has also been used as a sensor to detect the concentration of phenols in waste water [163, 164]. The detection of phenols is of importance also in the medical field. Tyrosinase has been used as part of an enzyme-electrode system to detect catechols and assess catecholamines in the urine of patients with neural crest tumors [165]. Since tyrosinase is responsible for the browning of fruits and vegetables it has also applications in the food industry. Interest in the enzyme has been demonstrated by tannin oil companies due to the role that it plays in melanogenesis. Also, it has been considered for use in melanin-related disorders, such as albinism, vitiligo, and melanoma [166].

Although tyrosinase has widespread applications, its use is limited by its inherent instability and rapid inactivation. By using enzyme immobilization technology, good operational stability and long-term stability can be achieved for tyrosinase.

Red and white wine contain many phenolic substances which have a number of important functions in wine. They affect the taste like bitterness and astringency, especially in red wines, the color of red wine is caused by phenolics, they are also bactericidal agents and impart antioxidant properties, being especially found in the skin and seeds of the grapes.

There are two types of phenols in wines. "flavonoids" and "non-flavonoids". The flavonoids are composed of three benzene rings and react readily, binding to other molecules and there are between 6,000 and 8,000 species of flavonoids. A group of flavonoids, called the flavon-3-ols, have been well characterized in wine. Flavon-3-ols are usually concentrated in grape seeds, stems and skin. When these parts of the grape are left in for as long as possible during the wine-making process, more flavon-3-ols end up in the resulting wine than if the seeds, stems and skin are removed earlier [167].

The non-flavonoids in wine comprise many classes of chemicals including hydroxyl cinnamates, benzoates, and stilbenes. The health benefits of a particular kind of stilbene, called "resveratrol," are known widely since it is unique to grapes and is not found in other fruits or vegetables [168].

Amount of phenolics vary from one brand and type of wine to another since the chemical composition of a wine is influenced by the climatic and atmospheric conditions, soil type, vine cultivation and the treatment to which it is subjected. Process difference cause the red wines to contain almost ten times higher amount of phenolics than the white wine.

The typical methods for the determination of phenolic compounds are gas and liquid chromatography [169, 170]. These methods involve complex sample pre-treatment procedures and are unsuitable for on site or field based analyses. A biosensing approach with advantages of high specificity, high sensitivity and rapid detection mechanism may provide a solution [171-175]. In this study immobilization of polyphenol oxidase enzyme in a conducting polymer electrode was studied as an alternative method for the determination of phenolic compounds [176, 177].

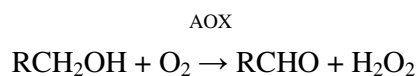
### **1.2.8. Alcohol Oxidase Immobilization**

The detection and quantification of alcohols with high sensitivity, selectivity and accuracy is required in many different areas. Accurate and rapid measurement of ethanol is very important in clinical and forensic analysis in order to analyse human body fluids, e.g. blood, serum, saliva, urine, breath and sweat, among others. The food, beverage (wine, beer and spirits) and pulp industries require simple, fast and economic analytical methods in order to control fermentation processes and the quality of products thereof [178, 179]. Moreover, the determination of ethanol is also important in agricultural and environmental analysis, e.g. for the assessment of ethanol at a spill site or in groundwaters.

Many analytical methods have been developed during the years for the determination of ethanol and other aliphatic alcohols, such as methanol. These include the use of chemical methods, such as redox titrations, colorimetric methods, specific gravity and refractive index measurements, chromatographic and spectroscopic methods. Although some of these methods are precise and reliable, they are complex, time consuming and require previous separations processes (distillation, pervaporation), expensive instrumentation and trained operators. Such disadvantages can be overcome by the use of enzymatic methods. Enzymes are one of the essential components of living systems, catalysing almost all chemical transformations that occur during cell metabolism. The nature and specificity of their catalytic activity makes them excellent tools for chemical analysis. The ability of a single enzyme molecule to catalyse the reaction of numerous substrate molecules also provides an amplification effect, which enhances the sensitivity of the analysis. A further advantage is that most enzyme-catalysed reactions can be followed by simple, widely available spectroscopic or electrochemical methods. Alcohol oxidase has been extensively used in the determination of alcohols.

Alcohol oxidase (AOX; Alcohol:O<sub>2</sub> oxidoreductase, EC 1.1.3.13) is an oligomeric enzyme consisting of eight identical sub-units arranged in a quasi-cubic arrangement, each containing a strongly bound cofactor, flavin adenine dinucleotide (FAD) molecule [180]. It is produced by methylotrophic yeasts

(e.g. *Hansenula*, *Pichia*, *Candida*) in subcellular microbodies known as peroxisomes, during growth on methanol. AOX is the first enzyme involved in the methanol oxidation pathway of methylotrophic yeasts and although its physiological role is the oxidation of methanol, it is also able to oxidise other short-chain alcohols, such as ethanol, propanol and butanol. AOX is thus responsible for the oxidation of low molecular weight alcohols to the corresponding aldehyde, using molecular oxygen (O<sub>2</sub>) as the electron acceptor, according to equation below. Due to the strong oxidizing character of O<sub>2</sub> the oxidation of alcohols by AOX is irreversible.



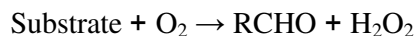
The classical ways to follow an oxidase-catalysed reaction have been by measuring either the decrease in O<sub>2</sub> tension or the increase in H<sub>2</sub>O<sub>2</sub> concentration.

Colorimetric, chemiluminescent and fluorescent methods can be used to detect the production of H<sub>2</sub>O<sub>2</sub> by AOX during the oxidation of ethanol. Colorimetric methods are based on the conversion of a chromogen substrate into a coloured product, which absorbs in the visible spectral region. Fluorescent methods are based on the formation of a fluorophore product, which emits visible light after being stimulated with a shorter wavelength radiation. Finally, chemiluminescence consists in the emission of visible light upon chemical reaction.

Most of the spectrometric methods described in the literature for the determination of ethanol are based on a bienzymatic system, comprising AOX and a peroxidase enzyme, which further reduces H<sub>2</sub>O<sub>2</sub> to H<sub>2</sub>O at the expense of hydrogen donor molecules. A wide range of substrates has been used, including chromogenic, fluorogenic and luminogenic substrates. One of the most popular substrate used is 2,2'-azino-di(3-ethylbenzthiazoline-6-sulfonate), ABTS [181-184]. The oxidized form of ABTS has a bluish green colour and is usually detected around 415 nm. Another currently used chromogen is 4-aminoantipyrine (4-AAP), which is used in combination with another reducing

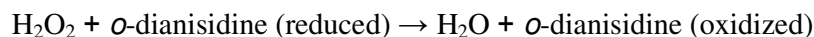
substrate such as phenol [185], 4-hydroxybenzenesulfonate [186,187], chromotropic acid (1,8-dihydroxy-3,6-naphthalene disulfonic acid) [188], 8-hydroxyquinoline [189]. Others chromogens used include 2,6-dichloroindophenol [190], *o*-dianisidine [191], 3,3',5,5'-tetramethylbenzidine (TMB) [192], etc. A well-known example is the estimation of ethanol with a combination of AOX, peroxidase (POD) and as *o*-dianisidine dye. The method involves two enzymatic reactions.

AOX



and,

POD



Although, most of the spectrophotometric methods used for the detection of ethanol are based on a bienzymatic system, comprising HRP and AOX, some methods have been proposed without the use of HRP. The group of Guilbault proposed a fibre-optic chemiluminescence method for the determination of ethanol in beverages [193]. In this method, the  $\text{H}_2\text{O}_2$  produced enzymatically by an AOX immobilised bioreactor was determined by measuring the luminescence of the oxidation of luminol, by  $\text{H}_2\text{O}_2$ , using  $\text{K}_3\text{FeIII}(\text{CN})_6$  as catalyst.

Other methods have also been reported to follow the oxidation of alcohols by AOX. Rank and co-workers have described a thermal biosensor for monitoring ethanol and other metabolites during industrial fermentations [194, 195]. This biosensor is based on the enthalpy change during the conversion of ethanol by an AOX immobilized column. A reference column, containing only BSA, was used in order to eliminate non-specific heat arising from mixing and salvation effects caused by high salt and metabolite concentrations in the fermentation broth.

### **1.3 Aim of the Study**

- (a) To achieve the syntheses of thiophene capped poly(ethylene oxide) coded as ThPEO and random copolymer containing 3-methylthienyl methacrylate and p-vinylbenzyloxy poly(ethylene oxide) coded as RPEO.
- (b) To synthesize the conducting copolymers of ThPEO and RPEO with thiophene or pyrrole and to investigate the electrochemical, morphological and electrochromic properties of resultant copolymers.
- (c) To check the possibility of enzyme immobilization, polyphenol oxidase and alcohol oxidase, in copolymers obtained via electrochemical polymerization and to characterize the enzyme electrodes.
- (d) To determine the phenolic compound concentration in red wines by using the tyrosinase electrodes.

## CHAPTER 2

### EXPERIMENTAL

#### 2.1. Chemicals

Pyrrrole (Merck) and thiophene (Merck) were distilled before use and stored at 4 °C. Acetonitrile (AN) (Merck) was used without further purification. Tetrabutylammonium tetrafluoroborate (TBAFB), borontrifluoride ethyl ether (BFEE) (Aldrich), *p*-toluene sulfonic acid (PTSA) (Sigma) and sodium dodecyl sulfate (SDS) (Sigma) were used as received. Tetrahydrofuran (THF) was purchased from Merck, and 3-thiophene ethanol was dried and distilled over CaH<sub>2</sub> under vacuum. Commercial reagents were purified according to usual procedures. Tetrahydrofuran (THF) was refluxed and distilled over sodium wire. Chloroform was dried over phosphorous pentoxide and distilled over calcium hydride. *α,α*-Azobisisobutyronitrile (AIBN) was recrystallized from methanol. The reagents used for anionic polymerization of ethylene oxide (EO) and its end-capping were purified and dried by the usual procedure using a vacuum line (10-5 mmHg), and sealed in ampoules fitted with breakable seals. EO was purified by repeated trap-to-trap distillations over calcium hydride and finally distilled over sodium mirror. 2-Methoxyethanol (Fluka, 99%) was dried and distilled under vacuum. *p*-Vinylbenzyl chloride (VBCl) was distilled over calcium hydride and stocked as THF solutions for end-capping reaction. Triethylamine (TEA) (Merck), dichloromethane (DCM) (Merck), chloroform (Merck), and methanol (Merck) were used without purification.

Tyrosinase (PPO) (E.C. 1.14.18.1), alcohol oxidase (AOX) (E.C. 1.1.3.13), peroxidase, type II, (POD) (E.C. 1.11.1.7) and *o*-dianisidine used in spectrophotometric activity determination of AOX was purchased from Sigma. 3-Methyl-2-benzothiozolinone (MBTH), acetone and sulfuric acid used in spectrophotometric activity determination of PPO were also obtained from Sigma. For the preparation of citrate buffer, citric acid and sodium hydroxide were used as received. Catechol was purchased from Sigma. All catechol solutions were prepared in citrate buffer. Hydrogen peroxide (H<sub>2</sub>O<sub>2</sub>) was supplied by Merck.

## **2.2. Electrochemical Polymerization**

Several different methods including cyclic voltammetry, constant current and constant potential methods can be utilized to carry out the electropolymerization of thiophene and pyrrole-based monomers. In each case, a solution of monomer in a high dielectric constant solvent (such as acetonitrile or propylene carbonate) suitable for electrochemistry is prepared. It is necessary that the solvent be electrochemically inert (meaning that it will not undergo electrochemical reactions itself within the potential range being used for the experiment) and non-nucleophilic. In addition to solvent, a supporting electrolyte (e.g. the sodium dodecylsulfate, tetrafluoroborate, and hexafluorophosphate) is also required to help current passage through the solution and to compensate charges that form on the polymer during oxidation and reduction.

### **2.2.1. Cyclic Voltammetry**

The most convenient method for initial studies on electrochemically polymerizable compounds is cyclic voltammetry (CV). This method consists of cycling the potential of an electrode immersed in an unstirred solution, and measuring the resulting current at the working electrode. The background of cyclic voltammetry was presented in Chapter 1.

### **2.2.2. Constant Current (Galvanostatic) Methods**

In this technique, the current is controlled by a galvanostat and it remains constant throughout the experiment while the potential is monitored as a function of time (chronopotentiometry). When a conducting polymer is deposited on the electrode surface, the potential of the monomer oxidation starts to decrease due to the reduction in monomer oxidation potential on the polymer, compared to the bare electrode. The thickness of conducting polymer films can be controlled by monitoring the charge which is obtained by following the time of experiment by the constant current. Although simple in application, this method has drawback of generation of unknown species since the potential is a variable parameter.

### **2.2.3. Constant Potential (Potentiostatic) Methods**

Potentiostatic method is also an effective means of polymer deposition and is mainly used when a specific amount of charge must be passed while the potential is maintained at a certain value. With this approach the potential is stepped from a potential where there is no reaction, to a set potential where the reaction occurs. This is often the onset potential recorded by during potentiostatic growth and current response is monitored with respect to time (chronoamperometry). By keeping the potential constant, the creation of undesired species is prevented, hence the reaction becomes selective.

## **2.3. Instrumentation**

In this work, synthesis of copolymers and enzyme immobilization processes were performed in a typical H-shaped electrolysis cell which is composed of anode and cathode compartments divided by a medium porosity sintered glass disc of 2.0 cm diameter. A Luggin capillary of reference electrode was inserted to working electrode compartment of the cell (Figure 2.1). Films were electrochemically polymerized potentiostatic methods by using Wenking Model POS 73 potentiostat. Platinum (Pt) flag electrodes as the working and counter electrodes and a silver (Ag) wire (pseudo reference) reference electrodes

were used during electrolyses, and all potentials were reported with respect to the Ag wire.

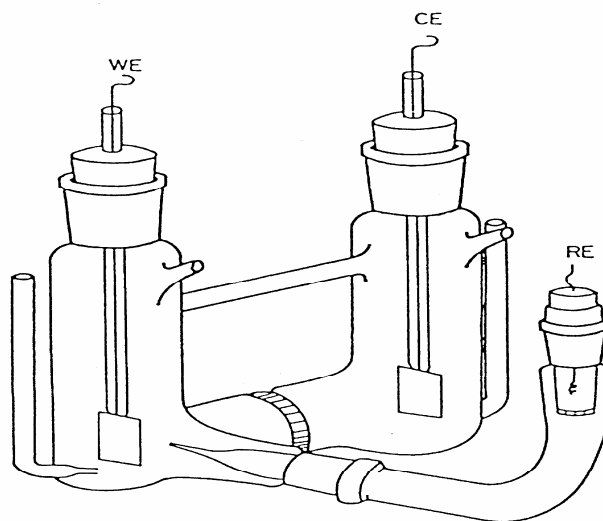


**Figure 2.1.** H-shaped electrolysis cell.

Cyclic voltammetry system is a convenient way of obtaining the oxidation-reduction peak potentials of the substrates such as monomers and to analyze the electroactivity of polymers. The cell (Figure 2.2) consists of a platinum bead working electrode of 1 cm wire in length, a platinum spiral counter electrode (3 cm), and a Ag/Ag<sup>+</sup> reference electrode. The volume of the cell was about 15 mL. CV experiments were carried out by a Bank Wenking POS 2 potentiostat/galvanostat. XY recorder was used to obtain the voltammograms.

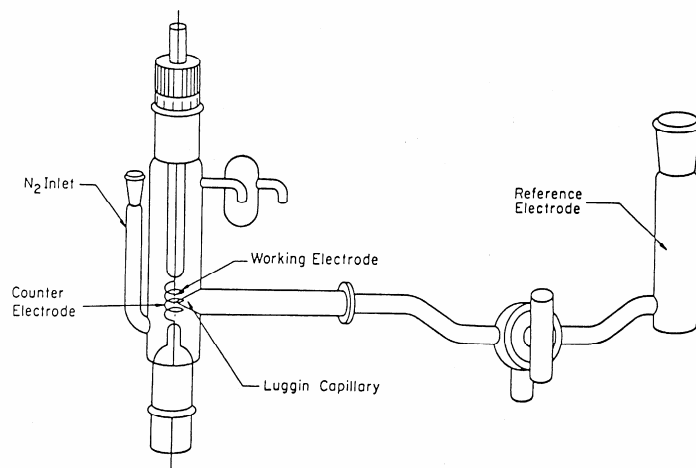


**Figure 2.2.** Cyclic voltammetry cell.

### **2.3.1. Nuclear Magnetic Resonance Spectrometer ( $^1\text{H}$ -NMR)**

NMR spectra of samples were taken by Bruker Instrument-NMR Spectrometer (DPX-400).

### **2.3.2. Fourier Transform Infrared Spectrophotometry (FTIR)**

FTIR is a useful method for the characterization of conducting polymers since it does not require polymers to be soluble. It is primarily used for the detection of functional groups, but analysis of spectra in the lower frequency finger print region can give evidence of degree of polymerization, the extent of mislinking within the polymer and the effect of substituents on the electronic properties of the polymer backbone. In this work, FTIR spectra of the polymers were recorded on a Nicolet 510 FT-spectrophotometer.

### **2.3.3. Gel Permeation Chromatography (GPC)**

A separation technique involving the transport of a liquid mobile phase through a column containing the separation medium, a porous material. Gel permeation chromatography (GPC), also called size exclusion chromatography and gel filtration, affords a rapid method for the separation of oligomeric and polymeric species. The separation is based on differences in molecular size in solution. It is of particular importance for research in biological systems and is the method of choice for determining molecular weight distribution of synthetic polymers.

For determination of  $M_n$  and  $M_w$  values of insulating precursor polymers (dissolved in tetrahydrofuran), GPC studies were conducted using Agilent 1100 RI equipped with three Waters Styragel columns HR series.

### **2.3.4. UV-Vis Spectrophotometry**

A Shimadzu UV-1601 model spectrophotometer was employed in the determination of activities of both free and immobilized enzymes.

### **2.3.5. Spectroelectrochemistry Experiments**

Spectroelectrochemical and kinetic studies were performed on Solatron 1285 potentiostat/galvanostat attenuated with Agilent HP8453A UV-Vis spectrophotometer in a cell furnished with ITO coated glass working, Pt wire counter electrodes and a  $Ag/Ag^+$  reference electrode at room temperature.

### **2.3.6. Colorimetry Measurements**

For colorimetry measurements Conica Minolta CS-100 A chromameter was used.

### **2.3.7. Scanning Electron Microscopy (SEM)**

SEM is a surface analytical technique which is employed to study the morphology of conducting polymer film surfaces and provides valuable information on the nature of dopant ion and the thickness of the film. SEM of both copolymer and enzyme entrapped films was performed using a JEOL model JSM-6400 scanning electron microscope at 20kV with varying levels of magnification. Polymer films were peeled back from Pt electrode and glued to copper holder, and then they were coated by sputtering with a thin gold film to avoid charge build-ups due to their low conductivity.

### **2.3.8. Four Probe Conductivity Measurements**

Four probe technique allows a number of conductivity measurements over a broad range of applied currents, usually varying between 1  $\mu$ A and 1 mA. In this device, four equally spaced points on a line make electrical contact with a polymer film on an insulating surface. Between the outer pair of these points, a constant current is applied while the potential difference arising from this current is measured at the two inner contacts. By applying a constant current across the two outer leads, the voltage drop across the two inner leads can be measured allowing for the calculation of resistance using Ohm's law. Figure 2.3 shows the simplest form of the device. A known current  $I$  is injected at the electrode 1 and collected at the electrode 4, while the potential difference between contacts 2 and 3 is measured. Conductivity is calculated from the following equation:

$$\sigma = \ln 2 / (\pi R t)$$

where  $R$  is the resistance of the sample,  $t$  is the thickness.

To measure the conductivities, electrochemically prepared polymers films at sufficient thickness were removed from the electrolysis medium, followed by rinsing, drying and removal of the film by peeling from the electrode surface. Their conductivities were determined by four probe technique.

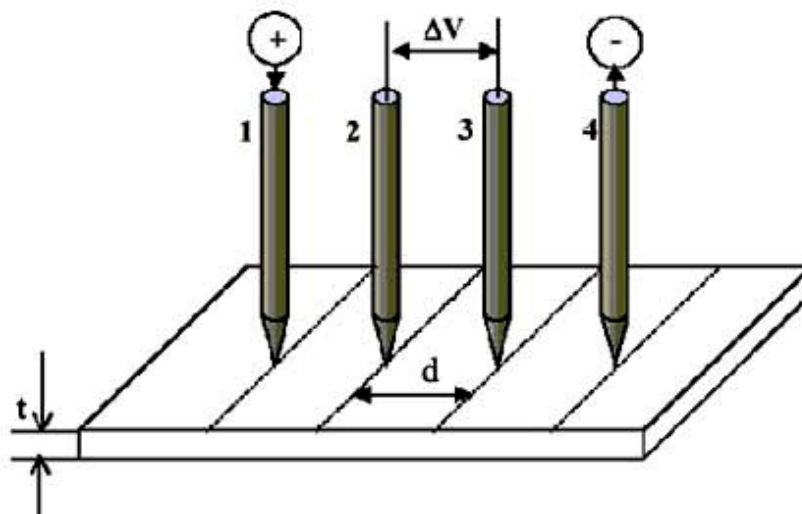


**Figure 2.3.** Four- probe conductivity measurement.

## **2.4. Experimental Procedures**

### **2.4.1. Synthesis of Conducting Copolymers of Thiophene Ended Poly (Ethylene Oxide) with Thiophene and Pyrrole**

#### **2.4.1.1. Synthesis of Thiophene Ended Poly(Ethylene Oxide) (ThPEO)**

Calculated amounts of 3-thiophene ethanol, potassium naphthalene in tetrahydrofuran (THF), THF and ethylene oxide (EO), each in an ampoule with a breakable seal, were fitted into a flask, baked under vacuum and sealed off the vacuum line. 3-Thiophene ethanol and THF were first introduced into the dried flask and then reacted with potassium naphthalene in THF. The dark green color due to potassium naphthalene almost immediately disappeared. Then EO, chilled by dry ice, isopropanol, was introduced to the flask and polymerized at 40 °C for 3 days. An aliquot was taken off to afford 3-thiophene ended

polyethylene oxide. The precipitated macromonomer was collected by filtration and freeze-dried from benzene. 95 % of product efficiency was obtained.

#### **2.4.1.2. Cyclic Voltammetry Studies of ThPEO**

The oxidation/reduction behavior of the ThPEO in the presence of pyrrole and thiophene was investigated by CV. The system consists of a potentiostat (HEKA), an X-Y recorder and a CV cell containing Pt foil working and counter electrodes, and a Ag/Ag<sup>+</sup> reference electrode. Measurements were carried out under N<sub>2</sub> atmosphere in acetonitrile and water at room temperature.

#### **2.4.1.3. Synthesis of Copolymers of ThPEO with Pyrrole by Electrochemical Polymerization**

Copolymer films of ThPEO with pyrrole were synthesized electrochemically under nitrogen atmosphere in conventional three-electrode cell by using platinum (Pt) electrodes as the working and counter electrodes. A Ag/Ag<sup>+</sup> electrode was utilized as the reference electrode.

For the synthesis of conducting copolymer of ThPEO with pyrrole, 20 mg ThPEO were dissolved in 10mL water and 20 μL pyrrole were put into electrolysis cell. The supporting electrolyte was SDS. Constant potential electrolysis was run at 1.1V for 30 min at room temperature under inert atmosphere.

#### **2.4.1.4. Synthesis of Copolymers of ThPEO with Thiophene by Electrochemical Polymerization**

Copolymer films of ThPEO were synthesized electrochemically under nitrogen atmosphere in a conventional three-electrode cell by using platinum (Pt) foils as the working and counter electrodes. A Ag/Ag<sup>+</sup> electrode was utilized as the reference electrode. For the synthesis of conducting copolymer of ThPEO with thiophene, 20 mg ThPEO were dissolved in 10mL acetonitrile and 20 μL thiophene were introduced into three compartment electrolysis cell. The supporting electrolyte was TBAFB. Constant potential electrolyses were run at 1.9V for 30 min at room temperature under inert atmosphere.

## **2.4.2. Synthesis of Copolymers of Random Copolymer (RPEO) 3-Methylthienyl Methacrylate and *p*-Vinylbenzyloxy Poly(Ethylene Oxide) with Thiophene and Pyrrole**

### **2.4.2.1. Synthesis of 3-Methylthienyl Methacrylate Monomer**

3-Thiophene methanol, 5.7 g (50 mmol), triethylamine, 7.3 g (71 mmol) and a small amount of CuCl were dissolved in 35 mL of dry ethyl ether. Freshly distilled methacryloyl chloride, 5.35 g (51 mmol), in 35 mL of dry diethyl ether were added slowly at 0°C. The mixture was stirred for two hours. Triethylammonium chloride was filtered off through a silica gel column. After solvent evaporation, the residue was stirred overnight in 1:1 mixture of methylene chloride and 2 M NaOH. The organic layer was separated, washed twice with water and dried over CaCl<sub>2</sub>. Following solvent evaporation residue was distilled in a vacuum over a Vigreux column. 80 % of product efficiency was obtained.

### **2.4.2.2. Synthesis of *p*-Vinylbenzyloxy Poly(Ethylene Oxide) Monomer (PEO-VB)**

PEO macromonomers bearing *p*-vinylbenzyl end-group was prepared by a conventional high vacuum line technique. 13.5 mmol of 2-methoxyethanol, 6 mmol of potassium naphthalene in THF, 295 mmol of EO and THF, each in an ampoule with a breakable seal, were fitted into a flask, baked under vacuum and sealed off from vacuum line. 2-Methoxyethanol and THF were introduced into a dried flask and then reacted with potassium naphthalene in THF. The dark green color due to potassium naphthalene almost immediately disappeared. Then, EO, chilled by dry ice/isopropanol, was introduced to the flask and polymerized at 40°C over 3 nights. Then, the flask was fitted into a vacuum line with the ampoules containing 50 mmol of *p*-vinylbenzyl chloride (VBCl) and 15 mmol of triethylamine (TEA). After evacuation, the system was sealed off and the contents were mixed to terminate the polymerization by breaking the seals. The reaction took place immediately to a cloudy appearance indicating formation of

KCl and Et<sub>3</sub>NHCl. The mixture was poured into a large amount of acetone (700 mL) to precipitate the salts, which were filtered off. The filtrate was concentrated by a rotary evaporator under a reduced pressure to about 70 mL and poured into a large amount of hexane (700 mL). The macromonomer was collected by filtration and freeze-dried from hexane. The yield was almost quantitative.

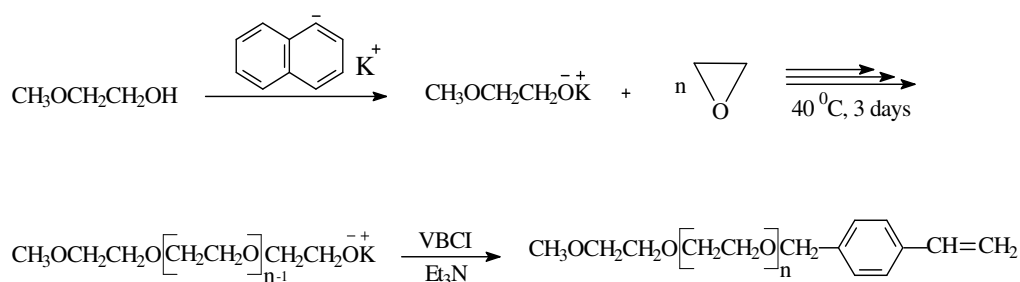


**Figure 2.4.** Synthesis route of *p*-vinylbenzyloxy poly(ethylene oxide) (PEO-VB).

#### 2.4.2.3. Synthesis of Random Copolymer (RPEO) of 3-Methylthienyl Methacrylate and *p*-Vinylbenzyloxy Poly(Ethylene Oxide)

*p*-Vinylbenzyloxy poly(ethylene oxide) (0.2 g) was dissolved in 1 mL dichloromethane. To this solution, 0.10 g ( $5.5 \times 10^{-4}$  mol) of 3-methylthienyl methacrylate was added. After adding AIBN, the tube was degassed by three freeze-pump-thaw cycles and sealed under vacuum. Polymerization was performed at 80°C for 3 hours. After the reaction time, the mixture was poured into n-hexane. The precipitated polymer was filtered off and dried in a vacuum oven.

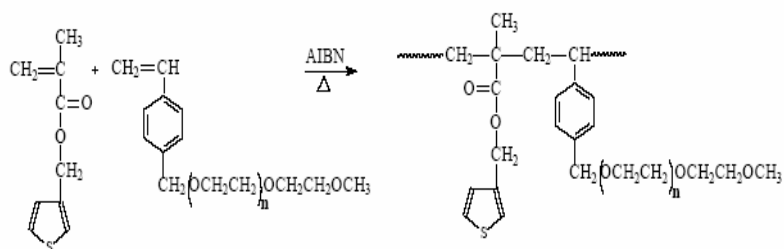


**Figure 2.5.** Synthesis route of random copolymer (RPEO) of 3-methylthienyl methacrylate and *p*-vinylbenzyloxy poly(ethyleneoxide).

#### 2.4.2.4. Cyclic Voltammetry Studies of RPEO

The oxidation / reduction behavior of the random copolymer RPEO in the presence of thiophene and pyrrole was investigated by cyclic voltammetry (CV). The system consists of a potentiostat (Wenking POS 2), and X-Y recorder and CV cell containing platinum foil working and counter electrodes and a  $\text{Ag}/\text{Ag}^+$  reference electrode. Measurements were carried out in AN-TBAFB solvent electrolyte couple under nitrogen atmosphere at room temperature.

#### 2.4.2.5. Synthesis of Copolymers of RPEO with Thiophene by Electrochemical Polymerization

A Wenking POS 73 potentiostat was used for the supply of a constant potential in the electrochemical polymerization. Electrolyses were performed under nitrogen atmosphere in conventional three-electrode cell by using platinum foils as the working and counter electrodes. A  $\text{Ag}/\text{Ag}^+$  electrode was utilized as the reference electrode. For the synthesis of copolymer of RPEO with thiophene, 15 mg of RPEO was dissolved in 15 mL of AN and 20  $\mu\text{L}$  of thiophene were added into 15 mL of AN. The supporting electrolyte was TBAFB. Constant potential was run at 2.0 V for one hour at room temperature under inert atmosphere. Films were washed with AN to remove excess TBAFB after electrolysis.

#### **2.4.2.6. Synthesis of Copolymers of RPEO with Pyrrole by Electrochemical Polymerization**

Electrolysis was performed in two different media; water-PTSA and water-SDS solvent-electrolyte couples under nitrogen atmosphere. In both media, RPEO was coated onto the working electrode surface from its (1 %, w/v) dichloromethane solution. Electrolyses were done at 1.1 V versus Ag/Ag<sup>+</sup> reference electrode. After electrolyses, films were washed several times with water to remove the supporting electrolyte adsorbed on the films.

#### **2.3.7. Spectroelectrochemical Studies of Copolymers**

Spectroelectrochemical analyses experiments of the copolymers of ThPEO and RPEO with thiophene were done on an HP 8453 Diode-array UV-Vis Spectrophotometer. For spectroelectrochemistry studies, copolymer films were electrochemically synthesized on indium tin oxide (ITO) coated glass slides in a strong Lewis acid, boron fluoride ethyl ether, BF<sub>3</sub>Et<sub>2</sub>O (BFEE) by potentiostatic methods. In this case, ITO, Pt and Ag/Ag<sup>+</sup> were used as the working, counter and reference electrodes respectively. The anodically coloring film was switched between the fully oxidized and fully reduced states. In order to ensure the access to maximum doping level, UV-Vis spectra of the film was recorded at various potentials in AN/TBAFB (0.1 M).

#### **2.3.8. Switching Properties of Polymers**

A remarkable color change and the switching ability between the two colored states of the polymer are crucially important for electrochromic applications. A square wave potential step method, coupled with optical spectroscopy known as chronoabsorptometry was used to probe switching time and contrast. During the experiments, the copolymers and the homopolymer (coated onto ITO) glass were switched at the wavelength of maximum contrast between its neutral and doped states for five seconds and % transmittance (%T) was measured. ThPEO-co-PTH and RPEO-co-PTH were switched via applying potentials between 0.2 V and +1.0 and 0.2 V and +1.4 V respectively.

## **2.4.9. Enzyme Immobilization**

### **2.4.9.1. Immobilization of Alcohol Oxidase**

#### **2.4.9.1.1. Preparation of Enzyme Electrodes PPy/AOX and RPEO-co-PPy/AOX**

Immobilization process was achieved by the electropolymerization of pyrrole on bare and RPEO coated platinum electrodes. The electrolysis solution contains 5mL AOX (100 units), 0.6 mg/mL SDS as the supporting electrolyte and 5 mL citrate buffer (pH 7.5). Polymerization reactions were carried out by applying 1.0 V. After polymerization was completed, electrodes were washed with distilled water and kept in pH 7.5 buffer at 4 °C.

#### **2.4.9.1.2. Determination of Alcohol Oxidase Activity**

The activity determination was performed by using a modified version of Janssen's study [196]. For free alcohol oxidase activity, alcohol solutions were placed in test tubes and incubated at 25 °C. After addition of 0.1mL enzyme solution to 0.5 mL alcohol, enzyme and substrate were allowed to react for specific times. Then, 0.1mL peroxidase (POD) (U/mL) (for catalyzing the reaction between hydrogen peroxide and *o*-dianisidine (2.4 mL, 0.21 mM)) were added. The reaction was stopped with the addition of 0.5 mL, 2.5M sulfuric acid. Spectrophotometric measurements were performed at 530 nm and the hydrogen peroxide standard calibration curve was used in order to define enzyme activity as the oxidation of 1  $\mu$ mol of alcohol to corresponding aldehyde and hydrogen peroxide per minute at pH 7.5 at 25 °C. For enzyme electrodes the same procedure was applied.

#### **2.4.9.1.3. Determination of Kinetic Parameters of Free and Immobilized AOX**

In order to determine maximum velocity of the reaction ( $V_{max}$ ) and the Michaelis–Menten constant ( $K_m$ ) for each electrode, activity assay was applied for different concentrations of methanol, ethanol and *n*-propanol solutions.

#### **2.4.9.1.4. Determination of Optimum pH and Optimum Temperature of Immobilized AOX**

The reaction temperature was changed between 10 and 60 °C while alcohol solution concentration was kept at 10 Km for each case. For pH optimization at 25 °C, the pH of the reaction was altered between pH 4 and 11 while alcohol concentration was kept at 10 Km. The rest of the procedure was the same as the determination of AOX activity.

#### **2.4.9.1.5. Operational Stability and Shelf Life of Immobilized AOX**

The stability of electrodes in terms of repetitive uses was studied at 25 °C. For three different substrates, the responses of both enzyme electrodes did not change significantly within 40 uses. For the shelf life determination of the enzyme electrodes, the activities were characterized everyday for a week and then once in 5 days throughout 40 days.

#### **2.4.9.2. Immobilization of Polyphenol Oxidase**

##### **2.4.9.2.1. Preparation of Enzyme Electrodes (PPy/PPO, RPEO-co-PPy/PPO and ThPEO-co-PPy/PPO)**

For the immobilization of PPO in ThPEO/PPy matrix, a solution of 0.2 mg/mL PPO, 2mg/mL ThPEO, 1.2 mg/mL supporting electrolyte (SDS), 0.01 M pyrrole and 10 mL citrate buffer (pH 6.5) were put in a typical three electrode cell. Immobilization was carried out at a constant potential of +1.0 V for 20 min at room temperature.

Immobilization of PPO in PPy and RPEO/PPy matrices was achieved by electropolymerization of pyrrole on bare and previously RPEO coated platinum electrode. Enzyme electrode was prepared in 10 mL citrate buffer (pH 6.5) containing 1.2 mg/mL SDS supporting electrolyte, 0.01 M pyrrole and 0.2 mg/mL PPO. Immobilization was carried out at a constant potential of +1.0 V for 20min at room temperature. Enzyme electrodes were kept at 4 °C in citrate buffer solution when not in use.

### 2.4.9.2.2. Determination of PPO Activity

The activities of free and immobilized PPO were determined by using Besthorn Hydrazone method [197]. For the determination activity of immobilized PPO different concentrations of catechol were prepared (3.0mL) and put in water bath at 25 °C. 1 mL of 3-methyl-2-benzothiozolinone (MBTH) solution was added. In this method, MBTH interacts with the quinones produced by the enzyme to yield red products instead of brown color pigments in the absence of the color reagent [198]. Enzyme electrode was immersed in the solution and shaken for 5 min. 1mL sulfuric acid and 1mL acetone were added for a total volume of 6 mL. After mixing, absorbances were measured at 495 nm [199] (Figure 2.6).

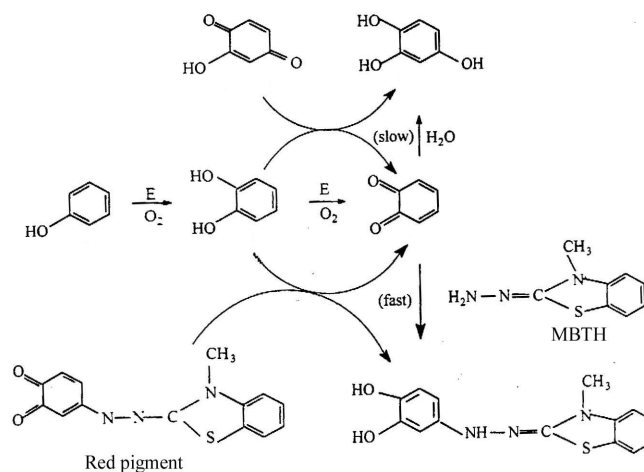


**Figure 2.6.** Assay reactions of PPO.

#### **2.4.9.2.3. Enzyme Activity Measurements for Free and Immobilized PPO**

In order to determine maximum velocity of the reaction ( $V_{max}$ ) and the Michaelis–Menten constant ( $K_m$ ) for each electrode, activity assay was applied with different concentrations of catechol solutions.

#### **2.4.9.2.4. Determination of Optimum pH and Temperature of Immobilized PPO**

Optimum temperature and pH determinations were carried out by changing incubation temperature and pH between 10–80 °C and 2–11, respectively while catechol concentration is 10  $K_m$ . The rest of the procedure was the same as the determination of PPO activity.

#### **2.4.9.2.5. Operational Stability and Shelf Life of Immobilized PPO**

The operational stability of enzyme electrode in terms of repetitive uses was studied by performing 40 successive measurements at 25 °C in one day.

For the shelf life determination of the enzyme electrodes, the activities were checked everyday for a week and then once in Five days throughout 40 days.

#### **2.4.9.2.6. Determination of Phenolic Compounds in Red Wines**

Immobilized enzyme electrodes were used to determine phenolic compounds in two kinds of Turkish red wines, Brand K and Brand D. Total phenolic compounds in wines produced in Turkey were reported as 2000-3000 mg/L [200-202]. Red wines are diluted with citrate buffer of pH 6.5 to a 1:3 volume and activity assay was applied as described in section 2.4.9.2.2.

#### **2.4.9.3. Protein Determination for Enzyme Electrodes**

Protein determination measurements were performed by Bradford's method [200]. Bradford's reagent was prepared by mixing 25mL phosphoric acid, 12.5 mL ethanol and 25 mg Coomassie Brilliant Blue (G-dye). The mixture was diluted to 50mL with distilled water. During measurements, a

solution of Bradford's reagent was prepared by mixing of one volume of stock solution with four volumes of distilled water.

For the preparation of protein calibration curve, bovine serum albumin (BSA) was used. Different concentrations of BSA were prepared as 1 mL. 2 mL of diluted Bradford's reagent was added to different concentrations of BSA solutions. The absorbance of these solutions was measured at 595 nm.

Since the protein entrapped in enzyme electrode can not be weighed, we measured the protein amount in the electrolysis solution before and after the electrolysis. The difference gives amount of protein entrapped in the enzyme electrode during the electrolysis.

## CHAPTER 3

### RESULTS AND DISCUSSION

#### 3.1. Conducting Copolymers

##### 3.1.1. Conducting Copolymers of Thiophene Ended Poly(Ethylene Oxide) (ThPEO) with Thiophene and Pyrrole

###### 3.1.1.1. Characterization of Thiophene Ended Poly(Ethylene Oxide) (ThPEO)

Thiophene ended Poly(Ethylene Oxide) was synthesized chemically. Figure 3.1 represents synthesis route of ThPEO.

###### 3.1.1.1.1. NMR Study of ThPEO

In  $^1\text{H}$  NMR spectrum of ThPEO, a signal was seen at 1.5 ppm due to the  $-\text{OH}$  group. Methylene protons attached to the thiophene give the peaks at 2.8 ppm. Also the other methylene protons attached to the oxygens yield the peaks at 3.65 ppm, and the peaks of repeating unit " $\text{CH}_2-\text{CH}_2-\text{O}$ " were obtained at 3.6 ppm. The protons which belong to the thiophene are 6.8, 6.9 and 7.1 ppm (Figure 3.2) [204].

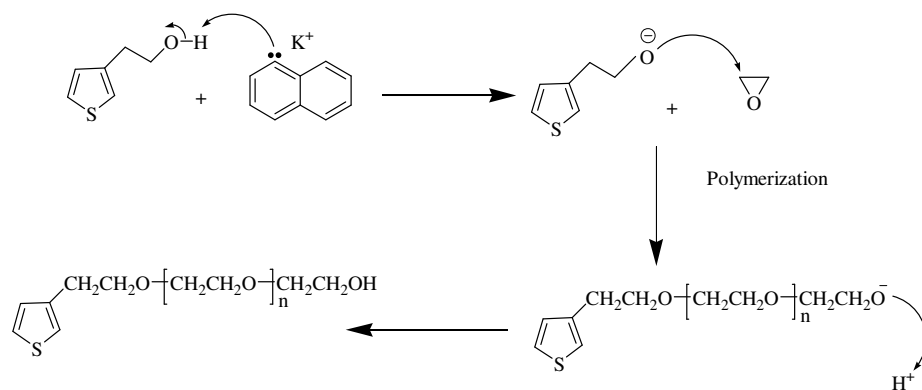


**Figure 3.1.** Chemical synthesis route of thiophene ended poly (ethylene oxide) (ThPEO).

#### 3.1.1.1.2. FTIR Study of ThPEO

The spectrum of ThPEO showed characteristic peaks of 1106 and 1250  $cm^{-1}$  due to the C–O–C symmetric and asymmetric stretchings. Absorption peak at 846  $cm^{-1}$  and at 740  $cm^{-1}$  are due to the thienylene C-H $_{\beta}$  and C-H $_{\alpha}$  stretching modes, respectively. Peaks positioned at 2930  $cm^{-1}$  reveal aromatic C–H and aliphatic C–H stretchings. The peak observed at 1639  $cm^{-1}$  is due to C=C stretchings in the thiophene. Also, O-H stretchings caused broad peak at 3414  $cm^{-1}$  (Figure 3.3).

#### 3.1.1.1.3. GPC Study of ThPEO

ThPEO also was characterized via GPC technique. Mn data of PEO is given at Table 3.1.

#### 3.1.1.1.4. Cyclic Voltammetry Study of ThPEO

Acetonitrile and water were used as the solvent and TBAFB was used as the supporting electrolyte for cyclic voltammetry studies. Measurements were carried out under  $N_2$  atmosphere in acetonitrile using potentials between 0 and 2.5 volts. As seen from Figure 3.4, ThPEO has no redox peak which implies that ThPEO is not an electroactive material.

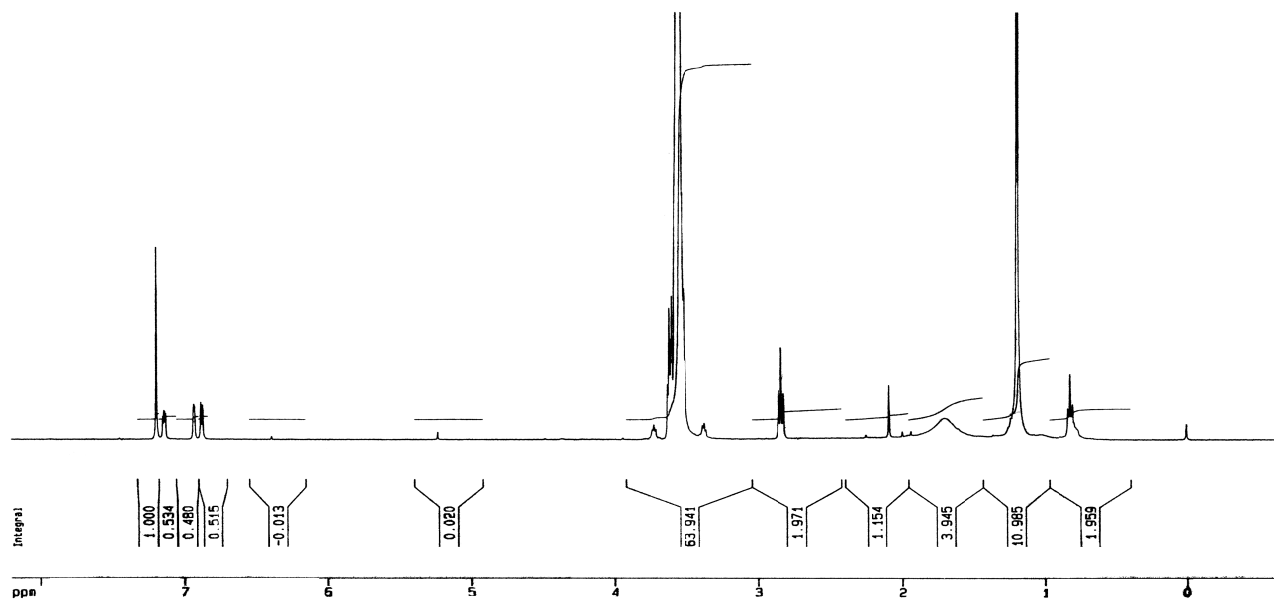


Figure 3.2. <sup>1</sup>H NMR spectrum of ThPEO

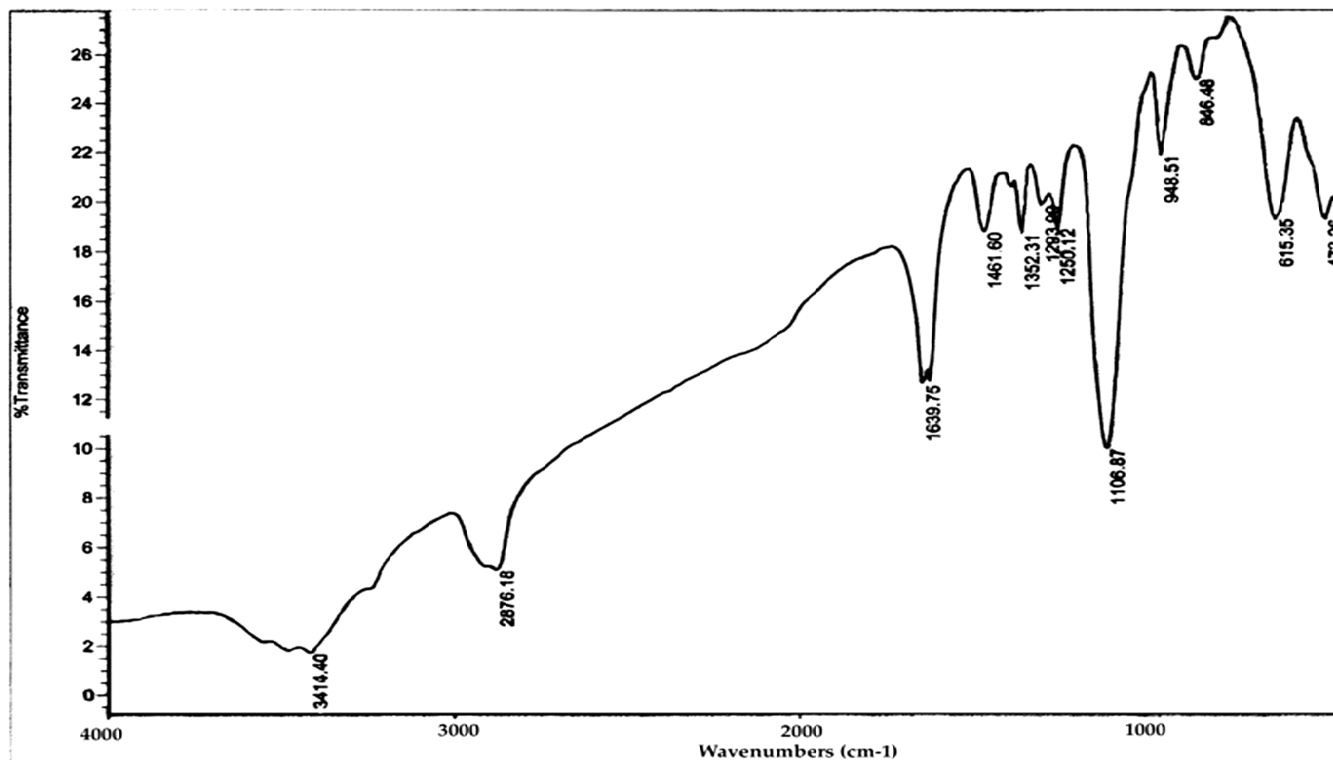


Figure 3.3. FTIR spectrum of ThPEO

**Table 3.1.** Synthesis of 3-thiophene-ended polyethyleneoxide

Code	Mn(GPC)	Mn(NMR)	Mn(Kinetic Calculation)	DP
ThPEO	1240	1096	1096	23

THF, 120 mL; 3-thiophene ethanol,  $13.5 \times 10^{-3}$  mol; potassium naphthalene,  $6.0 \times 10^{-3}$  mol; ethylene oxide,  $295 \times 10^{-3}$  mol.

### 3.1.1.2. Copolymers of PEO with Thiophene (ThPEO-co-PTh)

Electropolymerization of ThPEO was achieved in the presence of thiophene by constant potential electrolysis. Measurements were carried out under  $N_2$  atmosphere in conventional three-electrode cell. Constant potential electrolyses were run at 1.9 volt for 30 minutes. (Figure 3.5).

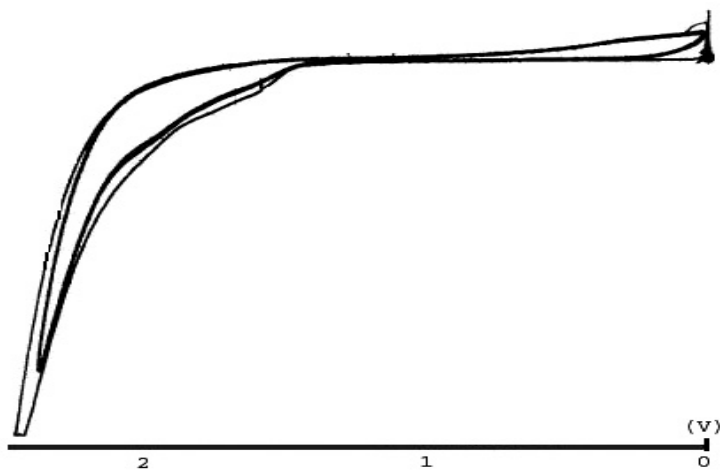


**Figure 3.4.** Cyclic voltammogram of ThPEO.

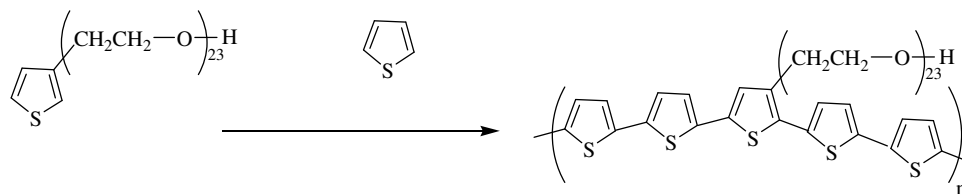


**Figure 3.5.** Electrochemical synthesis route for copolymerization of ThPEO-co-PTh.

### 3.1.1.2.2. FTIR Study of ThPEO-co-PTh

The copolymer spectrum exhibited the characteristic peaks of pristine polymer (ThPEO). Disappearance of the thiophene out of plane C–H stretching and in-plane C–H deformations, evolution of the new absorption peaks at  $858\text{ cm}^{-1}$  (three substituted thiophene), at  $1634\text{ cm}^{-1}$  (polyconjugation) at  $1121\text{ cm}^{-1}$  (C–O–C symmetric and asymmetric stretchings) and a shoulder at  $1080\text{ cm}^{-1}$  (dopant anion) and at  $1402\text{ cm}^{-1}$  (–OH group) were considered to be due to polymerization (Figure 3.6). Also because of the intramolecular hydrogen bond in the group, sharp peak at  $3424\text{ cm}^{-1}$  was observed.

### 3.1.1.2.1. Cyclic Voltammetry Study of ThPEO-co-PTh

As given in Figure 3.4, ThPEO is not electroactive. However, with the addition of thiophene to the solution, in the first run a peak at 1.8 V was observed. There was a gradual shift to 1.75 V throughout 20 runs. After the 20th run, there was no change in the peak height. This may be due to the growth of copolymer chains to a certain extent, where after stops, implying that copolymerization yields oligomers of certain sizes which then go into the solution without having a chance for further propagation (Figure 3.7 b)

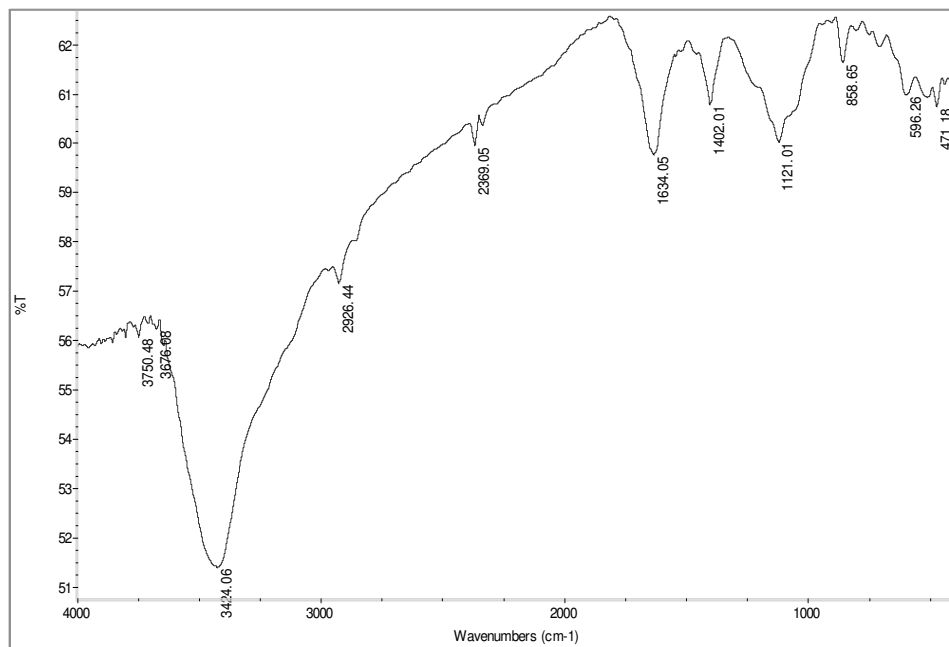


**Figure 3.6.** FTIR spectrum of ThPEO-co-PTh in AN-TBABF medium.

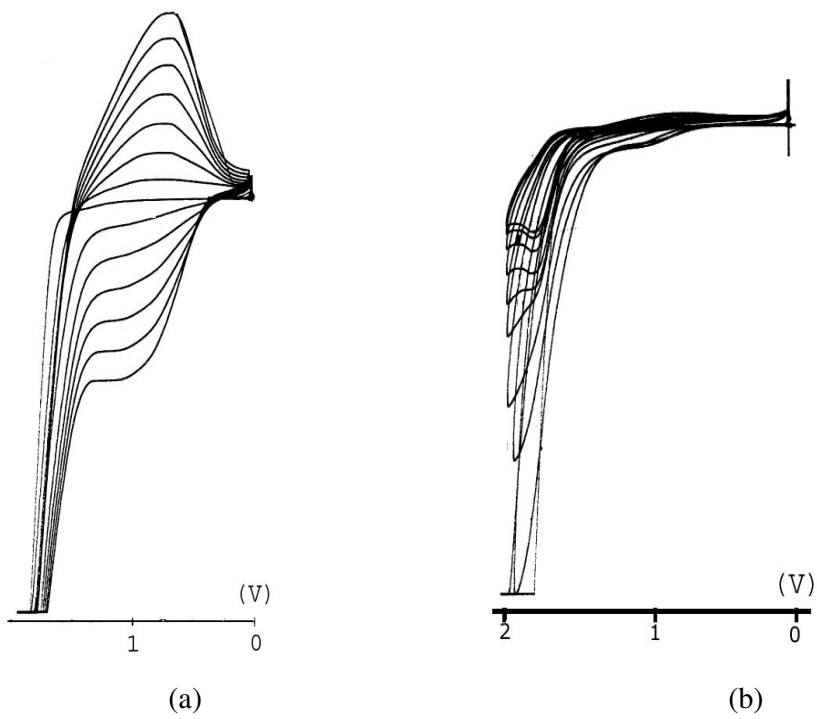


**Figure 3.7.** Cyclic voltammograms of a) PTh, b) ThPEO-co-PTh.

### 3.1.1.2.3. Morphologies of ThPEO-co-PTh Films

The structure of electrode side of ThPEO-co-PTh is smooth. The morphology of the solution side of ThPEO-co-PTh has cauliflower like structure. It has more compact globules than that of pure PTh. This may reveal that a copolymer was synthesized different than pure PTh (Figure 3.8).

### 3.1.1.2.4. Conductivity of ThPEO-co-PTh Film

Electrical conductivity measurements were carried out by using standard four-probe technique. For  $\text{BF}_4^-$  doped copolymer film, conductivities of the solution and electrode sides of the copolymer films were found to be  $0.8 \text{ S cm}^{-1}$ .

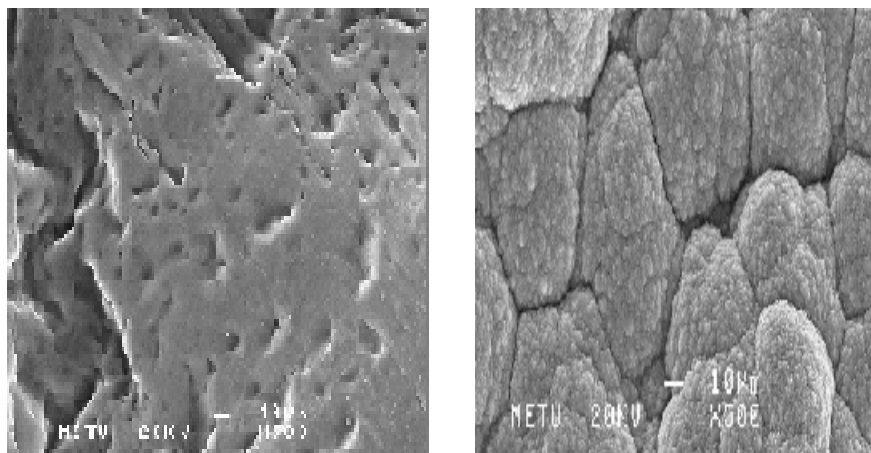


**Figure 3.8.** Scanning electron micrographs of a) ThPEO-co-PTh (electrode side), b) ThPEO-co-PTh (solution side).

### 3.1.1.2.5. Electrochromic Studies of ThPEO-co-PTh

Spectroelectrochemical studies were carried out to determine spectroelectrochemical and electrochromic properties of resulting copolymer, ThPEO-co-PTh polymerized potentiostatically on ITO-coated glass slides in BFEE [205]. At voltages between 0.0 and 0.9V, ThPEO-co-PTh layer has an absorptive brick red color with the  $\pi$ - $\pi^*$  transition at 515 nm. The polaron charge carrier band was detected at 740 nm. The electronic band gap defined as the onset energy for  $\pi$ - $\pi^*$  transition (Figure 3.9) was calculated as 1.95 eV. The film was switched between neutral state (brick red color) and fully oxidized state (greenish-blue colour). Films are seen to exhibit distinctive color changes upon doping and dedoping and this fact was confirmed by the differences in L (relative luminance) and the a and b values (CIE color space) (Figure 3.10 and 3.11) of pure PTh and ThPEO-co-PTh (Table 3.2).

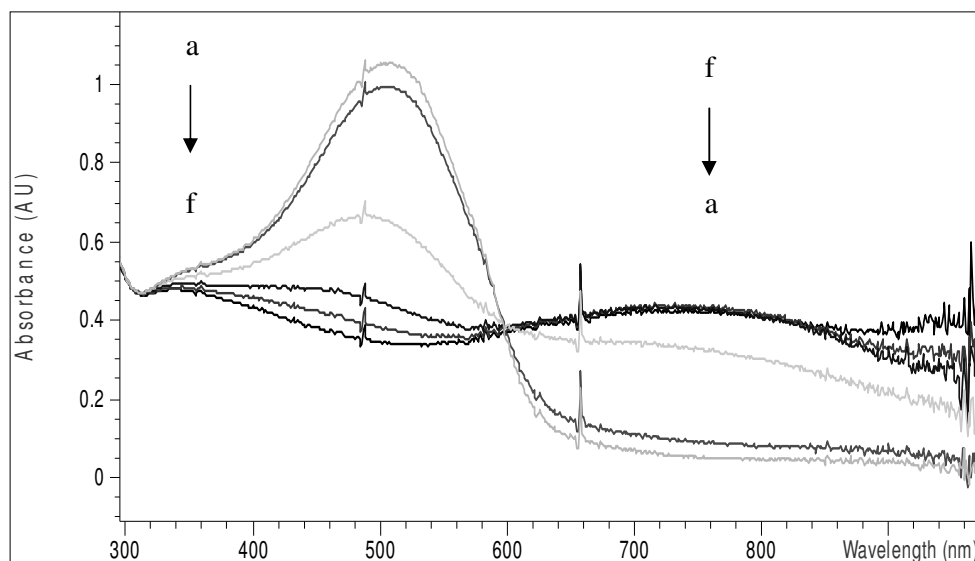


**Figure 3.9.** Spectroelectrochemical studies on ThPEO-co-PTh (a: 1.0 V; b: 0.9 V; c: 0.8 V; d: 0.6 V; e: 0.4 V; f: 0.2 V).

**Table 3.2.** Electrochemical, electronic and electrochromic properties of PTh and ThPEO-co-PTh.

	$\lambda_{max}$ (nm)	$L$	$a$	$b$	$E_g$ (eV)
PTh	495	(ox) 57	(ox) - 7	(ox) - 2	1.92
		(red) 51	(red) 52	(red) 46	
ThPEO-co-PTh	515	(ox) 52	(ox) - 10	(ox) - 4	1.95
		(red) 60	(red) 61	(red) 27	

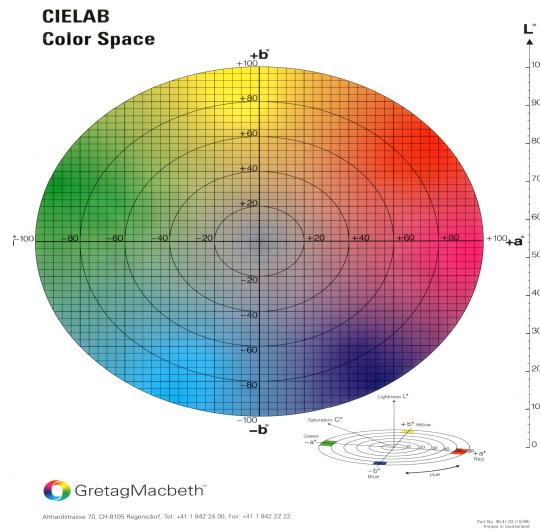


**Figure 3.10.** CIE color space.

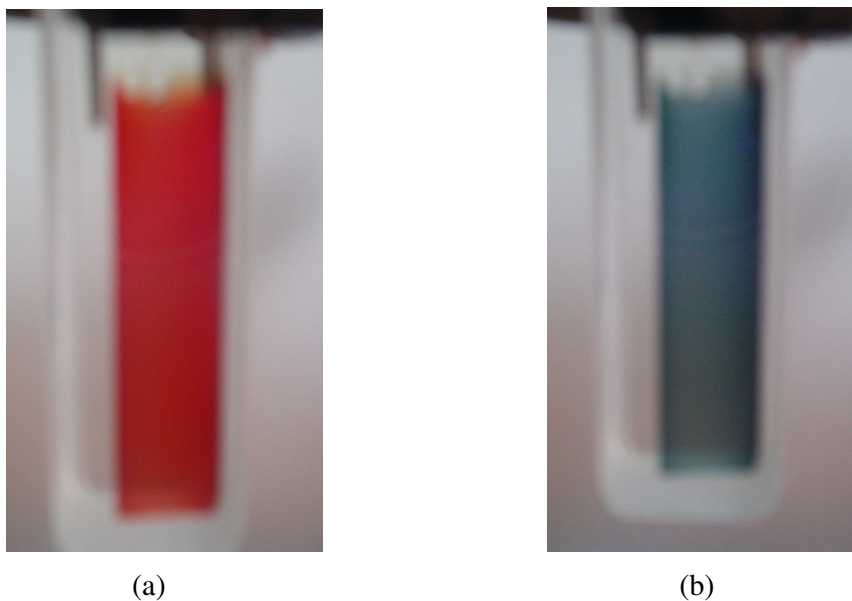


**Figure 3.11.** Photographs of a) reduced state of ThPEO-co-PTh and b) oxidized state of ThPEO-co-PTh.

### 3.1.1.3. Copolymers of ThPEO with Pyrrole (ThPEO-co-PPy)

Electropolymerization of ThPEO was achieved in the presence of pyrrole by constant potential electrolysis (Figure 3.12).

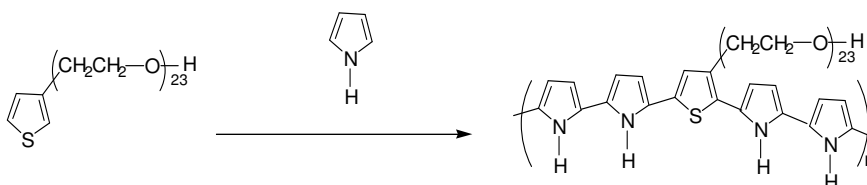


**Figure 3.12.** Electrochemical synthesis route for copolymerization.

### 3.1.1.3.1. FTIR Study of ThPEO-co-PPy

The copolymer spectrum exhibited the characteristic peaks of pristine polymer (ThPEO). FTIR spectra of SDS doped ThPEO-co-PPy showed peaks at  $1466\text{ cm}^{-1}$  due to C-N and C-C stretchings which are characteristic for PPy. The broad band related to C-O-C stretching is present at about  $1220\text{ cm}^{-1}$ . The peak of dopant ion is observed at  $1077\text{ cm}^{-1}$ . Also a shoulder at  $3500\text{ cm}^{-1}$  is coming from N-H stretchings and two sharp peaks at  $2852\text{ cm}^{-1}$  and  $2989\text{ cm}^{-1}$  are reason of  $\text{CH}_2$  stretchings (Figure 3.13).

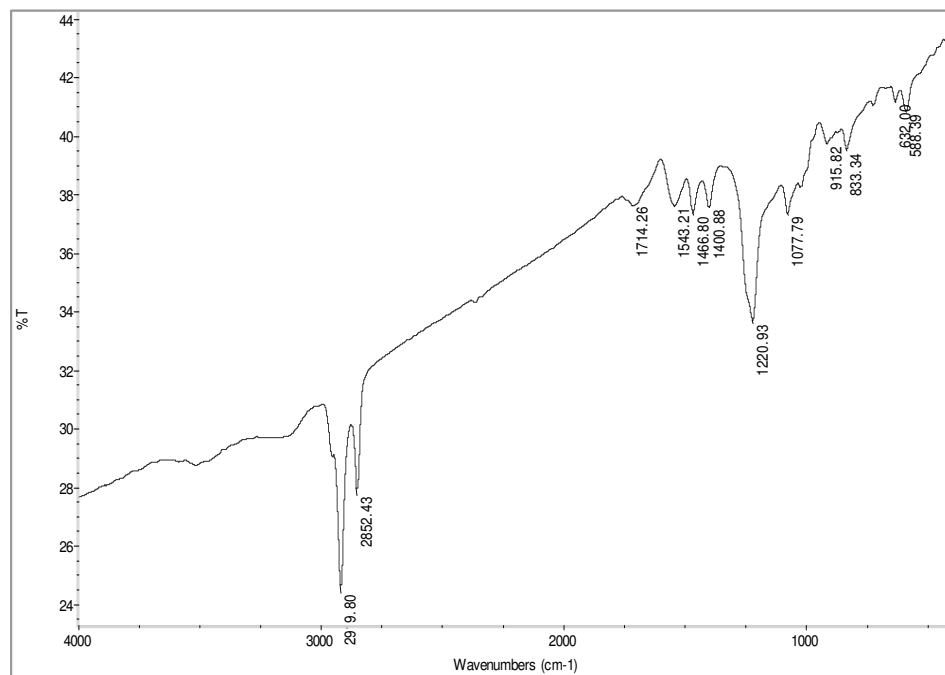


**Figure 3.13.** FTIR spectrum of ThPEO-co-PPy in water-SDS medium.

### 3.1.1.3.2. Cyclic Voltammetry Study of ThPEO-co-PPy

In the presence of pyrrole, at the first run a peak at 1.1V was observed (Fig. 3.14 a). With the further runs a redox couple below 1V was appeared. These redox peaks for ThPEO-co- PPy were narrower than that of pure PPy (Figure 3.14 b). Also the increase in the increments between the consecutive cycles and the oxidation–reduction potentials of the material were different. These events show us that electro-copolymerization between ThPEO and pyrrole occurs and the product does not behave like pure polypyrrole.

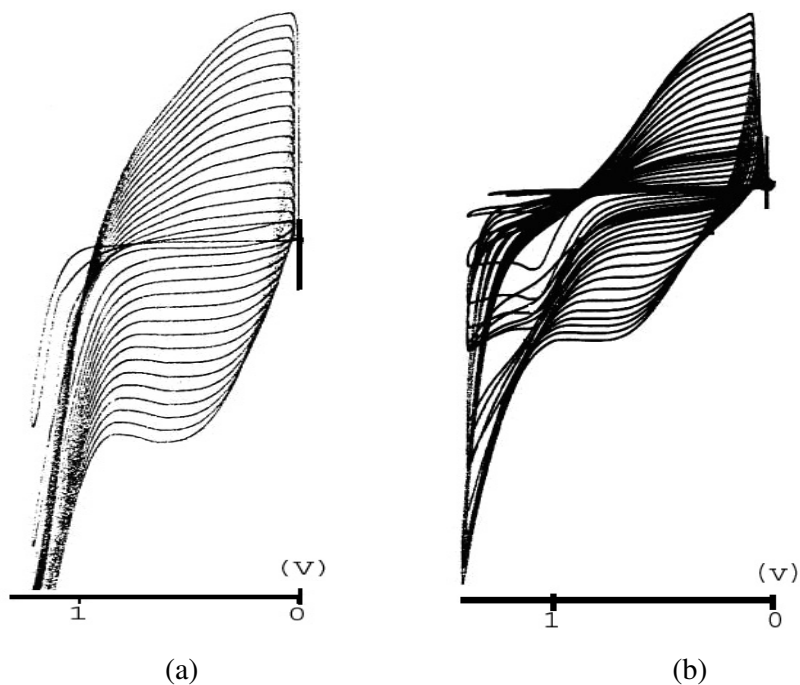


**Figure 3.14.** Cyclic voltammograms of a) PPy, b) ThPEO-co-PPy.

### 3.1.1.3.3. Morphologies of the ThPEO-co-PPy Films

The solution side of ThPEO-co-PPy showed cauliflower like structure. However, the electrode side of the ThPEO-co-PPy was not smooth as is the case for PPy. This proves that a new copolymer product was synthesized different than pure PPy (Fig. 3.15 a and b).

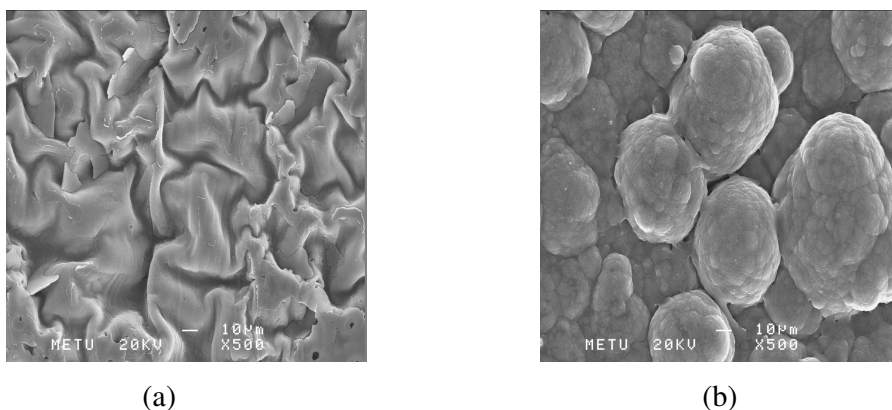


**Figure 3.15.** Scanning electron micrographs of a) ThPEO-co-PPy (electrode side), b) ThPEO-co-PPy (solution side).

### 3.1.1.3.4. Conductivity Measurements of ThPEO-co-PPy Film

Electrical conductivity measurements were carried out by using standard four-probe technique. For SDS doped copolymer film, conductivities of the solution and electrode sides of the copolymer films were found to be  $0.45 \text{ S cm}^{-1}$ .

### 3.1.2. Conducting Copolymers of Random Copolymer (RPEO) of 3-Methylthienyl Methacrylate and p-Vinylbenzyloxy Poly(Ethylene Oxide) with Thiophene and Pyrrole

#### 3.1.2.1. Characterization of 3-Methylthienyl Methacrylate

Synthesis of 3-methylthienyl methacrylate was explained in part 2.4.2.1. Characterization of this monomer was done using <sup>1</sup>HNMR. Table 3.3 shows the characteristic peaks for this monomer.

**Table 3.3.** The <sup>1</sup>HNMR spectrum of 3-methylthienyl methacrylate.

$\delta$ (ppm)	Assignment
1.9	s, 3H, CH <sub>3</sub>
5.1	d, 2H, OCH <sub>2</sub>
5.5	d, 2H, vinyl H
6.1	d, 2H, vinyl H
7.06	m, 2H, ring H
7.2	m, 1H, ring H

#### 3.1.2.2. Characterization of p-Vinylbenzyloxy Poly(Ethylene Oxide) (PEO-VB)

PEO macromonomers possessing p-vinylbenzyl end-group was prepared by a conventional high vacuum line technique. Synthesis route of PEO-OVB was shown in Figure 2.4. The characterization of PEO-OVB was done by <sup>1</sup>HNMR (Table 3.4) (Figure 3.16) [206].

**Table 3.4.**  $^1\text{H}$ NMR peaks of (PEO-OVB).

$\delta$ (ppm)	Assignment
3.3	s, 3H, $\text{OCH}_3$
3.8	m, 80H, $\text{OCH}_2\text{CH}_2$
4.5	s, 2H, $\text{OCH}_2$
5.4	t, 1H, vinyl H
5.6	t, 1H, vinyl H
6.7	t, 1H, vinyl H
7.2	m, 2H, ring H
7.4	m, 2H, ring H

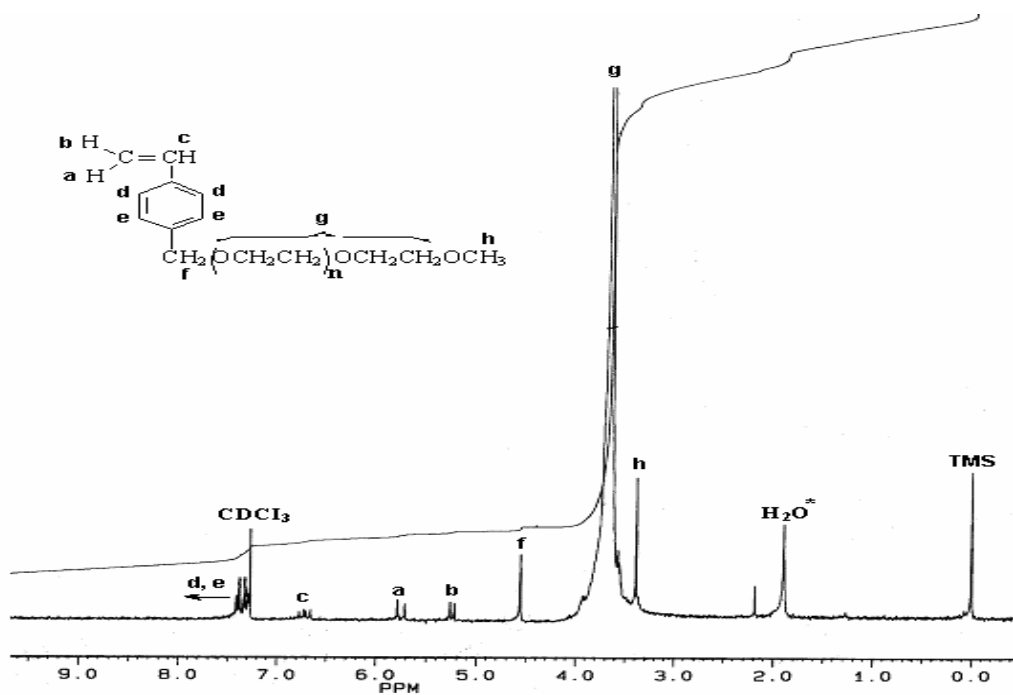


**Figure 3.16.**  $^1\text{H}$ NMR spectrum of PEO-OVB.

### 3.1.2.3. Characterization of Random Copolymer (RPEO) of 3-Methylthienyl Methacrylate and p-Vinylbenzyloxy Poly(Ethylene Oxide)

RPEO was synthesized using AIBN. The route of synthesis for RPEO was shown in Figure 2.5. RPEO was characterized by <sup>1</sup>HNMR, FTIR and GPC techniques.

#### 3.1.2.3.1. GPC Studies of RPEO

The GPC data of RPEO are showed in Table 3.5.

**Table 3.5.** Preparation of random copolymer (RPEO) of 3-methylthienyl methacrylate and PEO –VB.

Code	Time (h)	Random Copolymer composition RPEO (Mol %)		Conversion (%)	<i>M<sub>n</sub></i>	<i>M<sub>w</sub>/M<sub>n</sub></i>
		MTM	PEO-VB			
RPE O	3	91	9	62	13835	1.14

[AIBN] =  $2.8 \times 10^{-2}$  molL<sup>-1</sup>, [MTM] =  $5.5 \times 10^{-1}$  molL<sup>-1</sup>, Temp. = 80 °C.

#### 3.1.2.3.2. <sup>1</sup>HNMR Study of RPEO

<sup>1</sup>HNMR peaks of RPEO are showed in Table 3.6.

**Table 3.6.**  $^1\text{H}$ NMR peaks of RPEO.

$\delta$ (ppm)	Assignment
0.9	s, 3H, $\text{CH}_3$
1.2	m, 2H, vinyl H
1.3	m, 2H, vinyl H
2.2	m, 1H, vinyl H
3.3	s, 3H, O- $\text{CH}_3$
3.6	m, 80H, $\text{OCH}_2\text{CH}_2$
4.5	s, 2H, $\text{CH}_2$
4.8	m, 2H, benzylic $\text{CH}_2$
6.8	m, 1H, thienyl ring
6.9	m, 2H, thienyl ring
7.15	m, 2H, benzyl ring
7.2	m, 2H, benzyl ring

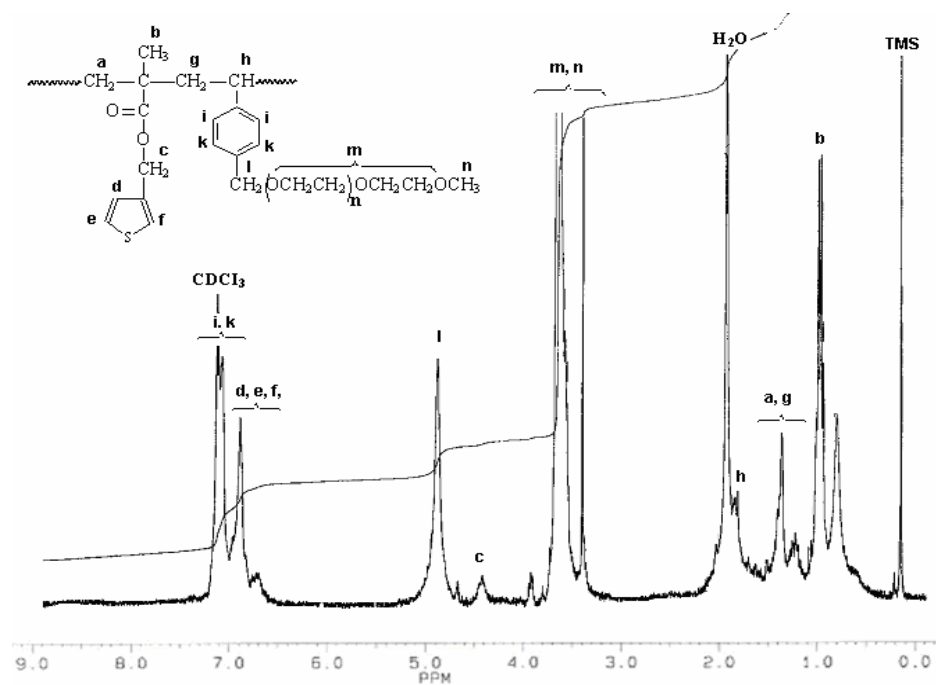


**Figure 3.17.**  $^1\text{H}$ NMR spectrum of RPEO.

### 3.1.2.3.3. FTIR Study of RPEO

The FTIR spectrum of the precursor copolymer (RPEO) was recorded on a Nicolet 510 FTIR spectrometer. Characteristic C-O-C asymmetric stretching peaks were detected at  $1146\text{ cm}^{-1}$ ,  $1114\text{ cm}^{-1}$ , and  $1061\text{ cm}^{-1}$ . The peaks at  $1230\text{ cm}^{-1}$  and  $1241\text{ cm}^{-1}$  are due to O=C-O-C stretching. The sharp intense peak at  $1726\text{ cm}^{-1}$  can be attributed to the carbonyl stretching vibrations. The peaks of  $\text{CH}_\alpha$  stretching and  $\text{CH}_\beta$  stretchings of Th moieties are at  $786\text{ cm}^{-1}$  and  $842\text{ cm}^{-1}$  respectively. Also the peak observed at  $2886\text{ cm}^{-1}$  is coming from C-H bending of  $\text{CH}_3$ ,  $\text{CH}_2$  groups. Also the peak at  $1467\text{ cm}^{-1}$  is due to the aliphatic  $\text{CH}_2$  vibrations (Figure 3.18).

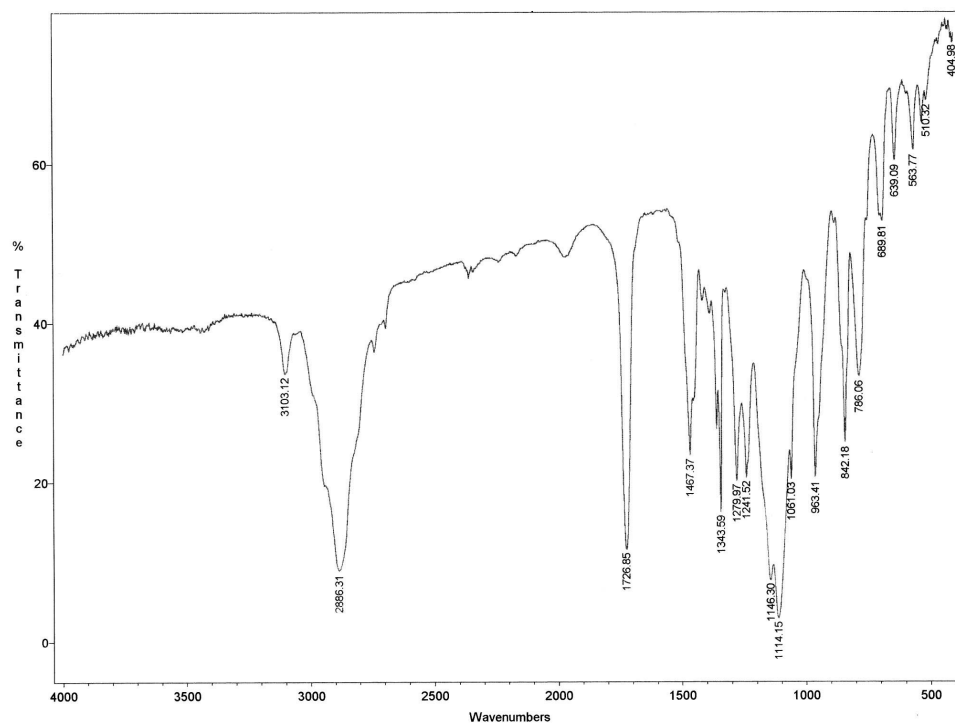
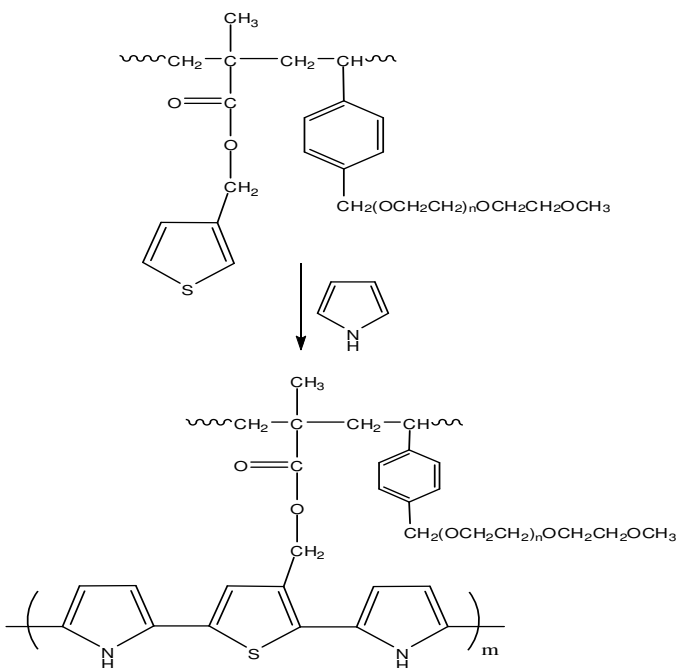


Figure 3.18. FTIR spectrum of RPEO.

### 3.1.2.4. Copolymerization of RPEO with Pyrrole (RPEO-co-PPy)

Electrocopolymerization of RPEO was achieved in the presence of pyrrole by constant potential electrolysis (under 1.1 V constant potential) (Figure 3.19).



**Figure 3.19.** Electrochemical synthesis route for RPEO-co-PPy.

#### 3.1.2.4.1. FTIR Study of RPEO-co-PPy

FTIR spectra of electrochemically synthesized copolymers of SDS doped RPEO-co-PPy revealed a peak at  $1715\text{ cm}^{-1}$  representing to the carbonyl group.

In addition, O=C-O-C and C-O-C stretchings are at  $1256\text{ cm}^{-1}$  and  $1084\text{ cm}^{-1}$  respectively. The peaks at  $1627\text{ cm}^{-1}$  and  $3421\text{ cm}^{-1}$  were due to the pyrrole chains. These data prove that RPEO-co-PPy copolymerization occurred successfully (Figure 3.20).

In the FTIR spectrum of PTSA doped RPEO-co-PPy, carbonyl group at  $1736\text{ cm}^{-1}$  is present. The peaks at  $1646\text{ cm}^{-1}$  and  $3408\text{ cm}^{-1}$  belong to pyrrole ring. The peaks at  $1237\text{ cm}^{-1}$  and  $1124\text{ cm}^{-1}$  are arising from O=C-O-C and C-O-C stretchings respectively. These data support the synthesis of RPEO-co-PPy copolymers (Figure 3.21)

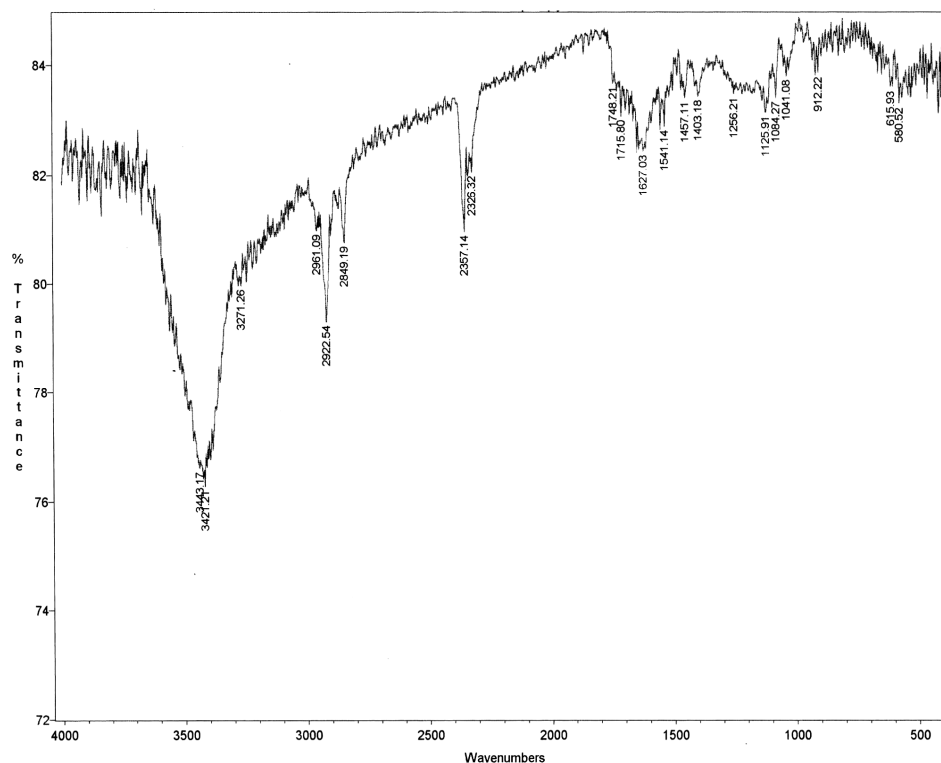


**Figure 3.20.** FTIR spectrum of RPEO-co-PPy in water-SDS medium.

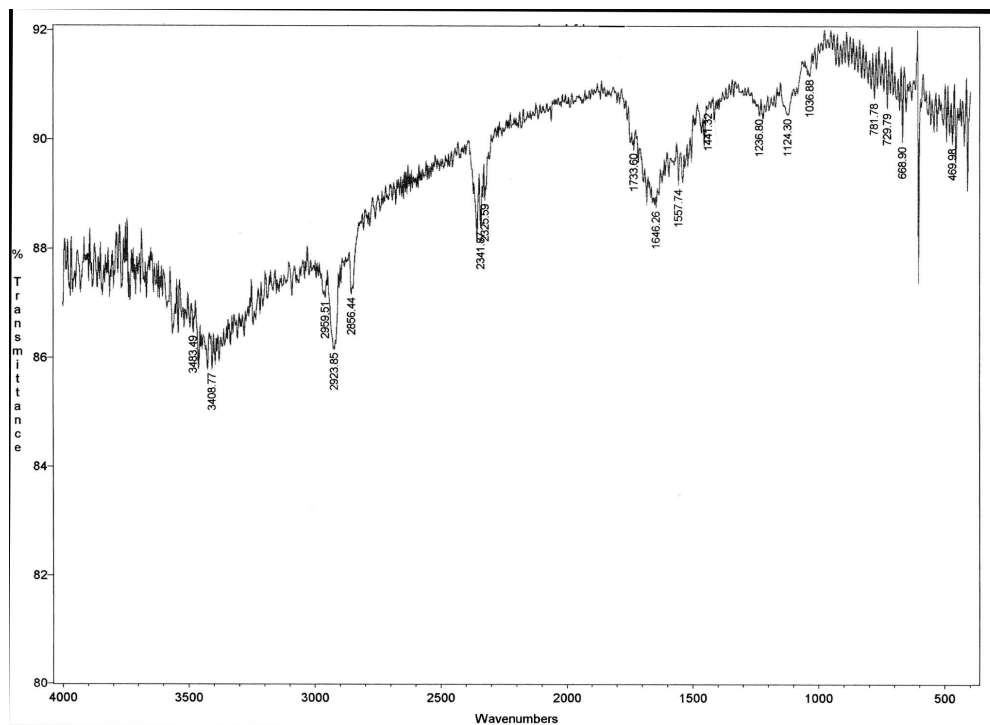


**Figure 3.21.** FTIR spectrum of RPEO-co-PPy in water-PTSA medium.

#### 3.1.2.4.2. Cyclic Voltammetry Study of RPEO-co-PPy

The pristine RPEO polymer is not electroactive. However, after introducing Py into the solution, an increasing redox peaks showing the increase in electroactivity with increasing scan number were observed. When voltammogram of RPEO in the presence of Py was compared with the voltammogram of pure PPy, two important differences were observed. The redox peaks of RPEO-co-PPy system were narrower than that of pure PPy. Also the first few scans did not reveal any electroactivity. These events prove us that electrocopolymerization between RPEO and Py is taking place and the product

(graft copolymer of RPEO-co-PPy) naturally does not behave like the pure PPy in voltammograms (Figure 3.22).

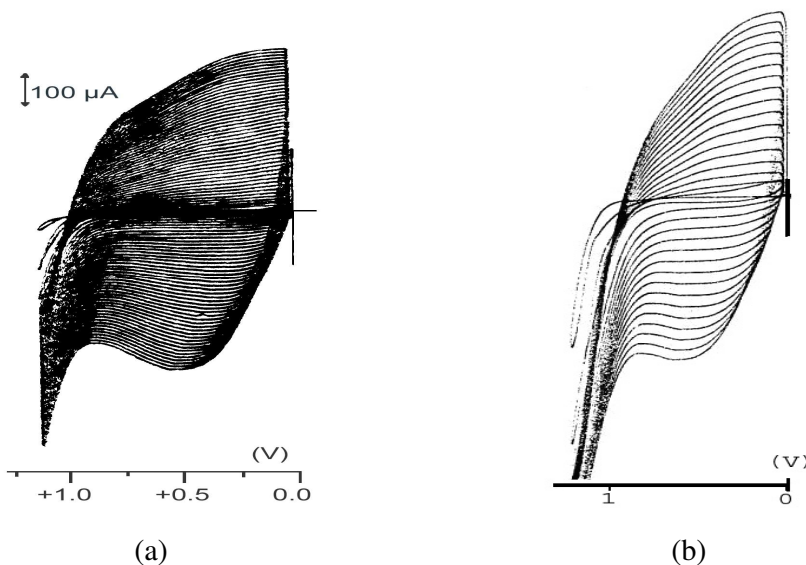
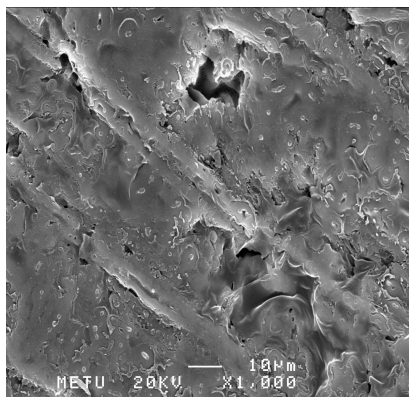


**Figure 3.22.** Cyclic voltammograms of a) RPEO-co-PPy and b) PPy.

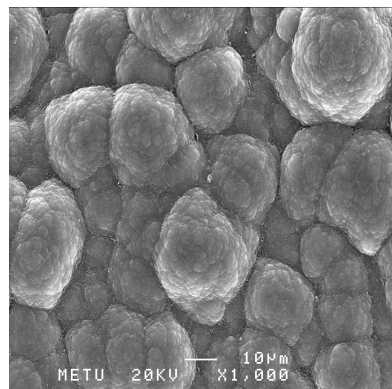
#### 3.1.2.4.3. Morphologies of RPEO-co-PPy Films

The morphologies of the copolymer films were investigated by scanning electron microscopy studies (SEM). JSM 6400 scanning electron microscope was used for this purpose.

The morphologies of the solution sides of RPEO/PPy copolymer synthesized in water-SDS and water-PTSA media, have cauliflowerlike structure. Yet, they have more compact globules than that of pure PPy. Also it can be said that the electrode side of the RPEO-co-PPy films was different from that of polypyrrole (Figures 3.23 and 3.24).

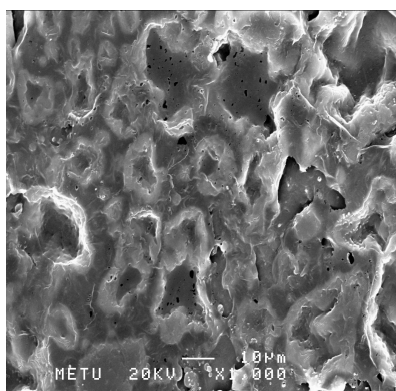


(a)

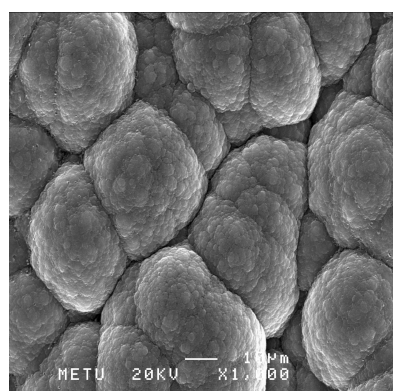


(b)

**Figure 3.23.** SEM micrographs of (a) electrode side of RPEO-co-PPy;  
(b) solution side of RPEO-co-PPy in water-PTSA medium.



(a)



(b)

**Figure 3.24.** SEM micrographs of (a) electrode side of RPEO-co-PPy;  
(b) solution side of RPEO-co-PPy in water-SDS medium.

#### 3.1.2.4.4. Conductivity Measurements of RPEO-co-PPy

Conductivities of the solution and electrode sides of the copolymer films were found to be the same. The conductivities of copolymers of RPEO/PPy synthesized in water-SDS and water-PTSA solvent-electrolyte couples are 0.3 S/cm and 0.7 S/cm respectively.

#### 3.1.2.5. Copolymerization of RPEO with Thiophene

Electropolymerization of RPEO was achieved in the presence of thiophene by constant potential electrolysis (Figure 3.25).

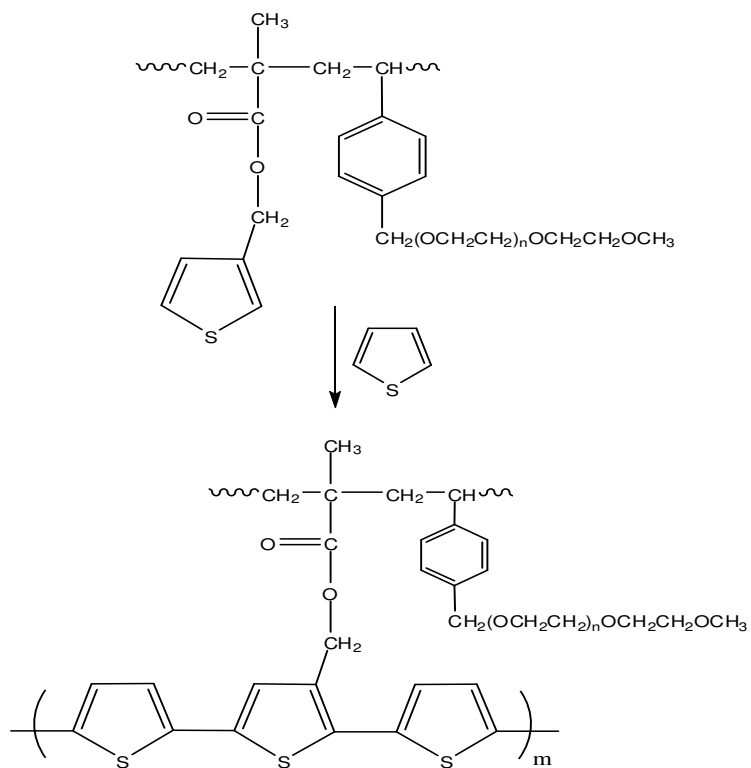


**Figure 3.25.** Electrochemical synthesis route for RPEO-co-PTh.

### 3.1.2.5.1. FTIR Study of RPEO-co-PTh

FTIR spectrum of  $\text{BF}_4^-$  doped RPEO-co-PTh showed a characteristic peak of C-O-C at  $1124\text{ cm}^{-1}$ . O=C-O-C stretching gave a peak at  $1397\text{ cm}^{-1}$ . The peak at  $871\text{ cm}^{-1}$  belongs to thiophene group. Also the peak observed at  $2883\text{ cm}^{-1}$  is coming from C-H bending of  $\text{CH}_3$ ,  $\text{CH}_2$  groups. Moreover, the characteristic peak of carbonyl group at  $1676\text{ cm}^{-1}$  was observed. This spectrum supports the synthesis of RPEO-co-PTh copolymers (Figure 3.26).

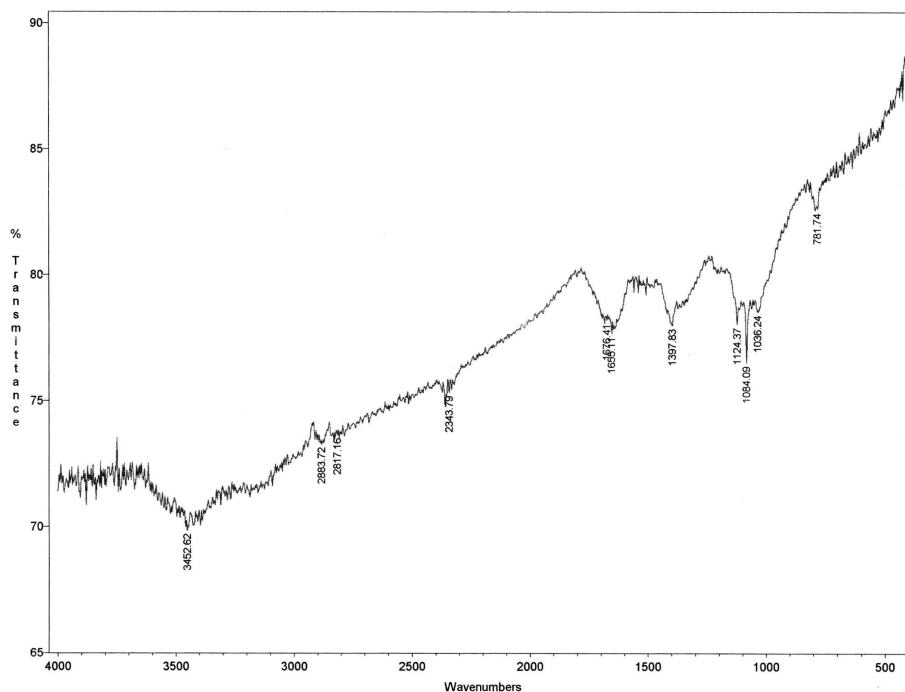


**Figure 3.26.** FTIR spectrum of RPEO-co-PTh in AN-TBAFB medium.

### 3.1.2.5.2. Cyclic Voltammetry Study of RPEO-co-PTh

A similar trend like addition of Py into the solution was seen upon addition of Th into the solution containing RPEO. When the voltammogram of RPEO/PTh was compared with that of pure Th system, it is seen that the redox

peaks of RPEO/PTh were narrower than that of pure PTh and a tilt was observed for the redox couple on the voltammogram of RPEO/PTh. These differences reveal that a reaction between RPEO and PTh occurs (Figure 3.27).

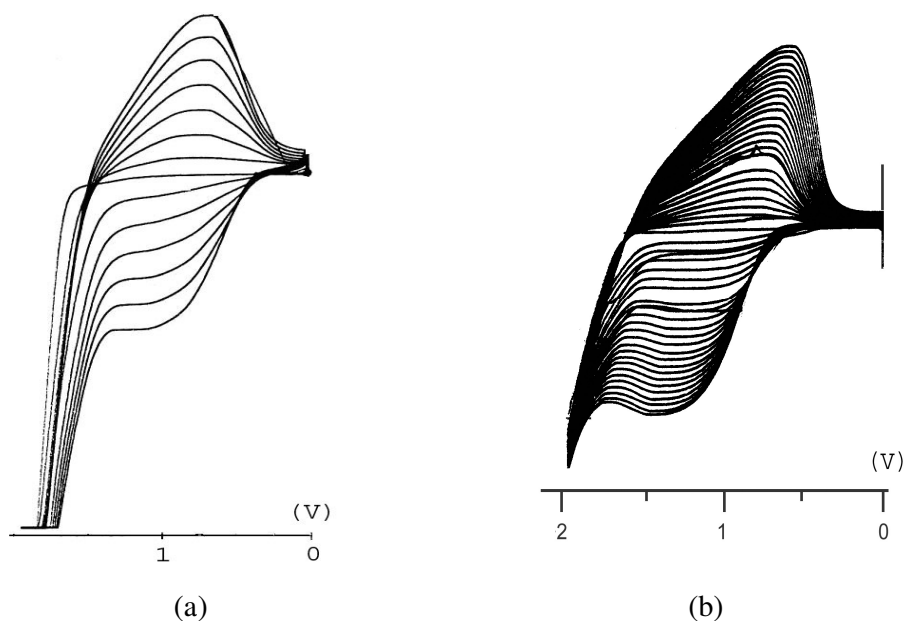


**Figure 3.27.** Cyclic voltammograms of a) PTh and b) RPEO-co-PTh.

### 3.1.2.5.3. Morphologies of the RPEO-co-PTh Films

The morphologies of the copolymer films were investigated by scanning electron microscopy studies (SEM). JSM 6400 scanning electron microscope was used for this purpose.

As far as the SEM micrographs of RPEO-co-PTh films are concerned, solution side morphologies of RPEO-co-PTh (Figure 3.28 (b)) species are

significantly different from standard cauliflower like structure. This provides yet another evidence that a new copolymer was synthesized.

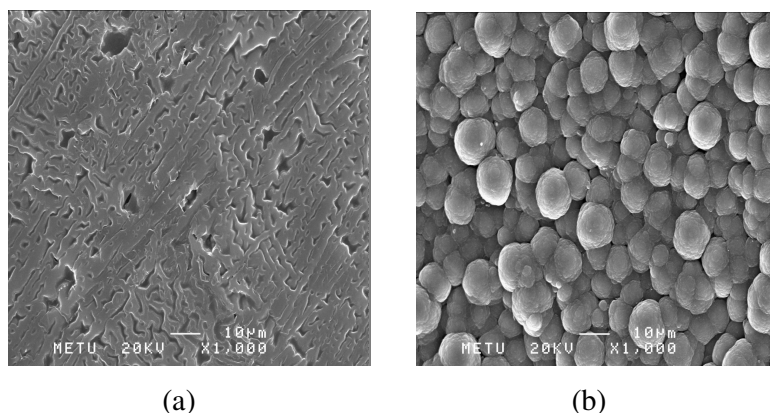


**Figure 3.28.** SEM micrographs of (a) electrode side of RPEO-co-PTh; (b) solution side of RPEO-co-PTh in AN-TBAFB medium.

#### 3.1.2.5.4. Conductivity Measurements of RPEO-co-PTh

The conductivity of copolymer of RPEO/PPy synthesized in AN-TBAFB solvent-electrolyte couple are 0.4 S/cm.

#### 3.1.2.5.5. Electrochromic Studies of RPEO-co-PTh

In order to obtain information on the spectroelectrochemical and electrochromic properties of the resulting graft copolymers, films were prepared by performing the polymerization on ITO-coated glass slides in BFEE potentiostatically at 1.4 V. At different potentials, a series of UV-Vis spectra were run. The  $\lambda_{\text{max}}$  values for the  $\pi$ - $\pi^*$  transitions in the neutral state of RPEO-co-PTh was found to be 510 nm (Table 3.7). For comparison, the values for the

PTh under the same conditions, 495 nm, is also given the Table 1. The electronic band gaps defined as the onset energy for the  $\pi$ - $\pi^*$  transition, are at 1.92 eV for PTh and at 1.97 eV for RPEO-co-PTh ( Table 3.7). This film was switched between the neutral (red color) and fully oxidized (blue color) states. With the applied voltage, the evolution of new absorption band ; the polaron band at 770 nm was observed while the intensity of the 510 nm band decreases. As the charge carrier bands at longer wavelengths (lower energy) increase in intensity with the application of increasing positive potentials with suitable increments, the  $\pi$ - $\pi^*$  transitions currently decrease. This strong shift of the maximum absorption upon applied voltage is related to the electrochromic property of the polymer. The spectra for PTh and RPEO-co-PTh are similar but different in the ratio of polaronic states accessed in the fully oxidized polymers (Figure 3.29). Colorimetry measurements were performed on the films in an electrolyte solution of TBAFB (0.1 M)/ AN/ BFEE and films were synthesized in BFEE. The relative luminescence (L) and the a, b- values (CIE color space) were measured at the fully oxidized and neutral states. The color of the copolymer film switches from transmissive blue in the oxidized form to brick red in the reduced (neutral) form (Figure 3.30).

**Table 3.7.** Electrochemical, electronic and electrochromic properties of PTh and RPEO/PTh.

	$\lambda_{max} (nm)$	<i>L</i>	<i>a</i>	<i>b</i>	<i>E<sub>g</sub>(eV)</i>
<b>PTh</b>	495	(ox) 57	(ox) – 7	(ox) –2	1.92
		(red) 51	(red) 52	(red) 46	
RPEO/PTh	510	(ox) 34	(ox) – 5	(ox) – 7	1.97
		(red) 44	(red) 19	(red) 13	

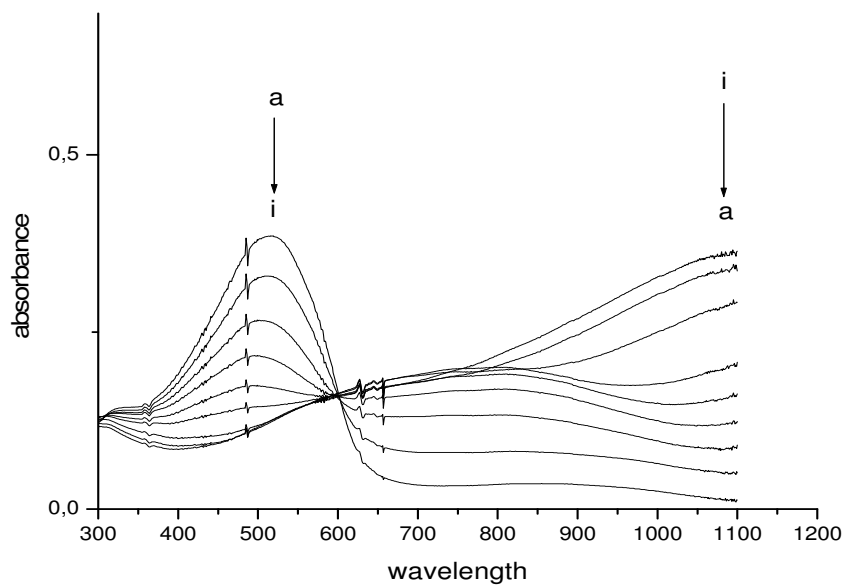


**Figure 3.29.** Spectroelectrochemical spectrum of RPEO/PTh (a: 0.2 V, b: 0.4 V, c: 0.5 V, d: 0.6 V, e: 0.7 V, f: 0.8 V, g: 1.0 V, h: 1.2 V, i: 1.4 V).

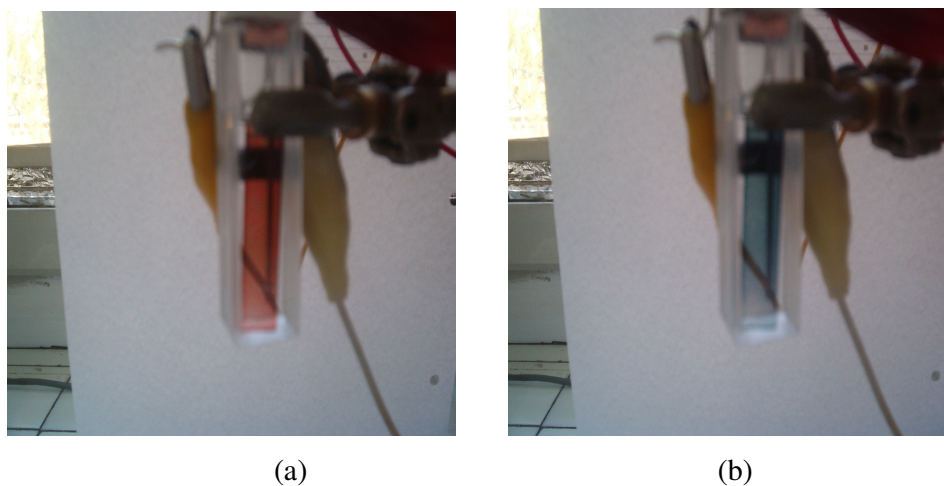


**Figure 3.30.** The photographs of a) reduced state of RPEO-co-PTh and b) oxidized state of RPEO-co-PTh.

## 3.2. Enzyme Immobilization Studies

### 3.2.1. Immobilization of Alcohol Oxidase

RPEO-co-PPy and PPy were used as the supporting materials to immobilize alcohol oxidase. Immobilization was achieved by electrochemical polymerization. This study describes a spectrophotometric method, Jansenn's Method, based on a bienzymatic system for the determination of primary alcohols. This method was described in section 2.4.9.1.2. It comprises the alcohol oxidase (AOX) and peroxidase (POD) enzymes, where POD further reduces  $\text{H}_2\text{O}_2$  produced by AOX during the oxidation of primary alcohol to  $\text{H}_2\text{O}$  at the expense of hydrogen donor molecules. A chromagenic substrate, *o*-dianisidine, was used (Figure 3.31 and 3.32). Methanol, ethanol and *n*-propanol were used as the substrates for alcohol oxidase.

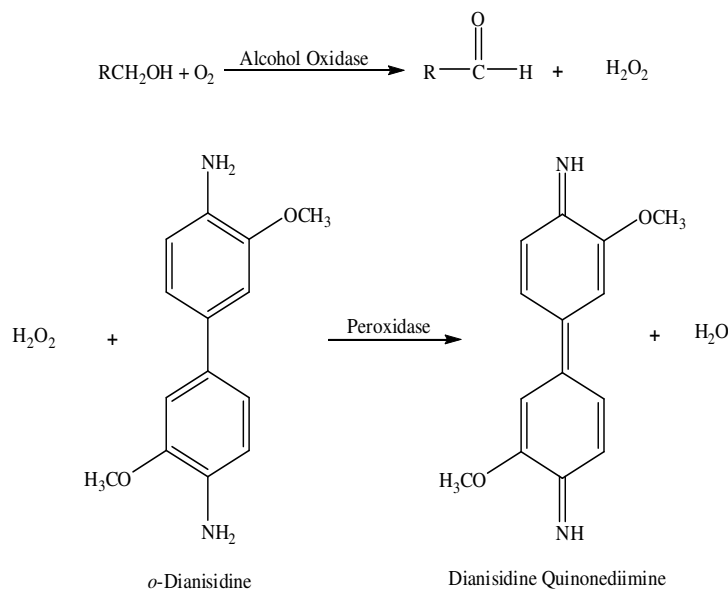


**Figure 3.31.** Reaction scheme for the enzymatic measurement of primary alcohols.

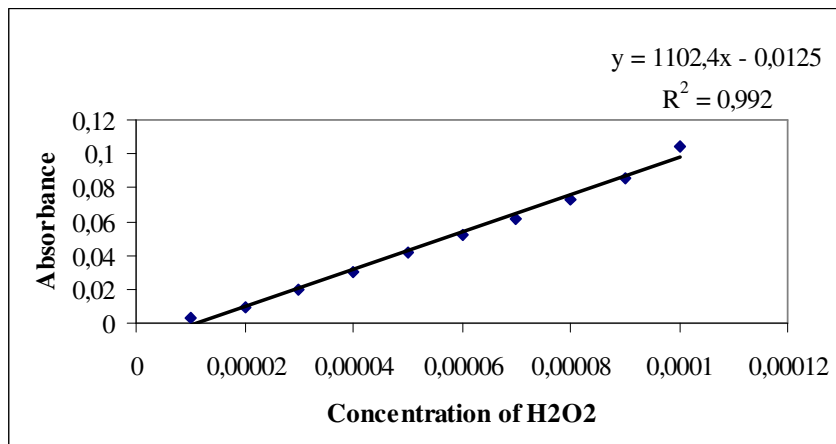


**Figure 3.32.** Calibration curve for Jansenn's Method.

### 3.2.1.1. Protein Determination for AOX

Determination of amount of immobilized protein was performed as it was described in section 2.4.9.3. Figure 3.33 shows the calibration curve which is prepared by using bovine serum albumin.

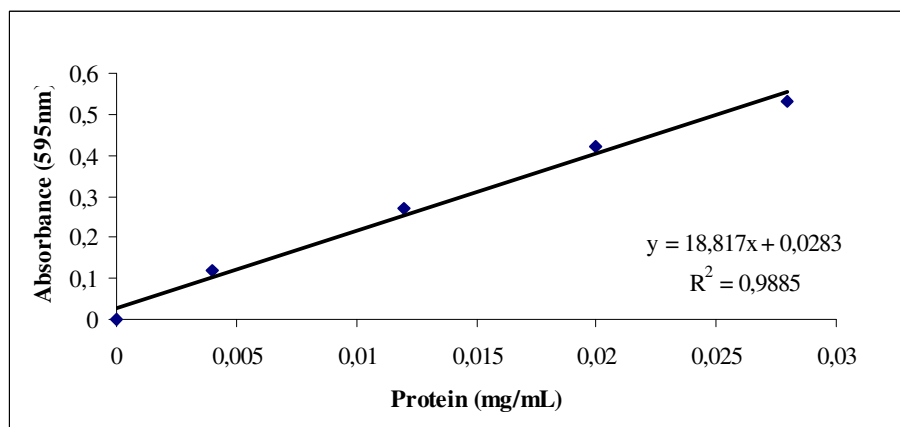


**Figure 3.33.** Calibration curve for protein determination.

Free enzyme was found to have reactivities of 11  $\mu\text{mol}/\text{min}\cdot\text{mg}$  protein for methanol, 9.20  $\mu\text{mol}/\text{min}\cdot\text{mg}$  protein for ethanol substrate and 7.50  $\mu\text{mol}/\text{min}\cdot\text{mg}$  protein for n-propanol. Results of protein determination for PPy/AOX and RPEO-co-PPy/AOX electrodes were  $9.1 \times 10^{-3}$  and  $8.7 \times 10^{-3}$  mg protein respectively.

### **3.2.1.2. Kinetic Studies of Free and Immobilized AOX**

Kinetic parameters include the maximum reaction rate ( $V_{\text{max}}$ ) of the enzymatic reaction and the Michaelis-Menten constant ( $K_{\text{m}}$ ) which defines the affinity of enzyme toward its substrate. Lower the  $K_{\text{m}}$  value means higher its affinity against its substrate. These parameters were obtained from Lineweaver-Burk plot which is a plot of  $1/V_0$  against  $1/[\text{Substrate}]$  for systems obeying the Michaelis-Menten equation. The graph being linear can be extrapolated at anywhere approximating to a saturating substrate concentration, and from the extrapolated graph, the values of  $K_{\text{m}}$  and  $V_{\text{max}}$  can be determined.

For methanol, ethanol and n-propanol which were used as substrates, free AOX has  $K_{\text{m}}$  values of 0.5, 1.5 and 9.70 mM respectively. It seems that  $V_{\text{max}}$  and  $K_{\text{m}}$  values decrease with increasing chain length of the substrates. Increasing chain length causes lower solubility of substrate in reaction media. Both  $V_{\text{max}}$  and  $K_{\text{m}}$  values for the two enzyme electrodes showed the same tendency as the free enzyme in the sense that they were inversely proportional to the chain length of substrates (Table 3.8) [207, 208].

$K_{\text{m}}$  values of enzyme electrodes in this study were high when compared to that of free enzyme. Changes in  $K_{\text{m}}$  values are related with the affinity of enzyme towards its substrates, thus the microenvironment in matrices used in this study gives rise to high  $K_{\text{m}}$  values, which indicate the difficulty of meeting of substrate with enzyme [209]. Lower  $K_{\text{m}}$  value for RPEO-co-PPy shows that this matrix provides a more suitable matrix for the enzyme than that PPy matrix does.

**Table 3.8.** Kinetic parameters for free and immobilized alcohol oxidase for methanol, ethanol and n-propanol substrates.

	Methanol		Ethanol		Propanol	
	Km (mM)	Vmax	Km (mM)	Vmax	Km (mM)	Vmax
<b>Free</b>	0.50	11.0 μmol/min.mg protein	1.5	9.2 μmol/min.mg protein	9.7	7.5 μmol/min.mg protein
<b>PPy</b>	3.70	1.4 μmol/min.electrode	6.8	1.0 μmol/min.electrode	23.4	0.6 μmol/min.electrode
<b>RPEO-co-PPy</b>	2.60	2.1 μmol/min.electrode	5.5	1.6 μmol/min.electrode	16.3	1.2 μmol/min.electrode

### 3.2.1.3. Influence of Temperature on the AOX Activity

The effect of temperature between 10 °C and 60 °C on the relative enzyme activity for three different substrates was investigated and illustrated in Figure 3.34 a-c.

For methanol the maximum activity temperature for free enzyme was found to be 30 °C. Maximum enzyme activity for PPy matrice was at 40°C and for RPEO-co-PPy it was at 50°C. RPEO-co-PPy/AOX enzyme electrode functions better than PPy/AOX electrode at low and low temperatures since even at 10°C and 60°C, it reveals high activity.

For ethanol the maximum activity was observed at 40 °C both for free enzyme and PPy/AOX enzyme electrode. RPEO-co-PPy/AOX enzyme electrode revealed a maximum activity at 50 °C and exhibits stability up to 60°C. However, at 50 °C, PPy/AOX electrode lost its 60 % of its activity. Due to that fact, RPEO-co-PPy/AOX electrode can be used effectively in this temperature range (between 10 °C and 60 °C).

For n-propanol, , free enzyme has the maximum relative enzyme activity at 40 °C. PPy/AOX and RPEO-co-PPy/AOX electrodes have the maximum relative enzyme activities at 50 °C. For this substrate, as in the case of methanol

and ethanol substrates, it was shown that RPEO-co-PPy/AOX is a better sensor than PPy/AOX electrode at all temperatures.

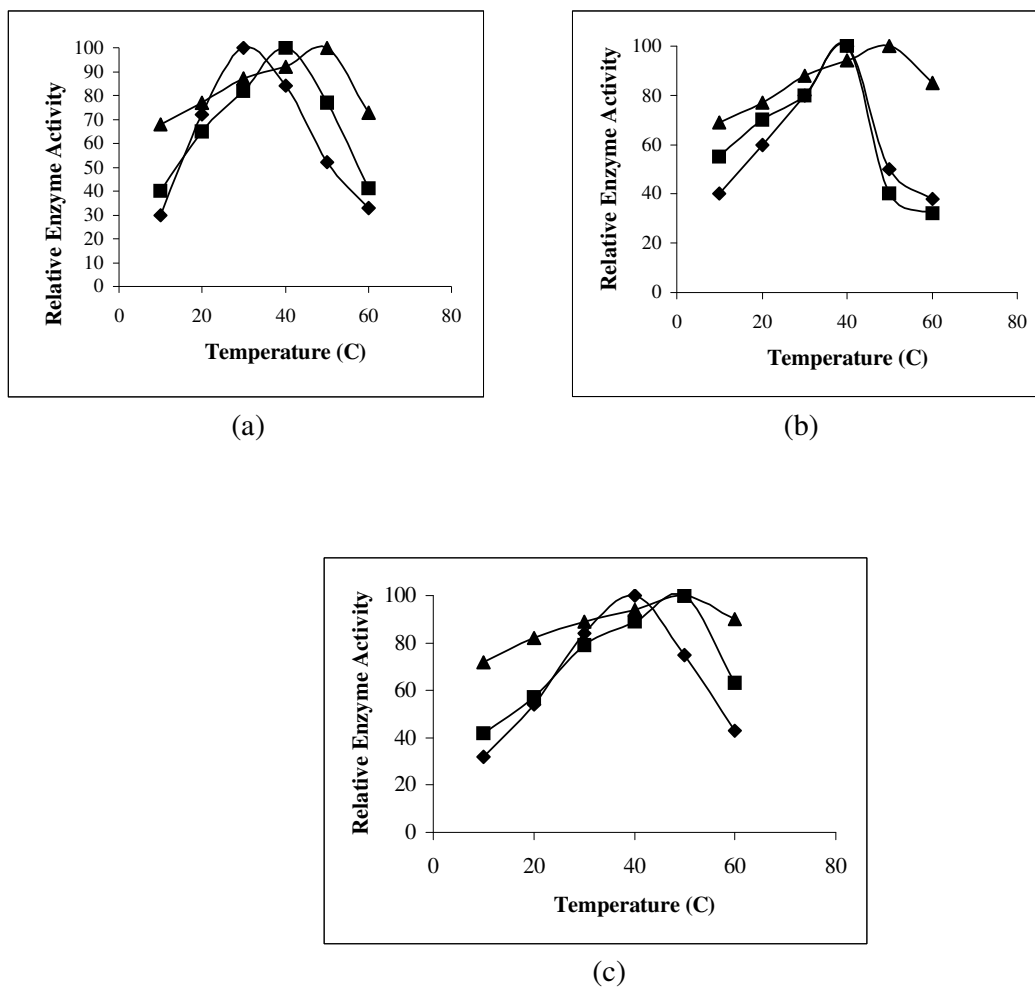
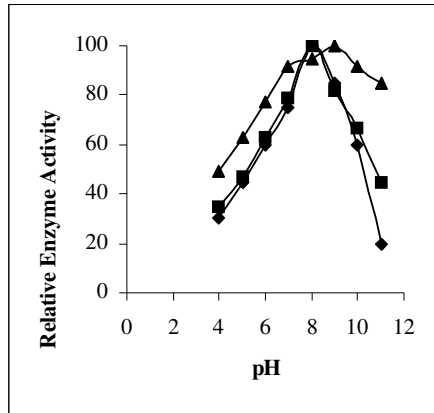


**Figure 3.34.** Effect of incubation temperature on alcohol oxidase activity for Free enzyme (◆); PPy/AOX (■) and RPEO-co-PPy/AOX (▲) in a) methanol; b) ethanol; c) n-propanol.

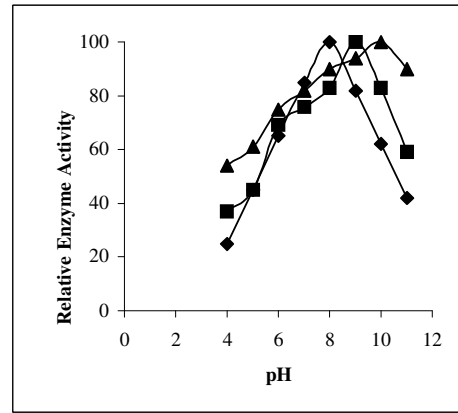
#### **3.2.1.4. Influence of pH on the AOX Activity**

Free AOX has an optimum pH of 8 for the three substrates. For pH optimization at 25°C, the pH of medium was changed between 4 and 11. Due to the denaturation of AOX in more acidic medium than pH 4, the optimization study started from pH 4 for enzyme electrodes. In methanol, immobilized AOX revealed an optimal pH for PPy and RPEO-co-PPy/AOX electrodes as 8 and 9 respectively, thus pH stability is increased for the RPEO-co-PPy/AOX electrode. For ethanol, the maximum activity was observed at pH 9 for PPy and 10 for RPEO-co-PPy matrix. For n-propanol, both enzyme electrodes revealed maximum activity at pH 9. In n-propanol, PPy and RPEO-co-PPy matrices lost only 40% and 20% of their activities respectively (up to pH 11). Moreover, RPEO-co-PPy matrix is stable in the pH range between pH 7 and 11 for methanol and ethanol. Hence, this enzyme electrode can be used reliably at high pH values (Figures 3.35 a-c).

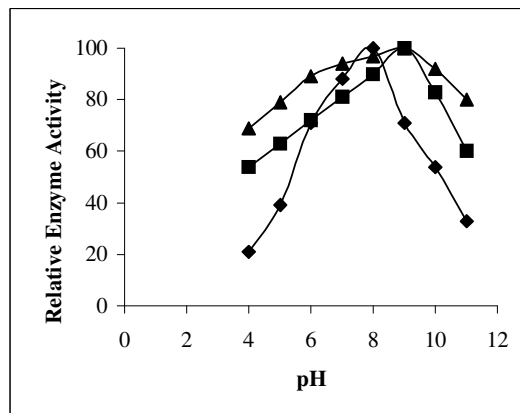
For the enzyme electrodes, the pH value that maximum activity was shifted towards the alkaline side when compared with that of the free enzyme. This can be explained by partitioning of protons. Negatively charged groups of matrix will tend to concentrate protons (lowering the pH) around the enzyme. Therefore, the pH around the enzyme will be lower than that of the bulk phase from which measurement of pH is carried out [210].



(a)



(b)



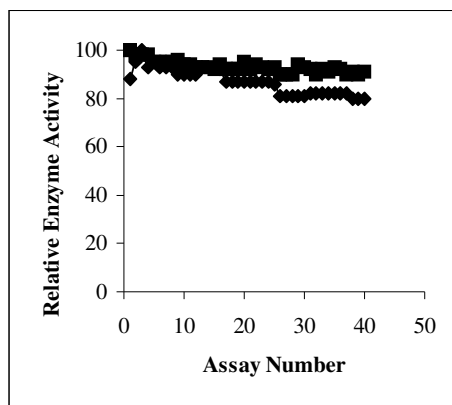
(c)

**Figure 3.35.** Effect of pH on alcohol oxidase activity for Free enzyme (♦); PPy/AOX (■) and RPEO-co-PPy/AOX (▲) in a) methanol; b) ethanol; c) n-propanol.

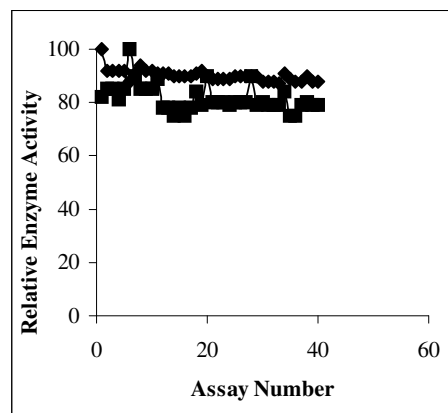
### **3.2.1.5. Operational Stability and Shelf Life of the AOX Electrodes**

Enzymes can easily lose their catalytic activity and get denaturated, hence careful storage and handling are important. The stability of electrodes in terms of repetitive uses was studied at 25°C. For three different substrates the responses of both enzyme electrodes did not change significantly. The slight increase in the responses of PPy/AOX in n-propanol and RPEO-co-PPy/AOX in ethanol are related to the swelling of the polymer structure and reorganization of the enzyme molecules in these matrices [211] (Figures 3.36 a-c).

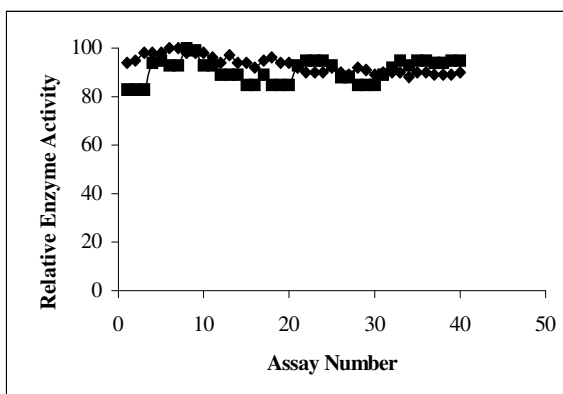
For the shelf life determination of the enzyme electrodes, the activities were characterized everyday for a week and then once in five days throughout 40 days. The enzyme in RPEO-co-PPy matrix maintained 65 % of its activity after 15 days in methanol substrate, 75% of its activity in ethanol after 20 days and 50 % of its activity in n-propanol after 20 days and stayed constant up to 40th day. PPy matrix maintained 80-85 % of its activity after about 20th day and stayed constant until 40th day for three substrates (Figures 3.37 a-c).



(a)

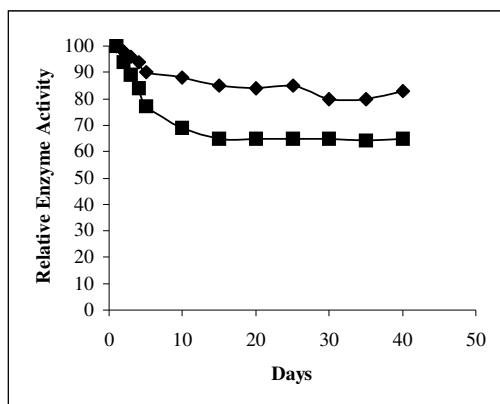


(b)

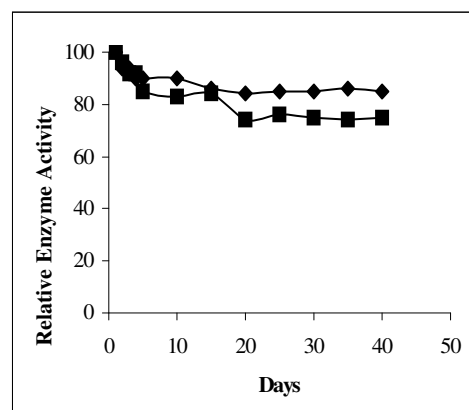


(c)

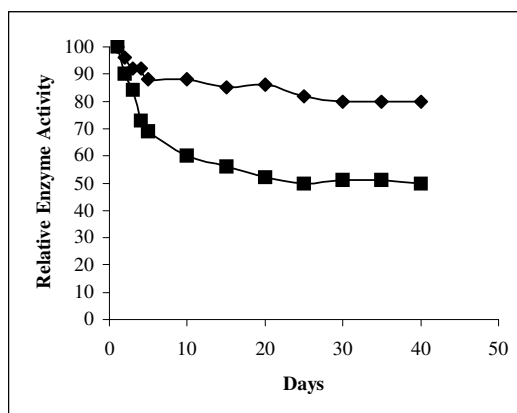
**Figure 3.36.** Operational stabilities of PPy/AOX (◆) and RPEO-co-PPy/AOX (■) electrodes in a) methanol; b) ethanol; c) n-propanol.



(a)



(b)



(c)

**Figure 3.37.** Shelf life of PPy/AOX (◆) and RPEO-co-PPy/AOX (■) electrodes in a) methanol; b) ethanol; c) n-propanol.

### 3.2.2. Immobilization of Polyphenol Oxidase

The enzyme assay is based on the measurement of *o*-quinone generated in enzymatic reaction.

The method described in section 2.4.9.2.2 is based on the spectrophotometric measurements of absorbance of the compound produced when the 3-methyl-2-benzothiozolinone (MBTH) interacts with the quinones produced by the enzyme to yield red products.

Figure 3.38 shows calibration curve for the reaction of *o*-quinone by Besthorn's Hydrazone Method.

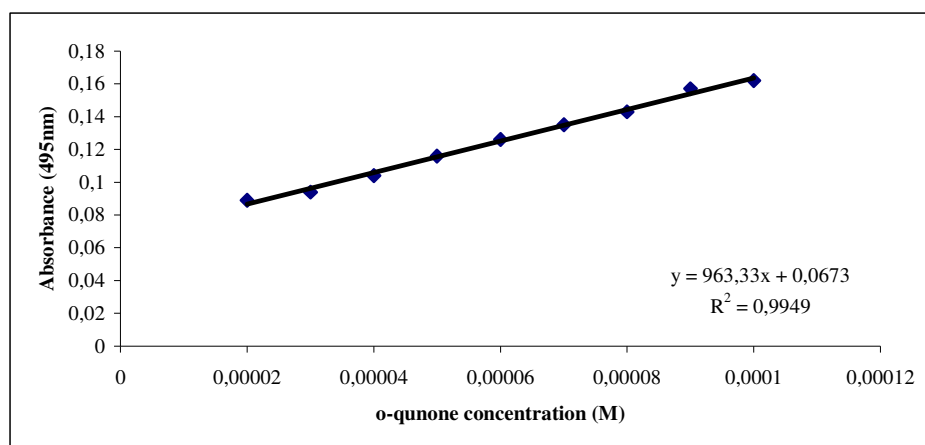


**Figure 3.38.** Calibration curve for Besthorn's Hydrazone method.

#### 3.2.2.1. Protein Determination for Polyphenol Oxidase

Determination of amount of immobilized protein was performed as described in section 2.4.9.3. Figure 3.29 shows the calibration curve which is prepared using bovine serum albumin.

Free enzyme was found to have a reactivity of 11.2  $\mu\text{mol}/\text{min}.\text{mg}$  protein [177]. Results of protein determination experiments for ThPEO-co-PPy/PPO

and RPEO-co-PPy/PPO electrodes were  $2.9 \times 10^{-3}$  and  $2.8 \times 10^{-3}$  mg protein respectively.

### **3.2.2.2. Kinetic Studies for Polyphenol Oxidase**

$V_{max}$  and Michaelis-Menten constants ( $K_m$ ) for enzyme electrodes were found from Lineweaver-Burk plot [199]. The results are collected in Table 3.9.

Decrease in kinetic parameters is an expected result since enzyme is entrapped in a matrix which provides many advantages.

$V_{max}$  values for ThPEO/PPO and RPEO/PPO enzyme electrodes were determined as  $0.033 \mu\text{mol}/\text{min}\cdot\text{electrode}$  and  $0.030 \mu\text{mol}/\text{min}\cdot\text{electrode}$  respectively.  $V_{max}$  values for both enzyme electrodes are very close.  $V_{max}$  value for PPy/PPO was found as  $0.11 \mu\text{mol}/\text{min}$  in a previous study [177]. When the  $V_{max}$  results of ThPEO-co-PPy and RPEO-co-PPy electrodes are compared with that of PPy matrix, it is seen that  $V_{max}$  value of PPy electrode was 3.5 times higher than those of the ThPEO-co-PPy and RPEO-co-PPy matrices. These results were supported by the amount of protein entrapped in the electrodes which are  $9.6 \times 10^{-3}$  and  $2.9 \times 10^{-3}$  and  $2.8 \times 10^{-3}$  mg protein for PPy, ThPEO-co-PPy, and RPEO-co-PPy respectively.

$K_m$  values of enzyme electrodes in this study were very high when compared to that of free enzyme. Changes in  $K_m$  values are related with the affinity of enzyme towards its substrate thus, the microenvironment in matrices used in this study give rise to high  $K_m$  values which indicate the difficulty of meeting of substrate with enzyme. When we compare the  $K_m$  values of copolymers of ThPEO and RPEO with that of PPy matrix, lower  $K_m$  values imply that these copolymers provide a more suitable microenvironment.

### **3.2.2.3. Influence of Temperature on the PPO Activity**

The effect of temperature between  $10-80^\circ\text{C}$  on the relative enzyme activity was investigated and illustrated in Figures 3.39. The maximum activity temperature for free enzyme was found to be at  $40^\circ\text{C}$  [177]. Maximum enzyme activity for ThPEO-co-PPy matrix was at  $70^\circ\text{C}$  and for RPEO-co-PPy matrix  $60$

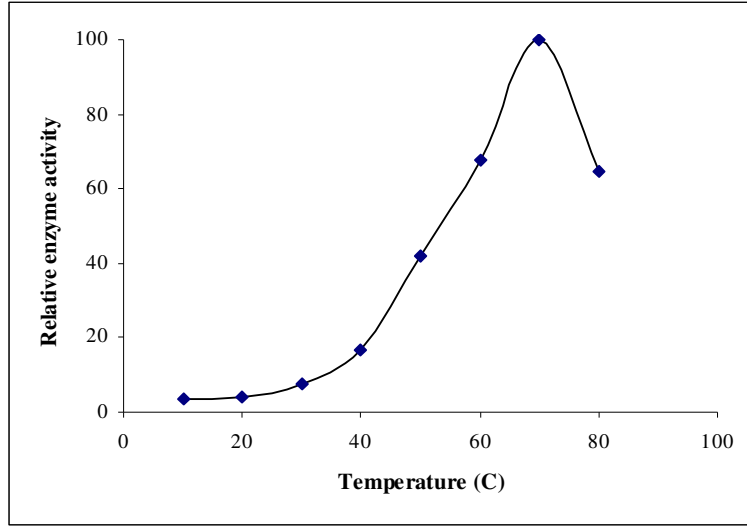
°C. At temperatures up to 80°C, they lost about 40% of their activity. These matrices showed high stability against temperature.

**Table 3.9.** Kinetic parameters for free and immobilized PPO.

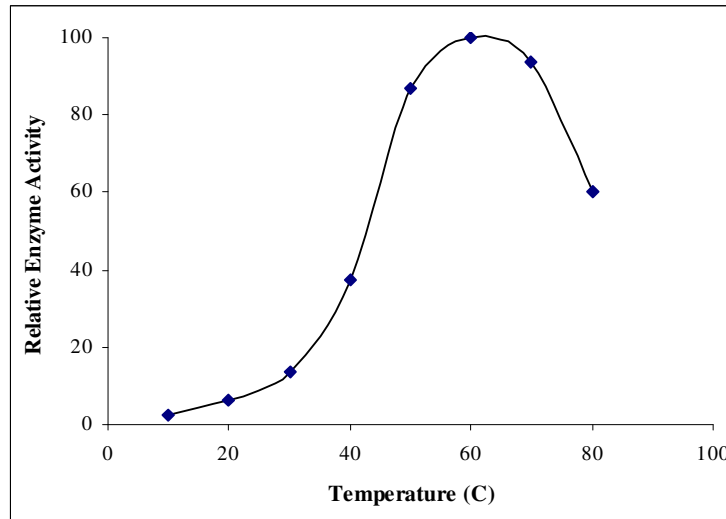
	$V_{\max}$	$K_m$
<b>Free</b>	11.2 $\mu\text{mol}/\text{min}.\text{mgprotein}$	4 mM
<b>PPy/PPO</b>	0.11 $\mu\text{mol}/\text{min}.\text{electrode}$	100 mM
<b>ThPEO-co-PPy/PPO</b>	0.033 $\mu\text{mol}/\text{min}.\text{electrode}$	33 mM
<b>RPEO-co-PPy/PPO</b>	0.030 $\mu\text{mol}/\text{min}.\text{electrode}$	35 mM

#### 3.2.2.4. Influence of pH on the AOX Activity

The maximum pH values were found as 9.0 for ThPEO-co-PPy and 8.0 for RPEO-co-PPy matrices. They are illustrated in Figure 3.40. This might be explained by the partitioning of protons explained in 3.2.1.4 [177, 209, 210]. Negatively charged groups of matrix will tend to concentrate protons and this cause lowering the pH around the enzyme. Therefore, the pH around the enzyme will be lower than that of the bulk from which the measurement of pH is carried out. ThPEO-coPPy and RPEO-co-PPy matrices lost only 20% and 40% of their activity respectively up to pH 11. Moreover, ThPEO-co-PPy matrix is stable on the pH range between the pH 7 and 10. Hence, this matrix can be used reliably at high pH values for enzyme reactions.

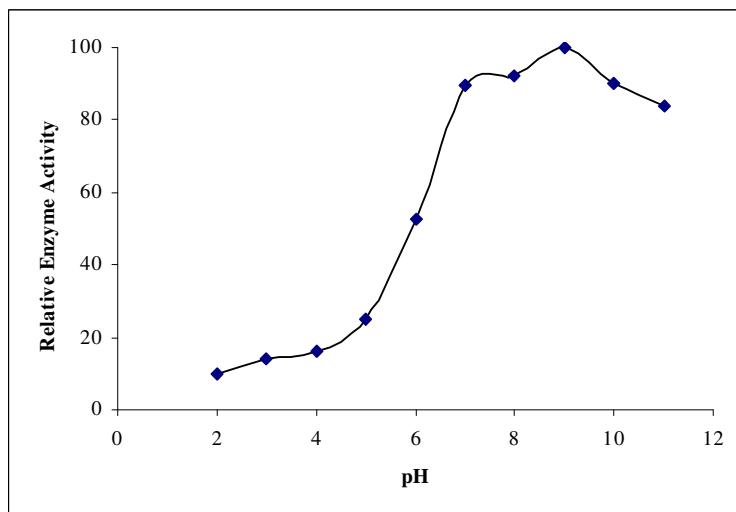


(a)

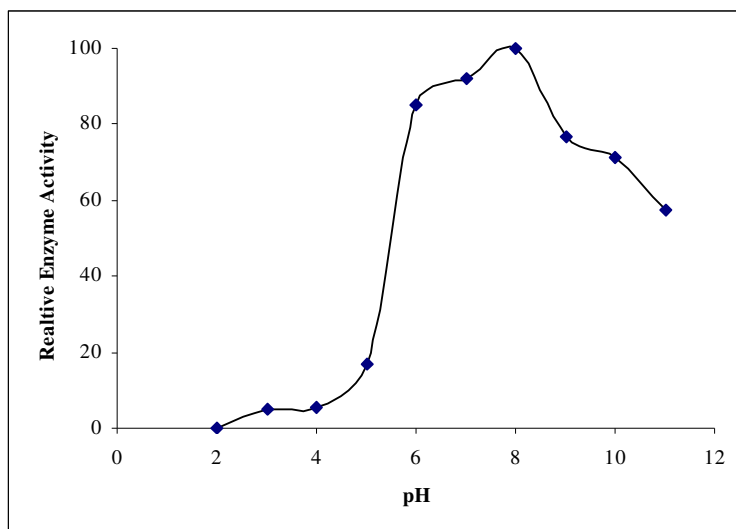


(b)

**Figure 3.39.** Temperature dependence of a) ThPEO enzyme electrode, b) RPEO enzyme electrode.



(a)



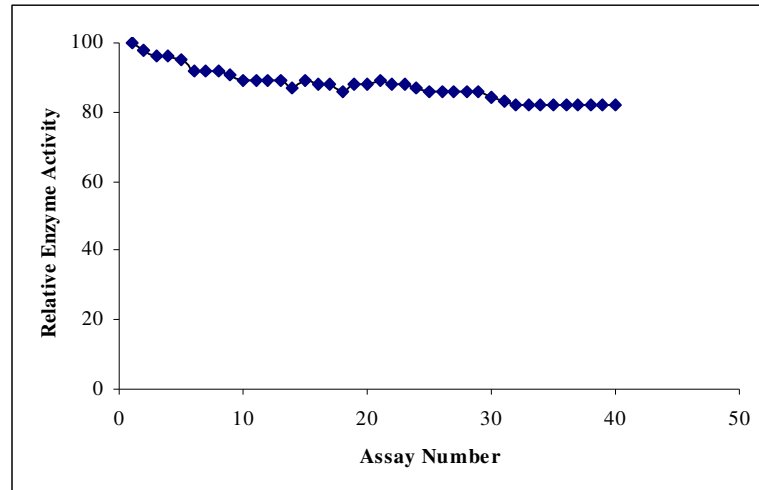
(b)

**Figure 3.40.** pH dependence of a) PEO enzyme electrode, b) RPEO enzyme electrode.

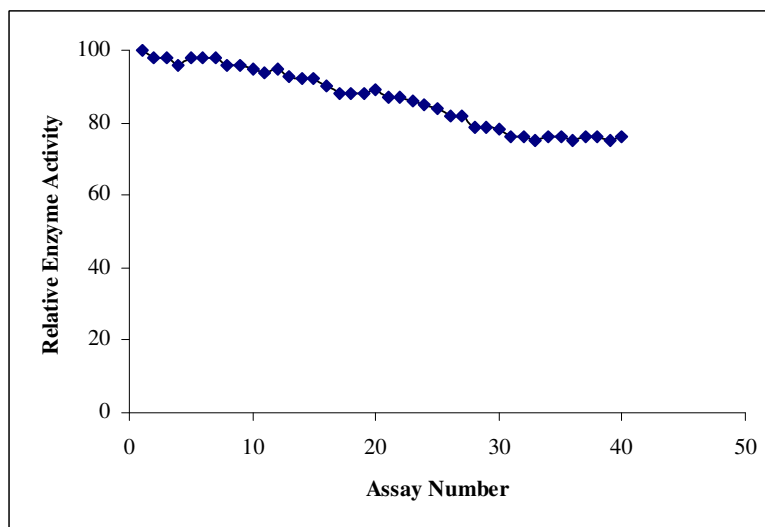
### **3.2.2.5. Operational Stability and Shelf Life of the PPO Electrodes**

The stability of enzyme electrode in terms of repetitive uses was studied by performing 40 successive measurements at 25°C in one day. RPEO-co-PPy/PPO electrode revealed an activity that gradually decreased until 25<sup>th</sup> use and stayed constant at 75% of its activity. As to the temperature and pH stability, ThPEO-co-PPy/PPO electrode exhibits very high operational stability and retained 82% of its activity after 40<sup>th</sup> use (Figure 3.41).

For the shelf life determination of the enzyme electrodes, the activities were checked everyday for a week and then once in five days throughout 40 days. The enzyme for ThPEO-co-PPy matrix maintained 65% of its activity after 20 days and stayed constant up to 40<sup>th</sup> day. RPEO/PPy matrix maintained 75% of its activity and stayed constant until 40<sup>th</sup> day (Figures 3.42).

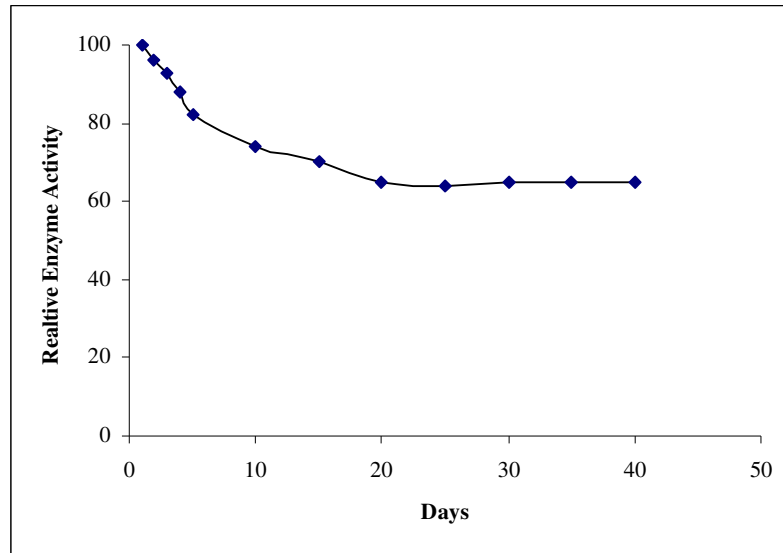


(a)

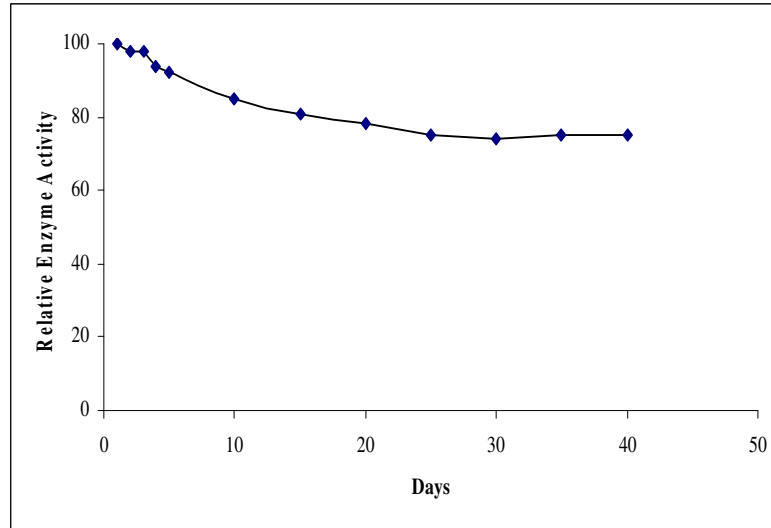


(b)

**Figure 3.41.** Operational stability of a) PEO enzyme electrode, b) RPEO enzyme electrode.



(a)



(b)

**Figure 3.42.** Shelf life of a) PEO enzyme electrode, b) RPEO enzyme electrode.

### 3.2.2.6. Determination of Total Phenolic Amount in Red Wines

Turkish red wines, Brand K and Brand D were used in the analysis of phenolic amount in wines. Total phenolic compounds in Turkish wines are reported as 2000-3000 mg/L [202, 212, 213]. Polyphenol oxidase enzyme acts on –OH groups on phenolic compounds. Via activity determination of enzyme in red wine, the total –OH groups were obtained.

Results for phenolic determination by using free PPO enzyme give very small values when compared with both enzyme electrodes. As it is known from the literature, benzoates act as inhibitors for free PPO. Thus PPO is inhibited by benzoates found naturally in wines before it completes enzymatic reactions. In previous studies, immobilized PPO was protected by the several matrices decreasing the effect of inhibitors found in wines [176, 177, 214, 215]. In these studies the range of phenolic amount was reported as 3000-4000 mg/L for the Brand K and 1500-2000 mg/L for Brand D. As it is seen in Table 3.10, the values for both matrices are in good agreement with both literature and previous studies.

Brand K contains twice the amount of phenolics compared to Brand D. This result was obtained by both enzyme electrodes. High amount of phenolics in Brand K is responsible for the bitter taste of the wine.

**Table 3.10.** Total phenolics in two different red wines, determined by the two enzyme electrodes.

	<i>Free PPO</i>	<i>PPy/PPO</i>	<i>ThPEO/PPO</i>	<i>RPEO/PPO</i>
<b>Brand K</b>	0.004M –OH 220 mg/L*	0.072M –OH 4000 mg/L*	0.059 M –OH 3334 mg/L*	0.065 M –OH 3625 mg/L*
<b>Brand D</b>	0.005 M –OH 270 mg/L*	0.04M –OH 2200 mg/L*	0.029 M –OH 1650 mg/L*	0.031M –OH 1747 mg/L*

\*Total phenolics are expressed as Gallic acid equivalents [215].

## CHAPTER 4

### CONCLUSION

A random copolymer (RPEO) of 3-methylthienyl metacrylate and *p*-vinylbenzyloxy poly(ethylene oxide) and thiophene ended poly(ethylene oxide) (ThPEO) were synthesized chemically. Synthesized monomers were characterized by several techniques like GPC, <sup>1</sup>HNMR, FTIR. Cyclic voltammetry was utilized as the major characterization technique to get information about electrochemical behavior of monomers. CV studies of monomers were performed in TBAFB/AN supporting electrolyte/solvent system. From these studies, it was understood that both monomers have no electroactive properties.

ThPEO and RPEO were used to synthesize copolymers with pyrrole and thiophene under conditions of constant potential electrolyses. Resultant copolymers were characterized by CV, FTIR, SEM, and conductivity measurements. Copolymerizations were proven by the drastic difference in the voltammograms such as the presence characteristic peaks that belonged to PPy and PTh. Difference in morphology of films and conductivity of copolymers compare to those of PTh and PPy supported the above argument..

The third part of the study was devoted to investigate one of the most interesting property of conducting polymers, electrochromism. In recent years there has been a growing interest in the application of conducting polymers in electrochromic devices. Thus electrochromic properties of the synthesized conducting polymers were investigated by the techniques like

spectroelectrochemistry and colorimetry studies. Spectroelectrochemistry experiments were performed in order to investigate key properties of conjugated polymers such as band gap, maximum absorption wavelength, the intergap states that appear upon doping and evolution of polaron and bipolaron states. Coupled with colorimetry, these films were observed to exhibit distinctive and aesthetically pleasing color changes between blue to red.

Copolymers of RPEO and ThPEO with pyrrole were used as enzyme immobilization matrices. This study shows that alcohol oxidase and polyphenol oxidase can be successfully immobilized in conducting RPEO-co-PPy and ThPEO-co-PPy copolymer matrices by electrochemical methods. The immobilization procedure is simple to carry out. Kinetic parameters for enzyme activity,  $V_{\max}$  and  $K_m$ , temperature and pH effect on the enzyme electrodes and storage and operational stabilities were investigated. AOX enzyme electrodes exhibited better  $V_{\max}$  and  $K_m$  values. Although they have limited storage capacities, these enzyme electrodes are very useful as their high kinetic parameters point. In addition to that, they exhibit very good operational stability and wide pH working range. PPO enzyme electrodes show wider pH and temperature working range than the ones obtained with the other electrodes constructed. Two copolymer matrices; ThPEO-co-Py and RPEO-co-Py show comparable results since they have no superior performance over one another as enzyme electrodes.

Immobilization of polyphenol oxidase enzyme in conducting polymer electrodes were studied as an alternative method for determination of phenolic compounds in wines and obtained results reveal that this significant development can successfully replace the classical methods.

## REFERENCES

1. M.A. DePaoli, R. J. Waltman, A. F. Diaz, J. Bargon, *J. Polym. Sci. Polym. Chem. Ed.*, **23**, 1687 (1985).
2. C.K. Chiang, C.R. Fincher, Y.W. Park, A.J. Heeger, H. Shirakawa, E.J. Louis, A.G. MacDiarmid, *Phys. Rev. Lett.*, **39** 1098 (1977).
3. T.A. Skotheim, R.L. Elsenbaumer, J.R. Reynolds, *Handbook of Conducting Polymers*, 2<sup>nd</sup> Ed., (1998) Marcel Dekker: New York, New York.
4. T.A. Skotheim, *Handbook of Conducting Polymers*, (1986) Marcel Dekker: New York, New York.
5. P. Chandrasekhar, *Conducting Polymers, Fundamentals and Applications: A Practical Approach*, (1999) Kluwer Academic Publishers: Boston, Massachusetts.
6. H.S. Nalwa, *Handbook of Conducting Organic Conductive Molecules and Polymers*, 2<sup>nd</sup> Ed, (1987) John Wiley and Sons: New York, New York.
7. A.J. Heeger, *Angew. Chem. Int. Ed.*, **40** 2591 (2001).
8. J.C.W. Chien, *Polyacetylene: Chemistry, Physics, and Materials Science*, (1984) Academic Press, Harcourt Brace Jovanovich: Orlando.
9. G. Green, G. Leditzky, B. Ullrich, G. Leising, *Adv. Mater.*, **4** 36 (1992).
10. B.D. Reeves, PhD. Dissertation, University of Florida, 2005.
11. H. Shirakawa, E.J. Louis, A.G. MacDiarmid, C.K. Chiang, A.J. Heeger, *J. Chem. Soc., Chem. Commun.*, (1977) 578.
12. P. Bauerle, *Adv. Mater.*, **5** (1993) 879.
13. A.G. MacDiarmid, A.J. Heeger, *Synth. Met.*, **1**(1979) 101.
14. G. Wegner, *Angew. Chem., Int. Ed.*, **20** (1981) 361.

15. K.J. Wynne, G.B. Street, *I&EC Product Research and Development*, **21** (1982) 23.
16. R.H. Baughman, E.J. Vanderberg (ed), *Contemporary Topics in Polymer Science Vol 5*, (1987) Plenum Publishing, New York.
17. R.L. Greene, G.B. Street, *Science*, **226** (1984) 651.
18. P. Kovacic, M.B. Jones, *Chem. Rev.*, **87** (1987) 357.
19. P. Kovacic, K.N. McFarland, *J. Polym. Sci., Polym. Chem. Ed.*, **17** (1979) 1963.
20. T. Yamamoto, Y.K. Sanechika, A. Yamamoto, *J. Polym. Sci., Polym. Lett. Ed.*, **18** (1980) 9.
21. J. Lin, L.P. Dudek, *J. Polym. Sci., Polym. Chem. Ed.*, **18** (1980) 2869
22. G. Kossmehl, G. Chatzitheodorou, *Makromol. Chem. Rapid. Commun.*, **2** (1981) 551
23. A. Dall'Olio, G. Dascola, V. Varacca, V. Bocchi, *R Acad Sci C*, **267** (1968) 433.
24. A.F. Diaz, K.K. Kanazawa, G.P. Gardini, *J. Chem. Soc., Chem. Commun.*, (1979) 635.
25. K.K. Kanazawa, A.F. Diaz, R.H. Geiss, W.D. Gill, J.F. Kowak, J.A. Logan, J.F. Rabolt, G.B. Street, *J. Chem. Soc., Chem. Commun.*, (1979) 854.
26. K.J. Wynne, G.B. Street, *Macromolecules*, **18** (1985) 2361.
27. A.F. Diaz, J. Bargon, *Handbook of Conducting Polymers*, T.A. Skotheim (ed), (1986) Marcel Dekker Inc, New York.
28. G.B. Street, *Handbook of Conducting Polymers*, T.A. Skotheim TA (ed), (1986) Marcel Dekker Inc, New York.
29. B.D. Malhotra, N.H. Kumar, S. Chandra, *Progr. Polym. Sci.*, **12** (1986) 179.
30. B.R. Saunders, R.J. Fleming, K.S. Murray, *Chem. Mater.*, **7** (1995) 1082.
31. P. Novak, *Electrochim. Acta*, **37** (1992) 1227.
32. P.N. Bartlett, P.R. Birkin, *Synth. Met.*, **61** (1993) 15.
33. H. Letheby, *J. Chem. Soc.*, **15** (1862) 161.

34. D.M. Mohilner, R.N. Adams, W.J. Argersinger Jr, *J. Am. Chem. Soc.*, **84** (1962) 3618.
35. M. Jozefewicz, L.T. Yu, G. Belorgey, R. Buvet, *J. Polym. Sci., Part C*, **16** (1967) 2931.
36. J. Honzl, M. Tlustakova, *J. Polym. Sci., Part C*, **22** (1968) 451.
37. M. Jozefewicz, L.T. Yu, J. Perichon, R. Buvet, *J. Polym. Sci., Part C*, **22** (1969) 1187.
38. A.G. MacDiarmid, A.J. Epstein, *Faraday Discuss Chem. Soc.*, **88** (1989) 317.
39. Epstein AJ, *Makromol. Chem., Macromol. Symp.*, **51** (1991) 217.
40. A.G. MacDiarmid, *Synth. Met.*, **84** (1997) 27.
41. J.L. Reddinger, J.R. Reynolds, *Adv. Polym. Sci.*, **145** (1999) 57.
42. T. Okada, T. Ogata, M. Ueda, *Macromolecules*, **29** (1996) 7645.
43. A. Dodabalapur, L.Torsi, H.E.Katz, *Science*, **268** (1995) 270.
44. J.C.Gustafson, O. Inganas, A.M. Andersson, *Synth. Met.*, **62** (1994) 17.
45. A. Kraft, A.C. Grimsdale, A.B. Holmes, *Angew. Chem. Int.Ed.*, **37** (1998) 402.
46. F. Jonas, G.Heywang, W. Schmidtberg, J. Heinze, M. Dietrich, *M. Europ. Pat. Appl.*, **339** (1988) 340.
47. J.C. DuBois, O. Sagnes, F.Henry, *Synth. Met.*, **28** (1989) 871.
48. J.P. Ferraris, M.M. Eissa, I.D. Brotherson, D.C. Loveday, *Chem. Mater.* **10** (1998) 3528.
49. G. Heywang, F. Jonas, *Adv. Mater.*, **4** (1992) 116.
50. P.N. Bartlett, R.G.Whitaker, *J. Electroanal. Chem.*, **224** (1987) 37.
51. N.C. Foulds, C.R. Lowe, *J. Chem. Soc. Faraday Trans.*, **82** (1986) 1259.
52. W. Schuhmann, *Microchim. Acta.*, **121** (1995) 1.
53. P. Novak, K. Muller, K.S.V. Santhanam, O. Hass, *Chem. Rev.*, **97** (1997) 207.
54. T.F. Otero, H. Grande, *Handbook of Conducting Polymers*, (1998) 2nd ed.; T.A, Skotheim, R.L. Elsenbaumer, J.R.Reynolds (Eds), (1998) Marcel Dekker: New York.
55. D.T. McQuade, A.E. Pullen, T.M. Swager, *Chem. Rev.* **100**, (2000) 2537.

56. J. Pernaut, J.R. Reynolds, *J. Phys. Chem. B*, **104**, (2000) 4080.
57. B. Sankaran, J.R. Reynolds, *Macromolecules*, **30**, (1997) 2582.
58. S.A. Sapp, G.A. Sotzing, J.R. Reynolds, *Chem. Mater.*, **10**, (1998) 2101.
59. P.M.S. Monk, R.J. Mortimer, D.R. Rosseinsky, *Electrochromism: Fundamentals and Applications*, (1995) VCH Inc: Weinheim.
60. R. Hoffmann, *Angew. Chem. Int. Ed.*, **26** (1987) 846.
61. S.N. Hoier, S.M. Park, *J. Phys. Chem.*, **96** (1992) 5188.
62. J.L. Bredas, G.B. Street, *Acc. Chem. Res.*, **18** (1985) 309.
63. K. Yoshino, R. Hayashi, R. Sugimoto, *Jpn. J. Appl. Phys.*, **23**, (1984) 899.
64. N. Toshima, S. Hara, *Prog. Polym. Sci.*, **20** (1995) 155.
65. P. Marque, J. Roncali, F. Garnier, *J. Electroanal. Chem.*, **218** (1981) 107.
66. F. Beck, P. Brawn, M. Oberst, *Ber. Bunsenges. Phys. Chem.*, **91** (1987) 967.
67. B.D. Malhotra, N. Kumar, S. Chandra, *Prog. Polym. Sci.*, **12** (1986) 179.
68. M. Graztl, H. Duan-Fu, M. Riley, J. Janata, *J. Phys. Chem.*, **94** (1990) 5973.
69. B.R. Scharitker, E.G. Pastariza, W. Marina, *J. Electroanal. Chem.*, **85** (1991) 300.
70. C.P. Andrieux, P. Audebert, P. Hapiot, J.M. Saveant, *J. Phys. Chem.*, **95** (1991) 10158.
71. P.S. Sargin, L. Toppare, E. Yurtsever, *Polymer*, **37** (1996) 1151.
72. P. Flugar, P. Street, *J. Chem. Phys.*, **533** (1984) 80.
73. R. John, G.G. Wallace, *J. Electroanal. Chem.*, **27** (1983) 342.
74. A. Battacharya, A. De, *Prog Solid St Chem.*, **24** (1996) 141.
75. O. Niwa, T. Tamamura, M. Kakuchi, *Macromolecules*, **20** (1987) 749.
76. D.B. Hibbert, *Introduction to Electrochemistry*, (1993) Macmillan Press, London.
77. H. Abuna, *Coord. Chem. Rev.*, **86** (1998) 135.
78. E. Laviron, *J. Electroanal. Chem.*, **39** (1972) 1.
79. D. Stanke, M.L. Hallensleben, L. Toppare, *Synth. Met.*, **73** (1995) 261.
80. D. Stanke, M.L. Hallensleben, L. Toppare, *Macromol. Chem. Phys.*, **196**

- (1995) 1697.
81. D. Stanke, M.L. Hallensleben, L. Toppare, *Synth. Met.*, **72** (1995) 167.
82. D. Stanke, M.L. Hallensleben, L. Toppare, *Synth. Met.*, **72** (1995) 89.
83. N. Balci, U. Akbulut, L. Toppare, D. Stanke, M.L. Hallensleben, *Mater. Sci. Bull.*, **32** (1997) 1449.
84. J.C.W Chien, G.E. Wnek, F.E. Karazs, J.A. Hirsch, *Macromolecules*, **23** (1985) 1687.
85. J.R. Reynolds, P.A. Poropatic, R.L. Toyooka, *Macromolecules*, **20** (1987) 1184.
86. A. Çırpan, S. Alkan, L. Toppare, Y. Hepuzer, Y. Yagci, *J. Polym. Sci. Part A: Polym. Chem.*, **40** (2002) 4131.
87. C. Biran, L. Toppare, T. Tincer, Y. Yagci, V. Harabagiu, *J. Appl. Polym. Sci.*, **86** (2002) 1663.
88. C. Biran, L. Toppare, T. Tincer, Y. Yagci, V. Harabagiu, *Chem. Eng. Commun.*, **87** (2003) 1720.
89. M.A. DePaoli, R.J. Waltman, A.F. Diaz, J. Bargon, *J. Polym. Sci. Polym. Chem. Ed.*, **23** (1985) 1687.
90. G. Nagaubramanian, S. DiStefano, *J. Electrochem. Soc. Extended Abstr.*, **85-2** (1985) 659.
91. H.L. Wang, L. Toppare, J.E. Fernandez, *Macromolecules*, **23** (1990) 1053.
92. D. Stanke, M.L. Hallensleben, L. Toppare, *Synth. Met.*, **56** (1994) 1108.
93. F. Selampinar, U. Akbulut, T. Yılmaz, A. Güngör, L. Toppare, *J. Polym. Sci. Polym. Chem.*, **5** (1997) 3009.
94. F. Selampinar, U. Akbulut, T. Yalçın, S. Süzer, L. Toppare, *Synth. Met.*, **62** (1999) 201.
95. E. Kalaycıoğlu, L. Toppare, Y. Yagci, V. Harabagiu, M. Pintela, R. Ardelean, B. Simunescu B, *Synth. Met.*, **97** (1998) 7.
96. N. Kizilyar, L. Toppare, A. Onen, Y. Yagci, *Polym. Bull.*, **40** (1997) 639.
97. S. Oztemiz, L. Toppare, A. Onen, Y. Yagci, *J.M.S.-Pure Appl. Chem. A*, **37** (2000) 277.
98. J.S. Miller, *Adv. Mater.*, **5** (1993) 587.

99. J.S. Miller, *Adv Mater.*, **5** (1993) 671.
100. A.M. Rocco, M.A. DePaoli, A. Zanelli, M.Mastrogostino, *Electrochim. Acta*, **41** (1996) 2805.
101. I. Jin, Ph.D Thesis, University of California (2005).
102. D.N Buckley, L.D. Burke, *J. Chem. Society-Faraday Transac. Int.*, **71** (1975) 1447.
103. D.N. Buckley, L.D. Burke, *J. Chem. Society-Faraday Transac. Int.*, **72** (1976) 1896.
104. L.D. Burke, E.J.M. Osullivan, *J. Electroanal. Chem.*, **93** (1978) 11.
105. L.D. Burke, D.D. Whelan, *J. Electroanal. Chem.*, **103** (1979) 179.
106. L.D. Burke, T.A.M. Twomey D.D. Whelan, *J. Electroanal. Chem.*, **107** (1980) 201.
107. L.D. Burke, O.J. Murphy, *J. Electroanal. Chem.*, **109** (1980) 373.
108. P.M.S. Monk, R.J. Mortimer, D.R. Rosseinsky, *Electrochromism: Fundamentals and Applications*, (1995) Wanheim, Germany, New York.
109. H.W. Heuer, R. Wehrmann, S. Kirschmeyer, *Adv. Funct. Mater.*, **12** (2002) 89.
110. S.A. Sapp, G.A. Sotzing, J.R. Reynolds, *Chem. Mater.*, **10** (1998) 2101.
111. C.G. Granqvist, *Handbook of Inorganic Electrochromic Materials*, (1995) Elsevier, Amsterdam, New York.
112. P.R. Somani, R. Radhakrishnan, *Mater. Chem. Phys.*, **77** (2003) 117.
113. K. Krishnamoorthy, M. Kanungo, A.V. Ambade, A.Q. Contractor, A. Kumar, *Synth. Met.*, **125** (2001) 441.
114. C.A. Cutler, M. Bougettaya, J.R. Reynolds, *Adv. Mater.*, **14** (2002) 684.
115. B.D. Reeves, B.C. Thompson, K.A. Abboud, B.E. Smart, J.R. Reynolds, *Adv. Mater.*, **14** (2002) 717.
116. H. Meng, D. Tucker, S. Chaffins, Y.S. Chen, R. Helgesen, B. Dunn, F. Wudl, *Adv. Mater.*, **15** (2003) 146.
117. Y. Lee, S. Sedki, B. Tsuie, J.R. Reynolds, *Chem. Mater.*, **13** (2001) 2234.
118. R.A. Copeland, *Enzymes: A Practical Introduction To Structure, Mechanism and Data Analysis*, (2000) Wiley-VCH Inc., New York.

119. P.W.Carr, L.D.Bowers, *Immobilized Enzymes in Analytical and Clinical Chemistry*, (1980) John Wiley & Sons, Inc.New York.
120. K.Mosbach (Ed.), *Methods in Enzymology, Immobilized Enzymes*. (1976). Academic Press, New York.
121. P.V. Sundaram, E.M. Crook, *Can. J. Biochem.*, **49** (1971) 1388.
122. G. Pozniak, B. Krajewska, W. Trochimczuk, *Biomaterials*, **16(2)** (1995) 129.
123. C.L. Dueck, R.J. Neufeld, T.M.S. Chang, *Can. J. Chem. Eng.*, **64** (1986) 540.
124. K. Raghunath, K.P. Rao, K.T. Joseph, *Biotech.Bioeng.*, **26** (1984) 104.
125. N.Das, P. Prabhakar, A.M. Kayastha, R.C. Srivastava, *Biotech.Bioeng.*, **54(4)** (1997) 329.
126. M.A. Arnold, *Anal.Chem.*, **57** (1985) 565.
127. D. Liu, K. Ge, K. Cheng, L. Nie, S. Yao, *Anal.Chim.Acta.*, **307** (1995) 61.
128. O.R. Zaborsky, *Immobilized Enzymes*, (1973) CRC Press, Cleveland.
129. W.Hartmeimer, *Immobilized Biocatalysts*, (1998) Springer-Verlag, Berlin.
130. G. B. Broun, *In Methods in Enzymology*, K. Mosbach, ed., (1976) Academic, New York, XLIV.
131. N.C. Foulds, C.R. Lowe, *J. Chem. Society-Faraday Trans.*, **82** (1986) 1259.
132. P.N. Bartlett, J.M. Cooper, *J. Electroanal. Chem.*, **363** (1993) 1.
133. W. Schuhmann, *Mikrochim. Acta.*, **121** (1995) 3.
134. S. Cosnier, *Electroanalysis*, **9** (1997) 894.
135. P.N. Bartlett, D.J. Caruana, *Analyst*, **117** (1992) 1287.
136. S. Cosnier, B. Galland, C. Gondran, A. Le Pellec, *Electroanalysis*, **10** (1998) 808.
137. C. Kranz, H. Wohlschlager, H.L. Schmidt, W. Schuhmann, *Electroanalysis*, **10** (1998) 546.
138. M. Umana, J. Waller, *Anal. Chem.*, **58** (1986) 2979.
139. M.D. Trevan, *Immobilized Enzymes: An Introduction and Applications*

- in Biotechnology*, (1980) John Wiley and Sons, New York.
140. H. Hossain, Ph.D. Thesis, McGill University (2004).
  141. S.Y. Seo, V.K. Sharma, *J. Agric. Food Chem.*, **51** (2003) 2837-2853.
  142. S.G. Burton, *Catal. Today*, **22** (1984) 459-487.
  143. S.G. Burton, A. Boshoff, W. Edwards, P.D. Rose, *J. Mol. Catal. B:Enz.*, **51** (1998) 411-416.
  144. D. Barbanti, D. Mastrocola, C.R. Lerici, *Lebens. Wiss. Technol.*, **23** (1990) 495-498.
  145. P.M. Lee, K. Lee, M.I.A. Karim, *J. Sci. Food Agric.*, **59** (1991) 251-260.
  146. A.M. Mayer, E. Harel, Phenol Oxidases in Fruit and Vegetables, *in Food Enzymology*, (1991) Elsevier, New York.
  147. V.F. Cheynier, N. Basire, J. Rigaud, *J. Agric. Food Chem.*, **37** (1989) 1069-1071.
  148. L.G. Fenoll, J.N. Rodriguez-Lopez, F. Garcia-Sevilla, P.A. Garcia-Ruiz, R. Varon, F. Garcia-Canovas, J. Tudela, *Biochim. Biophys. Acta*, **1548** (2001) 1-22.
  149. M.A. Rouet-Mayer, A.M. Klibanov, *Phytochem.*, **29** (2000) 435-440.
  150. E. Roux, C. Billoud, C. Maraschin, S. Brun-Marimee, J. Nicolas, *Food Chem.*, **81** (2003) 51-60.
  151. J.R. Ros-Martinez, J.N. Rodriguez-Lopez, R.V. Castellanos, F. Garcia-Canovas, *Biochem J*, **294** (1993) 621-623.
  152. C.J. Cooksey, P.J. Gariat, E.J. Land, S. Pavel, C.A. Ramsden, P.A. Riley, N.M.P. Smit, *J. Biol. Chem.*, **272** (1997) 26226-26235.
  153. H. Ozoglu, A. Bayindirli, *Food Control*, **13** (2002) 213-221.
  154. C. Severini, A. Baiano, T. De Pilli, R. Romaniello, A. Perossi, *Food Sci. Technol.*, **36** (2003) 655-657.
  155. M.R. Ullah, *Tea in Food Enzymology*, (1991) Elsevier Science Publishing, New York.
  156. J.R.L. Whitaker, Enzymatic Browning in Fruits: Its Biochemistry Control in *Enzymatic Browning and Its Prevention*, (1995) American Chemical Society, Washington D.C.

157. R. Yoruk, M.R. Marshall, *J. Food. Sci.*, **69** (2003) 2479-2485.
158. J. Zawistowski, C.G. Bliaderis, N.A.M. Eskin, *Polyphenol Oxidase in Oxidative Enzymes in Food*, (1991) Elsevier Science, London.
159. C.K. Wang, W.H. Lee, *J. Agric. Food. Chem.*, **44** (1996) 2014-2019.
160. A. Sanchez-Ferrer, J.N. Rodriguez-Lopez, F.G. Garcia-Cannovas, F. Garcia-Carmona, *Biochem. Biophys. Acta*, **1247** (1995) 1-11.
161. K.H. Lanouette, *Chem. Eng.*, **84** (1977) 99.
162. S.C. Atlow, L. Banadonna-Aparo, A.M. Klibanov, *Biotech. Bioeng.*, **26** (1984) 599.
163. J.G. Schiller, A.K. Chen, C.C. Liu, *Anal. Biochem.*, **85** (1978) 25.
164. K. Zachariah, H.A. Mottola, *Analytical Letters*, **22** (1989) 1145.
165. C.R. Tiliyer, P.T. Gobin, *Biosens. Bioelectron.*, **6** (1991) 569.
166. A.J. Winder, H. Harris, *Eur. J. Biochem.*, **198** (1991) 317.
167. K.E. Heim, A.R. Tagliaferro, J.B. Dennis, *J. Nutr. Biochem.*, **13**, (2002) 572.
168. S. Kallithraka, I. Arvanitoyannis, A. El-Zajouli, P. Kefalas, *Food Chem.*, **75** (2001) 355.
169. L. Campanella, A. Bonanni, E. Finotti, M. Tomassetti, *Biosensors and Bioelectronics*, **19** (2004) 641.
170. S. Malovana, F.J. Garcia Montelongo, J.P. Perez, M.A. Rodriguez-Delgado, *Anal. Chim. Acta*, **428**, (2001) 245.
171. N. Duran, M.A. Rosa, A. D'Annibale, L. Gianfreda, *Enz. Mic. Tech.*, **31** (2002) 907.
172. P. Vinas, C. Lopez-Erroz, J.J. Marin-Hernandez, M. Hernandez-Cordoba, *J. Chrom. A*, **871** (2000) 85.
173. S. Zhang, H. Zhao, R. John, *Anal. Chim. Acta*, **441** (2001) 95.
174. H. Xue, Z. Shen, H. Zheng, *J. Appl. Electrochem.*, **32** (2002) 1265.
175. A. Boshoff, M.H. Burton, S.G. Burton, *Biotech. Bioeng.*, **83** (2003) 1.
176. S. Kiralp, L. Toppare, Y. Yagci, *Int. J. Biol. Macrom.*, **33** (2003) 37.
177. S. Kiralp, L. Toppare, Y. Yagci, *Des. Mon. Pol.*, **7** (2004) 3.

178. A.M. Azevedo, D.M.F Prazeres, J.M.S. Cabral, L.P. Fonseca, *Biosens. Bioelectron.*, **21** (2005) 235-247.
179. N.G. Patel, S. Meier, K. Cammann, G.C. Chemnitz, *Sens. Actuat. B: Chem.*, **75** (1-2), (2001) 101.
180. J. Vonck, E.F. van Bruggen, *Biochim. Biophys. Acta*, **1038** (1990) 74.
181. H. Jurgens, R. Kabub, T. Plumbaum, B. Weigel, G. Kretzmer, K. Schugerl, K. Andreas, E. Ignatzek, F. Giffhorn, *Anal. Chim. Acta*, **298**, (1994) 141.
182. J. Rhee, K. Schugerl, *Anal. Chim. Acta*, **355** (1997) 55.
183. H. Ukeda, M. Ohira, M. Sawamura, *Anal. Sci.*, **15** (1999) 447-450.
184. N. Majkic-Singh, I. Berkes, *Anal. Chim. Acta*, **115** (1980) 401.
185. A.M. Salgado, R.O.M. Folly, B. Valdman, O. Cos, F. Valero, *Biotechnol. Lett.*, **22** (2000) 327-330.
186. T.D. Gibson, I.J. Higgins, J.R. Woodward, *Analyst*, **117** (1992) 1293-1295.
187. A.M. Azevedo, J.M.S. Cabral, T.D. Gibson, L.P. Fonseca, *J. Mol. Catal. B: Enzym.*, **28** (2004) 45.
188. L. Prencipe, E. Iaccheri, C. Manzati, *Clin. Chem.*, **33** (1987) 486-489.
189. Y.V. Rodionov, O.I. Keppen, M.V. Sukacheva, *J. Chromatogr.*, **38** (2002) 395-396.
190. E. Barzana, A.M. Klibanov, M. Karel, *Anal Biochem.*, **182** (1989) 109-115.
191. F.W. Janssen, H.W. Ruelius, *Biochim. Biophys. Acta*, **151** (1968) 330.
192. M.V. Gonchar, M.N. Maidan, O.M. Moroz, J.R. Woodward, A.A. Sibirny, *Biosens. Bioelectron.*, **13** (1998) 945-952.
193. M. Rank, J. Gram, K.S. Nielsen, B. Danielsson, *Appl. Microbiol. Biotechnol.*, **42** (1995) 813-817.
194. X. Xie, A.A. Suleiman, G.G. Guilbault, Z.M. Yang, Z.A. Sun, *Anal. Chim. Acta*, **266** (1992) 326.

195. M. Rank, J. Gram, B. Danielsson, *Anal. Chim. Acta*, **281** (1993) 255-257.
196. F.W. Janssen, R.M. Kerwin, H.W. Ruelius, *Biochem. Biophys. Res. Commun.*, **20** (1965) 630-634.
197. F. Mazocco, P.G. Pilleri, *Anal. Biochem.*, **72** (1996) 647.
198. F. Ortega, E. Dominguez, *J. Biotechnol.*, **31** (1993) 289-300.
199. T. Palmer, *Understanding Enzymes*, (1995) Prentice Hall, London.
200. M. Lopez, F. Martinez, C. Del Valle, C. Orte C, M. Miro, *J. Chrom. A.*, **922** (2001) 359.
201. A.V. Sakkiadi, M.N. Stavrakakis, S.A. Haroutounian, *Lebensm. Wiss. Technol.*, **34** (2001) 410.
202. S. Karakaya, S.N. El, A.A. Taş, *Inter. J. Food Sci. Nutr.*, **52** (2001) 501.
203. M.M. Bradford, *Anal. Biochem.*, **72** (1976) 248-254.
204. H.B. Yildiz, S. Kiralp, L. Toppare, Y. Yagci, K. Ito, *Mater. Chem. Phys.*, **100** (2006) 124-127.
205. S. Jin, G. Xue, *Macromolecules*, **30** (1997) 5733.
206. H.B. Yildiz, S. Kiralp, L. Toppare, Y. Yagci, K. Ito, T. Senyo, *Polym. Bull.*, **53** (2005) 193-201.
207. H.B. Yildiz, L. Toppare, *Biosens. Bioelectron.*, **21** (2006) 2306-2310.
208. G. Dienys, S. Jarmalavicius, S. Budriene, D. Citavicius, J. Serekaite, *J. Mol. Catal. B: Enzym.*, **21** (2003) 47-49.
209. A. Cirpan, S. Alkan, L. Toppare, Y. Hepuzer, Y. Yagci, *Bioelectrochemistry*, **59** (2003) 29-33.
210. H.B. Yildiz, S. Kiralp, L. Toppare, Y. Yagci, *J. Appl. Polym. Sci.*, **96** (2005) 502-507.
211. A. Cirpan, S. Alkan, L. Toppare, L. Cianga, Y. Yagci, *Des. Monomers Polym.*, **6** (2003) 237-243.
212. A.V. Sakkiadi, M.N. Stavrakakis, S.A. Haroutounian, *Lebensm. Wiss. Technol.*, **34** (2001) 410-413.
213. S.E. Stanca, I.C. Popescu, *J. Mol. Catal. B-Enzym.*, **27** (2004) 221-225.
214. S. Kiralp, A. Cirpan, L. Toppare, *J. Appl. Polym. Sci.*, **100** (2005) 521-524.

215. M. Lopez, F. Martinez, C. Del Vale, C. Orte, M. Miro, *J. Chrom. A*, **922**  
(2001) 359-363.

## VITA

Hüseyin Bekir YILDIZ was born in Kastamonu on 17<sup>th</sup> February 1977. He graduated from Antalya High School in 1994. He received his B.S. Degree at the Chemistry Department, in Middle East Technical University (METU) in 1999. After working a year as a research assistant at Chemistry Department of Gazi University, he joined the Department of Chemistry, METU as a research assistant in 2000. He completed his M.S. degree in June 2002 under the supervision of Prof. Dr. Yavuz Ataman in the field of “Oxidation State Related Evaluation of Tellurium Determination by Flame AAS and Use of Slotted Silica Trap”. He began his PhD study in 2002 under the supervision of Prof. Dr. Levent Toppare in the field of conducting polymers and enzyme immobilization. In 2002 he joined the Academic Human Resources Program (ÖYP) which is supported by State Planning Organization, and he continued his studies in METU on behalf of Selçuk University. He worked as a visiting scientist at Chemistry Department of Bochum-Ruhr University in Germany on the topic of amperometric biosensors. Up to date he has eight published and two submitted articles in international journals.